TARGETING AN NRF2/G6PDH PATHWAY TO REVERSE MULTI-DRUG RESISTANCE IN DIFFUSE LARGE B-CELL LYMPHOMA

A Dissertation

by

SEYEDHOSSEIN MOUSAVIFARD

Submitted to the Office of Graduate and Professional Studies of
Texas A&M University
in partial fulfillment of the requirements for the degree of

DOCTOR OF PHILOSOPHY

Chair of Committee,	Steve Maxwell
Committee Members,	James C. Sacchettini
	Raquel Sitcheran
	David W. Threadgill
	Warren Zimmer
Head of Program,	Warren Zimmer

May 2017

Major Subject: Medical Sciences

ABSTRACT

A leading cause of mortality in diffuse large B-cell lymphoma (DLBCL) patients is the development of resistance to the CHOP regimen, the anthracycline-based chemotherapy consisting of cyclophosphamide, doxorubicin, vincristine, and prednisone. Our first objective of this work was to investigate the impact of Nuclear factor erythroid–related factor 2 (Nrf2)/ glucose-6-phosphate dehydrogenase (G6PDH) pathway on CHOP-resistance in DLBCL cell lines. We provide evidence here that a Nrf2/G6PDH pathway plays a role in mediating CHOP resistance in DLBCL. We found that CHOP-resistant DLBCL cells expressed both higher Nrf2 and G6PDH activities and lower reactive oxygen (predominantly superoxide) levels than CHOP-sensitive cells. We hypothesized that increased activity of the Nrf2/G6PDH pathway leads to higher GSH production, a more reduced state (lower ROS), and CHOP-resistance. In support of our hypothesis, direct inhibition of G6PDH or knockdown of Nrf2/G6PDH lowered both NADPH and GSH levels, increased ROS, and reduced tolerance or CHOP-resistant cells to CHOP. We also present evidence that repeated cycles of CHOP treatment select for a small population of $Nrf2^{High}/G6PDH^{High}/ROS^{Low}$ cells that are more tolerant of CHOP and might be responsible for the emergence of chemoresistant tumors. We propose that sensitive $Nrf2^{Low}$ /$G6PDH^{Low}$ /ROS^{High} cells are essentially killed off by CHOP allowing for the selective propagation of the small population of CHOP-resistant $Nrf2^{High}/G6PDH^{High}/ROS^{Low}$ cells, thereby resulting in relapse of lymphoma.

Our second objective was to study rifamycins' potency at sensitizing drug resistant cancer cells to chemotherapeutics. We have discovered a novel chemosensitizer (RTI-79, a rifamycin-derivative) with a broad spectrum of action that includes ovarian cancer and double and triple hit non-Hodgkin's lymphoma. RTI-79 is relatively non-toxic and has favorable in vivo safety and

pharmacokinetic (PK) profiles. RTI-79 in combination therapies is effective in multiple drug resistant cancers in mouse models. RTI-79 works by dramatically increasing intracellular reactive oxygen species (ROS), primarily superoxide, through redox cycling. The level of ROS induction is directly correlated with drug sensitivity. Importantly, RTI-79 also triggers the unfolded protein response (UPR) that results in increased ubiquitination and loss of Nrf2, the primary sensor for intracellular ROS. Thus, RTI-79 both increases ROS and squelches Nrf2's ability to respond to ROS. This unique mechanism provides a broad and novel approach for the very safe application of RTI-79, and other rifamycins, in treating drug resistant cancers.

We also showed that RTI-79 acts to increase the oxidative state in chemoresistant cancer cells by inducing superoxide ($O2^-$) and downregulating the Nrf2/G6PDH/NADPH/GSH pathway. RTI-79 also increased the ubiquitination state of several mitochondrial chaperone proteins (mtDnaJ [HSP40]), HSP60, HSP70mt [mortalin]) and decreased activated CREB, which are known to play roles in mitochondrial unfolded protein response (UPRmt) retrograde signaling.

In summary, this research explores a new way to overcome the chemoresistance particularly in DLBCL and ovarian carcinoma. The new findings of this study will significantly impact our understanding of the role of Nrf2/G6PDH signaling pathway in DLBCL, and provide hope for the development of rational therapies for both newly diagnosed patients with DLBCL and also patients with relapsing DLBCL.

ACKNOWLEDGEMENTS

I would like to thank my committee chair, Dr. Steve Maxwell, and my committee members, Dr. Sacchettini, Dr. Sitcheran and Dr. Threadgill, and Dr. Zimmer for their invaluable guidance, support, encouragement, and knowledge throughout the course of this research.

I would like to express my profound gratitude to Dr. Sacchettini for the financial support and scientific collaborations.

I also thank the department of Molecular and Cellular Medicine at Texas A&M Health Science Center for providing funds for this research.

Thanks also go to my friends and colleagues and the department of Molecular and Cellular Medicine faculty and staff for making my time at Texas A&M University a great experience.

Finally, thanks to my family for their encouragement and support over the years and to my wife for her patience and love.

CONTRIBUTORS AND FUNDING SOURCES

Contributors

This work was supported by a dissertation committee consisting of Dr. Steve Maxwell, Dr. Raquel Sitcheran and Dr. David W. Threadgill of the Department of Molecular and Cellular Medicine, Dr. James C. Sacchettini of the Department of Biochemistry and Biophysics, and Dr. Warren E. Zimmer of the Department of Medical Physiology.

Steve Maxwell and Seyed Hossein Mousavi-Fard researched and prepared the manuscript for chapter I.

Seyed Hossein Mousavi-Fard and Steve Maxwell designed experiments and analyzed the data for Chapter II. Seyed Hossein Mousavi-Fard carried out the transductions, western blots, GSH, and NADPH experiments. Seyed Hossein Mousavi-Fard and Timothy Davis conducted experiments on G6PDH activities and effects on cell growth. Seyed Hossein Mousavi-Fard and Steve Maxwell carried out the reactive oxygen species analyses. Steve Maxwell conceived the idea for the project and generated the cell lines. Deeann Wallis and Jim Sacchettini commented on the data.

Deeann Wallis involved in much of the conception and experimental design, data generation, analysis, writing and editing the manuscript for Chapter III. Nian Zhou leads medicinal chemist determined SAR, conceived, designed and generated all analogs. Dwight Baker designed and implemented initial HTS and validated hits and determined synergy, edited manuscript. Seyed Hossein Mousavi-Fard, Kimberly Loesch, Stacy Galaviz, Qingan Sun, Thomas Ioerger, Michael DeJesus, Wen Dong, and Gwen Seemann involved in experimental design, data generation, and analysis. Carolina Mantilla Rojas and David W. Threadgill generated, analyzed, and interpreted

mouse echocardiogram data. Maureen T. O'Brien and Theresa Fossum generated, analyzed, and interpreted histology on mouse hearts. Theresa Fossum, Steve Maxwell, and James C. Sacchettini conceived the initial idea, involved in experimental design, data generation, and analysis, writing and editing manuscript.

All other work conducted for the dissertation was completed by Seyed Hossein Mousavi-Fard independently.

Funding Sources

The preparation of this dissertation was supported by institutional funds provided to Dr. Steve Maxwell from the Texas A&M Health Science Center of the Department of Molecular and Cellular Medicine. In addition, James C. Sacchettini provided funding for data generation and analysis for chapter III.

TABLE OF CONTENTS

LIST OF FIGURES

Page

LIST OF TABLES

Page

CHAPTER I

GENERAL INTRODUCTION AND LITERATURE REVIEW: NON-HODGKIN'S B CELL LYMPHOMA: ADVANCES IN MOLECULAR STRATEGIES TARGETING DRUG RESISTANCE *

1.1 Introduction

1.1.1 The problem of multidrug resistance in non-Hodgkins lymphoma

Non-Hodgkins lymphoma (NHL) is a heterogeneous class of cancers displaying a diverse range of biological phenotypes, clinical behaviors, and prognoses. The majority of NHL cases originate from B cells with about 10% arising from T cells (1, 2). B cells that normally undergo clonal expansions at different stages of differentiation can give rise to the B cell type of NHL (3).The standard treatment for NHL is the anthracycline-based chemotherapy regimen, termed CHOP, which is composed of cyclophosphamide, doxorubicin, vincristine, and prednisolone (4). The addition of rituximab (monoclonal antibody to CD20) to CHOP (R-CHOP) has provided the first major improvement in therapy in over three decades and is now the new standard for treatment (5). Most NHL patients initially respond to chemotherapy yielding complete response rates of 40–50% (6-10). Regrettably, a substantial population of patients undergo relapse, resulting in disappointing 3-year overall survival rates of only about 30% (11). The problem is compounded by the higher doses of CHOP administered to relapsed patients, which have resulted in severe side-effects and a response in only about one-third of relapsed patients (12-14). Relapsed lymphomas are not only refractory to subsequent treatments with the initial chemotherapy regimen but also can exhibit cross-resistance to a wide variety of anticancer drugs.

* Reprinted with permission from "Non-Hodgkin's B-cell lymphoma: advances in molecular strategies targeting drug resistance." by Maxwell SA, Mousavi-Fard S, 2013. Exp Biol Med (Maywood). 238(9):971-90, Copyright 2013 by SAGE Publishing.

Acquisition of chemoresistance in B cell lymphomas is due to the emergence of subpopulations of drug-resistant tumor cells, which leads to the failure of standard CHOP therapies. Chemoresistance in NHL is not consistently associated with the upregulation of multidrug pump (i.e. P-glycoprotein; MDR1) expression indicating the existence of other drug-resistant mechanisms (15, 16). Inherent genetic heterogeneity and instability of the tumor cells drive the acquisition of drug resistance in lymphoma (17). It is now apparent that a new generation of less toxic and more targeted approaches based on rational drug design is needed to prevent and/or reverse chemoresistant disease (18). The purpose of this article is to highlight the many new insights into the molecular basis of chemorefractory NHL, which are leading the way to the rational design of novel drugs to overcome chemoresistance. Due to the genetic heterogeneity of B-cell NHL, many different pathways leading to drug resistance have been identified. Successful treatment of chemoresistant NHL will thus require cocktails of combinatorial drugs targeting multiple pathways specific to different subtypes of NHL as well as the development of personalized approaches to address patient-to-patient genetic heterogeneity.

1.1.2 Innate and acquired drug resistance varies among subtypes of NHL

Aggressive NHL includes diffuse large B cell lymphoma (DLBCL), mantle-cell lymphoma (MCL), Burkitt's lymphoma (BL), follicular lymphoma (FL) and peripheral T-cell lymphoma (PTCL). Each of these subtypes of NHL display a wide range of responses and outcomes to standard chemotherapeutic regimens due to genetic heterogeneities. Despite remarkable advances in chemotherapy, more than half of patients with aggressive B cell NHL (B-NHL) are incurable (6). PTCL, in particular, remains a challenge for chemotherapy since there are no drugs that can prevent progression of the disease (19). The two most common types of NHL are DLBCL and FL, representing more than half of all patients with B-NHL (1). The most common

histological type is DLBCL and is classified as an aggressive subtype, but potentially is curable with chemotherapy (1, 20-22). The second most frequent type of NHL is FL, which is usually incurable with conventional chemotherapy, and exhibits a median survival of 10 years postdiagnosis (23). MCL is an aggressive disease with a 3–4-year median survival and poor responsiveness to conventional chemotherapy (24-27).

1.1.3 Drug-resistant DLBCL

Most DLBCL patients initially respond favorably to CHOP, but 50% eventually relapse with CHOP-resistant disease that disseminates and is highly lethal without transplantation (28). Even though CHOP-resistant DLBCL affects about 10,000 new cases in USA each year, the molecular features of CHOP-resistant DLBCL have not been adequately defined. Drug resistance can be inherent (innate) from the beginning (29) or develop from prior exposure to chemotherapy (acquired) (30, 31). The varied responses of DLBCL to chemotherapy are due to aberrations in multiple molecular pathways, which are attributed to the heterogeneous genetic nature of DLBCL (32). Gene expression profiling (GEP) of patient tumors has better defined the molecular heterogeneity underlying the heterogeneous clinical behavior of DLBCL. Patients with DLBCL have been classified into three groups according to their GEP patterns based on the three cell-of-origin signatures, activated B cell–like DLBCL (ABC-DLBCL), germinal-center B cell–like DLBCL (GCB–DLBCL) and mediastinal (33-36). The GCB and ABC subcategories are characterized by distinct differences in survival, chemoresponsiveness and dependence on signaling pathways (37). ABC–DLBCL resembles in vitro activated B cells. In a separate multiple clustering array analysis (38), DLBCLs were categorized into Ox-phos, BCR/proliferation and host-response signatures. The BCR/proliferation subset displayed the upregulation of genes involved in B cell activation and proliferation.

1.1.4 Mantle-cell lymphoma

Mantle-cell lymphoma (MCL) is an aggressive disease that has a poor response to conventional chemotherapy resulting in an overall survival of about 3–4 years (27, 39). A major problem in treating MCL is the occurrence of relapse caused by resistance to chemotherapy. Many different drug combinations comprised of alkylating agents, anthracyclines and purine analogs have been tested in MCL patients (40). One of the unique features of MCL is a cluster differentiation (CD) phenotype associated with a specific chromosomal translocation, t(11;14)(q13;q32), which translocates the cyclin D1 gene to be under the control of the immunoglobulin heavy chain gene enhancer, resulting in upregulation of cyclin D1 (41). Overexpression of cyclin D1 plays a critical role in the pathogenesis and chemorefractoriness of MCL. However, accumulating evidence indicates that MCL frequently is dysregulated not only in cell-cycle regulation but also in apoptosis and DNA repair (42, 43). MCL frequently can also be innately resistant to anticancer agents (43). A number of dysfunctional biochemical pathways have been identified that may contribute to the relatively high resistance of MCL to chemotherapy-induced apoptosis (44), including the activation of NFκB pathway (45-47), overexpression of antiapoptotic proteins and the absence of proapoptotic proteins (48). GEP has also identified the upregulation of genes associated with multidrug resistance in MCL (49). The resistance of MCL to alkylating agents and to anthracycline can also result from the upregulation of the glutathione S-transferase (GST) gene, which is located in 11q13 and thus co-amplified along with the cyclin D1 gene (50) as well as the phosphoinositide 3-kinase/Akt pathway (PI3K/Akt) (51, 52). Despite the generation of several new therapeutic agents directed against PI3K/Akt, B cell receptor signaling and Bcl-2, poor clinical outcomes continue to be a problem in a significant population of MCL patients (43, 53).

1.2 Drug-resistance pathways in B-cell NHL

1.2.1 PI3K/Akt pathway in B cell NHL drug resistance

The PI3K/Akt pathway plays a central role in promoting survival and chemoresistance in NHL (54-58). Dysregulation of the PI3K/Akt pathway is frequent in DLBCL and worsens prognosis (58-65). New drugs targeting this pathway have shown encouraging results in treating relapsed NHL patients (66-71). However, not all chemorefractory DLBCL patients show positive responses to current Akt pathway inhibitors, and many experience severe side-effects (72, 73). A primary mediator of PI3K signaling is the Akt/protein kinase B kinase, which acts to promote cell survival through direct phosphorylation of apoptotic regulators. Akt phosphorylation of proapoptotic substrates (including Bad, FOXO, GSK-3b and ASK1) targets them for binding to 14-3-3 proteins (74-80), which effectively neutralizes their ability to induce apoptosis. A role for the activation of the Akt pathway in promoting chemoresistance in NHL was shown by treatment with pharmacological inhibitor (LY-294002) and by Akt siRNA, both of which inhibited Bcl-xL expression and sensitized the cells to chemotherapeutics (81). Moreover, higher Akt activity was observed in CHOP-resistant DLBCL cells than in CHOP-sensitive cells, which was associated with the upregulation of 14-3-3zeta (82, 83). Chemical inhibition of Akt (82) or shRNA-mediated knockdown of 14-3-3zeta (83) restored CHOP sensitivity to the resistant cells, indicating that CHOP resistance was mediated by these proteins, was reversible and might be targeted as a clinical strategy for CHOP resensitization. mTOR in the Akt pathway is an important therapeutic target for DLBCL. Rapamycin inhibited mTORC1 in DLBCL lines and primary tumors with minimal cytotoxicity (84). Clinical trials of the rapamycin analogs, temsirolimus and everolimus have demonstrated overall response rates of about 30% for relapsed DLBCL (85-87). However, only about half of relapsed patients respond to mTOR inhibitors. A

critical focus needs to be on the development of new inhibitors of the PI3K/Akt pathway that bypass resistance mechanisms. As an example, addition of a histone deacetylase inhibitor reversed resistance to rapamycin (84).

1.2.2 Dysregulated apoptotic pathways

The germinal center (GC) is the location of immune surveillance in the lymph node. B cells that express functional B cell receptors and have a block to execution of an activated apoptotic program migrate to the GC (88). One hallmark of germinal center-derived B cell NHL (GC-DLBCL) is resistance to apoptosis characterized by the dysregulation of apoptotic control mechanisms (37, 89, 90). In addition, dysregulation of genes involved in apoptotic pathways has also been reported to be associated with chemoresistance in activated B cell-like DLBCL (ABC-DLBCL). Thus, a promising approach in both frontline and salvage therapeutic strategies in B cell NHL is targeting altered apoptotic pathways. Strategies targeting the two main apoptotic pathways, extrinsic and intrinsic, are summarized below.

1.2.2.1 Extrinsic (death receptor) pathway

The tumor-necrosis factor receptor (TNFR) family of transmembrane proteins, including the death receptors for Fas (CD95) and tumor necrosis factor-related apoptosis-inducing ligand (TRAIL), induces cell death. TRAIL mediates apoptosis by binding to cell-surface transmembrane receptors, either death receptor 4 (DR4/APO2/TRAIL-R1) or death receptor 5 (DR5/KILLER/TRAIL-R2/TRICK2) (91), which recruit the death-inducing signaling complex composed of FADD and the inactive proenzymatic form of the apoptosis-initiating proteases caspase-8 (92, 93). Self-activation of caspase-8 by autoproteolysis leads to the activation of the executioner caspase-3 to carry out apoptosis. TNFR family members can selectively induce

apoptosis in some drug-resistant B cell lymphomas (94-97). Twelve out of 22 primary lymphoma cell cultures derived from biopsied DLBCL samples were sensitive to TRAIL, (97) which included seven clinically chemoresistant lymphomas. TRAIL was found to induce apoptosis in DLBCL cells expressing the upregulation of prosurvival molecules, Bcl- 2 and/or X-linked inhibitor of apoptosis (XIAP). Thus, TRAIL might be an effective therapy for drug-resistant DLBCL patients that show dysregulated extrinsic apoptosis pathways (96, 98, 99). The Bfl-1 protein is required for the survival of malignant B cells and might be a potential target against drug resistant B cell lymphoma (100). Bfl-1 is a direct transcriptional target of nuclear factor-kappa B (NF-kB) (101-103), and its upregulation is associated with an increased resistance to tumor-necrosis factor (TNF)-α, anti-CD95, TRAIL and chemotherapeutic drugs (102-104). In DLBCL, downregulation of Bfl-1 occurs in tumor cells induced to undergo apoptosis by inhibition of the activated NF-kB pathway (105). Moreover, short-hairpin RNA silencing of Bfl-1 in DLBCL cell lines sensitized those cell lines to anti-CD20 (rituximab) - mediated cell death and chemotherapeutic agents. Thus, Bfl-1 will be a candidate target in the design of new strategies for drug-resistant cancer therapy.

1.2.2.2 Intrinsic pathway

The Bcl-2 family regulates an apoptotic pathway that is initialized at the mitochondrion known as the intrinsic apoptotic pathway. Bcl-2 family members function through mutual interactions with each other and the balance between the anti-apoptotic (Bcl-2, Bcl-xL, Mcl-1) and the proapoptotic (Bax, Bak; and the BH3-only Bid, Bim and PUMA protein) members are critical for preventing or initiating apoptosis (106, 107). The BH3-only proapoptotic (Bid, Bim, PUMA) proteins act as molecular sensors of cellular stress or damage and are activated in response to DNA damage, growth factor withdrawal and oncogene activation (108). Many chemotherapeutic

drugs activate the intrinsic apoptosis pathway, leading to the release of proapoptotic molecules, including cytochrome c, from the intermembrane space of mitochondria into the cytosol. Cytochrome c, Apaf-1 and procaspase-9 complex together to form the apoptosome machinery in the cytoplasm. The apoptosome promotes oligomerization of Apaf-1, which then triggers the activation of the initiator procaspase-9. The active caspase-9, in turn, cleaves and activates downstream executioner caspases, including pro-caspase-3, which cleaves proteins, thus producing the characteristic apoptotic phenotype of blebbing, nuclear condensation and cell shrinkage. Dysregulation of apoptosome formation and caspase activation has been associated with chemoresistance in B cell lymphoma. BL cells commonly are resistant to apoptosis induction by chemotherapeutic agents, which has been attributed to deficient levels of Apaf-1, thus leading to the failure of cytochrome c to promote apoptosome formation and caspase activation (109). Overexpression of antiapoptotic family members in B cell lymphomas is associated with the inhibition of apoptosis and chemotherapy resistance, resulting in lower clinical response rates and shortened survival (110-114). Bcl-2 was observed overexpressed in about 80% of FL and 20% of DLBCL as a result of the t (14; 18) translocation and amplification of the Bcl-2 gene, respectively (115-117). Bcl-2 expression was also correlated with a higher relapse-rate, shorter disease-free survival and shorter overall survival (16, 118-121). Antisense-mediated repression of Bcl-2 expression resulted in significant increases in the sensitivity of lymphoma cells to chemotherapeutic drugs (122-124). Oblimersen (Genta Inc.) is a phosphorothioate Bcl-2 antisense oligonucleotide, which in combination with rituximab, resulted in an overall response rate of 42% including 10 complete responses and 8 partial responses in relapsed B cell NHL patients (125). Median duration of response was 12 months with minimal toxicities. Thus, co-administration of Oblimersen and rituximab is a safe treatment that will be most beneficial in patients with refractory NHL.

1.2.3 IAP proteins

Inhibitor of apoptosis (IAP) proteins can block executioner caspases (126). Overexpression of IAPs (XIAP) has been shown to result in resistance to agents that induce apoptosis pathways (127, 128). XIAP is the most potent inhibitor of the apoptosis cascade and can repress apoptosis induced by TNF, TRAIL, Fas-L and conventional chemotherapeutics (127, 128). In DLBCL, XIAP expression was associated with a poor prognosis (129). A small-molecule XIAP antagonist re-activated the intrinsic apoptosis pathway in drug-resistant DLBCL cell lines (130, 131).Peripheral blood mononuclear cells and tonsil germinal-center B cells from healthy donors were not affected, validating the XIAP antagonist for possible development as a therapy for chemotherapy-refractory DLBCL. The sensitivity of DLBCL cells to the XIAP antagonist could be predicted from molecular markers, such as expression of XIAP, Bcl-2 and levels of constitutive caspase-9 activation (131), indicating a potential for selecting patients for XIAP therapy.

1.2.4 DNA damage response

Mutations in the DNA damage response (DDR) genes may promote tumor formation as well as drive emergence of drug resistance. The Atm gene product is a primary component of the DDR, which has a phosphatidylinositol-3- kinase-like protein kinase that phosphorylates many proteins upon DNA damage (132). Atm mutations have identified in hematologic malignancies. An association between Myc activation and Atm inactivation has been identified during the progression of human B cell lymphomas (133). In mice, Atm loss collaborated with Myc activation to accelerate the development of lymphomas (134-136). Following anticancer therapy, Atm (DDR)-compromised lymphomas exhibited defects in ability to undergo apoptosis and had

a poorer long-term outcome as compared to DDR-competent lymphomas. Atm thus appears to prevent tumor progression by converting oncogenic signaling into apoptosis, resulting in selection against an Atm-dependent DDR and the emergence of drug-resistant lymphomas

1.2.5 NFκB pathway

Activation of NF-kB is a driver in apoptosis resistance in a variety of B cell malignancies leading to poor outcome in lymphoma patients (137, 138). The NF-kB family has the capacity to regulate transcription of a diverse array of genes involved in cancer cell growth, including those involved in proliferation and resistance to apoptosis (139-142). Drug-resistant lymphoma cell lines have been sensitized by treatment with inhibitors of the NF-kB pathway (143, 144). Bfl-1 is a direct transcriptional target of NF-kB (101-103), and its upregulation is associated with decreased sensitivity in lymphomas to chemotherapeutic drugs and apoptotic stimuli, including TNF-α and anti-CD95 (102-104). Inhibition of NF-kB pathway in DLBCL (37, 105) led to the downregulation of Bfl-1 expression and apoptosis. Knockdown of Bfl-1 in sensitized DLBCL cell lines to anti-CD20 (rituximab) and standard chemotherapeutics (100).

1.2.6 microRNAs

A microRNA, miR-21, has been shown to influence sensitivity of DLBCL cells to CHOP by impacting the PI3K/Akt signaling pathway (145). Mir21 targets PTEN for downregulation and NFκB upregulates miR-21. Knockdown of NFκB decreased miR-21 and sensitized DLBCL cells to chemotherapy. A frequent genetic alteration that has been observed in MCL is chromosome 13q31–q32 amplification targeting a microRNA cluster termed miR-17–92 (146-148).Upregulation of miR-17–92 activated the PI3K/AKT pathway and inhibited apoptosis

induced by chemotherapeutics in MCL cell lines (149). Downregulation of miR-17–92 repressed the PI3K/Akt pathway and inhibited tumor growth in a xenograft MCL mouse model.

1.2.7 TGF-β pathway

Members of the transforming growth factor-b (TGF-β superfamily modulate proliferation, apoptosis and differentiation in many different cell types. TGF-β inhibits cell proliferation by arresting cells in the G1 phase of the cell cycle through the p15INK4b, p21Cip1/WAF1, p27 and c-Myc proteins (70). Binding of TGF-β receptors to their ligands activates the serine/threonine kinase activity of the TGF-β receptors (TbRI and TbRII). The ligand-activated TbRII phosphorylates and activates the TbRI, which in turn transmits the TGF-β signal by phosphorylating and activating the Smad2 and Smad3 proteins. The activated Smads oligomerize with Smad4, and the complexes then translocate to the nucleus where they regulate transcription of TGF-β target genes (66, 67, 150). Lymphoma cells can acquire resistance to TGF-β through promoter methylation of the TbRII gene (71). Promoter analysis in lymphomas revealed CpG methylations at 25 and 140 of the TRII promoter that correlated with the silencing of the TRII gene. Overexpression of BCL6 contributes to TGF-β resistance in B-cell lymphoma. BCL6 transcriptionally represses Smad4 (72). B cell lymphoma cells with upregulated BCL6 were refractory to TGF-β, whereas knockdown of BCL6 expression restored the response to TGF-β.

1.2.8 Oxidative stress pathways

Changes in oxidative stress pathways may explain the more aggressive tumor phenotype of drug-resistant lymphoma variants. In a murine lymphoma model, lymphoma cells transfected with catalase or selected for resistance to hydrogen peroxide were resistant to CHOP (151-153). Oxidative stress-resistant cells demonstrated an altered metabolic profile, including the ability to

generate ATP from alternative carbon sources such as glutamine (154, 155). When treated with glucocorticoids, the oxidative stress-resistant cells were better able to maintain ATP levels as compared to sensitive parental cells (155). Experiments with an uncoupler of mitochondrial respiration showed that the oxidative stress-resistant cells produced more ATP from mitochondria than the sensitive cells (154).

1.2.9 Reactive oxygen species

Once inside the cell, anthracyclines in the CHOP cocktail kill lymphoma cells by DNA intercalation, topoisomerase II inhibition and reactive oxygen species (ROS) induction. The type of ROS generated can be critical; superoxide anion and hydrogen peroxide inhibited cancer cell migration and invasion, whereas hydroxyl radical promoted cell migration and invasion (156). The Akt-survival pathway has been implicated in regulating ROS in lymphoma cells. Akt activation correlated with both decreased ROS and increased cell survival in lymphoma cells (157). Chronic ROS exposure can generate lymphoma cells with upregulated antioxidant defense systems, which results in chemoresistance (158). Oxidative stress-resistant variants expressed increased catalase and superoxide dismutase activities and increased phase 2 enzymes, NAD(P)H: quinone oxidoreductase and GST μ and π.

1.2.10 Proton pumps

The acidity of the tumor microenvironment due to hypoxic conditions, which influence ROS production, plays an important role in tumor progression, chemoresistance and metastatic behavior (159, 160). Cancers adjust to acidity by upregulating proton extrusion activity, thus allowing the tumor cells to survive (161-163). Tumor cells control intracellular pH through proton pumps like the vacuolar-type H + ATPase (V-ATPase). Modification of cellular pH

gradients by treatment with proton pump inhibitors (PPIs) sensitized B-lymphoma cells to chemotherapeutics through ROS production (164). Neutralization of ROS by the antioxidant, N-acetylcysteine, delayed apoptosis. PPIs also inhibited the growth of B-cell lymphoma in SCID mice. Thus, PPIs may provide for therapeutic approaches for drug-resistant B cell lymphomas.

1.2.11 GSH

The glutathione-S-transferases (GSTs) multigene family of enzymes detoxify electrophilic xenobiotics, including alkylating agents, and reduce oxidative stress (165-171). Overexpression of the GST-π isoenzyme has been associated with alkylating agent and anthracycline resistance in lymphomas (171).

1.2.12 CD antigens

1.2.12.1 CD20-rituximab

The coadministration of rituximab to CHOP chemotherapy has significantly increased the survival of DLBCL patients (172-179). Rituximab is a humanized monoclonal antibody that binds to the CD20 antigen on B lymphocytes (180). CD20 is expressed by >99% of B-cell NHL (2), which is not internalized following antibody binding (181) or secreted into the circulation (182). However, given that it is also expressed by normally differentiated pre-B cells and B cells (183, 184), normal B cells are also depleted during rituximab therapy, so that NHL patients have a prolonged B-lymphopenia following rituximab therapy (185). Regrettably, many patients will relapse after rituximab/ CHOP (R-CHOP) therapies (184, 186-193). Rituximab exerts its anti-lymphoma activity through multiple mechanisms, including growth inhibition, apoptosis, complement-dependent cell cytotoxicity (CDC) and antibody-dependent cellular cytotoxicity (ADCC) (60, 184). Although rituximab mediates CDC and ADCC of CD20- positive human B

cells (194), it can have direct apoptotic effects. Unfortunately, resistance to rituximab can eventually evolve in some patients during the course of the disease, which is only explained in part by the loss of CD20 expression (195).

A variety of signaling events have been observed in lymphoma cells exposed to rituximab in vitro, including the activation of Src-family of protein tyrosine kinases, decreased NFκB activity and downregulation of Bcl-2 levels (196-201). Rituximab inhibited Akt in B cell lymphoma cell lines, which contributed to the sensitization of drug resistant cells to chemotherapeutic drugs (81). B-lymphoma cell lines resistant to rituximab have cross-resistance to multiple chemotherapeutic agents and exhibit downregulation of the Bcl-2 family proteins Bax and Bak (202). Repeated exposure to rituximab generates a therapy resistant phenotype by modulating the expression of Bax and Bak. The development of new inhibitors of the Akt and Bcl-2 pathways will now allow rationally designed clinical trials addressing Rituximab resistance that employ combinations of the new inhibitors and rituximab.

1.2.12.2 CD147

Upregulation of extracellular matrix metalloproteinase inducer (EMMPRIN or CD147) drives lymphoma progression and induces resistance to chemotherapeutic drugs (203-208). CD147 is a transmembrane glycoprotein of the immunoglobulin superfamily that is expressed on the surface of lymphoma cells. It functions as a regulator of matrix metalloproteinase (MMPs) expression in the local lymphoma environment (204). High expression of MMPs has been correlated with tumor metastasis (209). Reduced CD147 expression led to reduced metastasis and sensitized drug resistant cells to chemotherapeutics (210).

1.2.13 MDR proteins

The ability of cancer cells to resist the cytotoxic effects of chemotherapeutic agents is termed multidrug resistance (MDR), which is manifested by a decreased sensitivity to a wide range of nonhomologous drugs targeting multiple diverse pathways (211). Overexpression of the 170–180 kDa ATP-dependent pump, P-glycoprotein (P-gp transporter), is frequently associated with resistance against a wide range of chemotherapeutics (212-215) and results in the MDR phenotype. P-gp transports or effluxes chemotherapeutics out of the cell, which reduces the intracellular concentration of the drugs, thus protecting cellular structures from damage and promoting cell survival. MDR due to the upregulated expression of P-gp product has been implicated as a critical factor in the prognosis and clinical outcome of refractory lymphoma patients (215-218). Expression of P-gp has been found in all histological types of NHL (219). Clinical trials combining chemotherapy with resistance modifiers have provided evidence for the role for P-gp in drug resistance in NHL (220-222). However, some reports have indicated a lack of correlation between clinical response and P-gp expression (29, 216, 223-225), possibly because MDR is mainly implicated in acquired drug resistance in lymphomas (226, 227). Thus, upregulation of P-gp is not consistently associated with chemoresistance in NHL, indicating the existence of additional drug-resistant pathways and mechanisms (15, 16).

Upregulation of the PI3K/Akt pathway can influence MDR in lymphoma. PI3K/Akt inhibition correlates with downregulation of NFκB activity and reduced P-gp function (228). PI3K/Akt activity was higher in drug-resistant lymphoma cell lines than in sensitive cells, and PI3K/Akt inhibitors inhibited P-gp function and increased sensitivity to chemotherapeutics in drug-resistant cell lines. Upregulation of the adenosine triphosphate-binding cassette drug transporter, ABCG2, in DLBCL correlated inversely with the disease-free survival (229). Activated hedgehog (Hh) signaling stimulated high-ABCG2 expression in DLBCL through direct

upregulation of ABCG2 gene transcription (230). Activation of Hh signaling in DLBCL cell lines led to co-upregulation of Bcl-2 and ABCG2, which was associated with increased resistance to chemotherapeutics. In addition to P-gp, the lung-resistance protein (LRP) is associated with MDR in lymphoma. LRP was first identified in a non-P-gp-multidrug-resistant lung cancer cell line (231). LRP is the major protein component of vaults, which are complex ribonucleoprotein particles located primarily in the cytosol and nuclear membrane and mediate nucleocytoplasmic transport (232, 233). Upregulation of LRP is associated with resistance to multiple chemotherapeutics (234, 235). High LRP expression was associated with more aggressive lymphomas and a lower response rate to chemotherapy than LRP-negative patients (236).

1.2.14 Drug metabolizing pathways

GSTs detoxify electrophilic chemotherapeutics, such as alkylating agents (166-171). GSTs act by promoting direct binding of drugs to alkylating agents and steroids and can also neutralize free radicals generated by anthracyclines (237-239). Drug resistance in lymphoma has been associated with an increase in glutathione content or GST activity (240-242). The GST-π isozyme is elevated in lymphoma cell lines resistant to anticancer agents (170). GST- π expression has been reported to have prognostic significance in DLBCL (243).

Glutathione S-transferase P1-1 (GSTP1-1) is a phase II detoxifying enzyme and plays a role in resistance to chemotherapeutics. GSTP1-1 may be a prognostic factor in late stage NHL (243, 244), since survival times were 64 and 25 months for the low and high GSTP1-1 groups, respectively. One strategy to overcome drug resistance would consist of treating relapsed NHL patients concomitantly with chemotherapeutics and GSTP1-1-specific inhibitors.

1.2.15 MAP kinase pathway

The MAP kinase signaling pathway may influence the sensitivity of B-lymphoma cells to chemotherapeutics. The contribution of the MAP kinase pathway and mitochondrial apoptotic pathways was studied in a panel of human B lymphoma cell lines exhibiting varying degrees of drug resistance and Bcl-2/Bax expression (245). Mitochondrial dysfunction was induced in these cells by the mitochondrial toxicants, carbonyl cyanide m-chlorophenylhydrazone (mClCCP) and antimycin A. The drug-resistant lines had higher Bcl-2/Bax expression ratios and were less sensitive to mitochondrial toxicant-induced apoptosis than the sensitive cell lines. Treatment with mitochondrial toxicants led to the activation of the MAP kinase pathway in only the drug-sensitive lines. Specific inhibition of the MAP kinase pathway augmented baseline and mClCCP-induced apoptosis, indicating that differential sensitivity to mitochondrial toxicants in B lymphoma cells involved regulation by MAP kinases.

1.2.16 Tyrosine protein kinases

Oncogenic tyrosine kinases regulate multiple signaling pathways involved in both cell survival and resistance to chemotherapeutics (246-252). Binding of antigen to the B-cell receptor (BCR) activates phosphorylation of Src family kinases (SFK), which is followed by the activation of MAP kinase, PI3kinase and NFκB pathways (253) resulting in B cell activation and survival (254, 255).

Over one-third of DLBCL patients tested expressed active SFKs in their tumors and thus may be candidates for treatment with the SFK inhibitor, dasatinib (256). Dasatinib is dual-kinase inhibitor that is currently approved for use in chronic myelogenous leukemia (257). In DLBCL cell lines, sensitivity to dasatinib varied by 400-fold, and resistance to dasatinib was associated with the dysregulation downstream of BCR activation.

The anaplastic lymphoma kinase (ALK) is a receptor tyrosine kinase involved in glucocorticoid-resistance in lymphomas (258). The glucocorticoids, prednisolone, and dexamethasone induce cell-cycle arrest and apoptosis in lymphoid cells and are included in chemotherapeutic regimens for lymphomas (259, 260). Unfortunately, glucocorticoid resistance commonly occurs in lymphomas (261-264). In about two-thirds of anaplastic large-cell lymphoma (ALCL), a rare type of NHL, a fusion of the nucleophosmin and ALK genes by the t(2;5) chromosomal translocation, gives rise to a hybrid NPM–ALK protein (265). Dysregulation of ALK caused by fusion to NPM is a causative factor in both ALCL and DLBCL (266-270). Abnormal activation of ALK is the result of the fusion of the N-terminal NPM partner encoding an oligomerization motif to activate the kinase domain of the ALK protein, which is critical for resistance to glucocorticoids (271-273).

1.2.17 p53 tumor suppressor gene

p53 mutations are often associated with decreased sensitivity to chemotherapeutics (274, 275), more aggressive clinical course (276) and higher relapse (16, 277-280). Lymphomas with a p53 mutation were more likely to be drug-resistant than those with normal p53 and to have a shorter progression-free survival (16).

The BH3-only genes, Puma and Noxa, are direct transcriptional targets of p53. The combinatorial action of the p53 target genes, Puma and Noxa, is important for the induction of apoptosis by chemotherapeutics in lymphoma cells (281). In nontransformed lymphoid cells, the loss of Puma and Noxa induced as much resistance to chemotherapeutics as loss of p53 itself.

1.2.18 Proteasome

The 26S proteasome complex is a large multisubunit catalytic complex that degrades ubiquitinated proteins (282). Proteasome inhibition has emerged as a new therapeutic option in lymphoma (283). The pharmacological proteasome inhibitor (PI), bortezomib (PS-341, Velcade) has shown efficacy against NHL through disrupting the equilibrium between protein biosynthesis and degradation (282, 284-286). Preclinical studies have demonstrated that proteasome inhibition potentiates the activity of other chemotherapeutics (287, 288). However, not all lymphomas are bortezomib sensitive, and acquired resistance to bortezomib can occur (284). Although bortezomib has single-agent efficacy in patients with relapsed or refractory MCL (289-292), about 40–50% of patients develop bortezomib-resistant disease. Bortezomib-resistant lymphoma cell lines exhibited residual proteasome activity in the presence of bortezomib (293), possibly due to increased expression of the b5, b2 and b1/b5 subunits of the proteasome. Alternative proteolytic systems may take the place of the proteasome leading to resistance to bortezomib (294-296). Targeting the PI3K/Akt signaling pathway may be a strategy to treat bortezomib resistant MCL, since the dual PI3K and mTOR inhibitor NVP-BEZ235 overcame bortezomib resistance in MCL cells. Activation of the endoplasmic reticulum (ER) stress pathway is correlated with resistance to doxorubicin-containing chemotherapy regimens, such as R-CHOP, in DLBCL patients. The 78-kDa glucose-regulated protein (GRP78), also known as immunoglobulin heavy chain binding protein, is an ER stress sensor commonly overexpressed in DLBCL that plays a role doxorubicin- and bortezomib-resistance (297). Small-interfering RNA silencing of Bip/GRP78 overcame bortezomib resistance (298).

1.2.19 Epigenetics

Epigenetics plays a critical role in many pathological processes of cancer (299). Histone deacetylases (HDACs) play a central role in cancer epigenetics (300). HDACs catalyze the removal of acetyl groups from core histones, which leads to the compaction of chromatin and repression of transcription (301). HDACs have been implicated in promoting drug resistance in B-cell malignancies (302, 303). Thus, HDAC inhibitors (HDIs) are being investigated as a new therapeutic approach to treat B cell lymphomas (304, 305). HDI-mediated inhibition of HDACS results in increased histone acetylation, which can reactivate silenced genes leading to the reversion of drug resistance (306-310).

Preclinical studies revealed synergistic interactions between proteasome inhibitors (PIs) and HDIs in lymphoma (311, 312). Coadministration of subtoxic concentrations of PIs with HDIs (vorinostat) synergistically increased apoptosis in both GC- and ABC-DLBCL cells, suggesting that a strategy using irreversible PIs to enhance the activity of HDIs might be effective in DLBCL. In other examples, HDIs reversed mTOR (mammalian target of rapamycin) resistance through a phosphatase that antagonized mTORC2 activation (84), suggesting a combination of HDI and mTOR inhibitors as a strategy for overcoming mTOR resistance in DLBCL. The coadministration of HDIs with rituximab may be a strategy to reverse rituximab resistance in B-cell lymphomas (313). HDIs enhanced the cytotoxic activity of rituximab by upregulating expression CD20 antigen on lymphoma cells.

1.2.20 MSI instability

MSIs are repetitive DNA sequences. Within MSIs, DNA polymerases are subject to slippage, and misalignments can form between the template and nascent strands. Mismatch repair (MMR) corrects these strand misalignments during DNA replication. MSI is a sign of deficient MMR

processes (314-318). In NHL, MSI may serve as a MMR biomarker that predicts lymphoma response to chemotherapy (319). MSI was found in 14% of tumors in NHL patients. Response to chemotherapy and outcomes were significantly worse in those NHL patients with MSI tumors.

1.2.21 Stromal influences

Stromal cells are an essential component of the bone marrow microenvironment that influences and supports tumor growth and survival (320-323). Resistance to chemotherapy can result from cytokines and growth factors released from stromal cells (320, 321). Bone marrow stroma can provide a protective 'sanctuary site' for lymphoma cells during chemotherapy (324), thus having an impact on the outcome of chemotherapy in DLBCL (325). Secretion of interleukin-4 and the integrin ligand VCAM-1 from stromal cells increase survival and rescue B cells from chemotherapy-induced apoptosis (326, 327). Another factor released from bone marrow stromal cells is the lymphoma cell adhesion induced B cell-activating factor (BAFF) protein, a member of the TNF superfamily of cytokines, which promotes B-cell activation, proliferation, and differentiation, thus enhancing B-lymphocyte survival (328-331). BAFF receptors are expressed on lymphomas originating from diverse subclasses of B cell lineages (332). Increased levels of BAFF were present in serum from NHL patients (332). Small-hairpin RNA depletion of BAFF increased sensitivity of lymphoma cells to chemotherapy and overcame stroma-mediated drug resistance.

Stroma-produced survival signals can influence the expression, conformation, and protein–protein interactions of Bax and Bcl-xL, which can then influence the sensitivity of a B cell lymphoma to chemotherapeutics (76, 333-337). Stroma-mediated activation of CD40 upregulated Bcl-xL protein levels via activation of NFκB. VCAM-1-mediated signals repressed

conformational changes in Bax protein and prevented etoposide-induced formation of Bax–Bcl-xL complexes. Stromal upregulation of IL-6 may contribute to the intrinsic chemoresistance commonly found in both primary and metastatic malignancies (338, 339). Additionally, tumor-directed inflammatory responses originating in the stroma that release IL-6 may reduce the efficacy of genotoxic agents.

Lymphocytes home into tissue stromas, which guide the lymphocytes by secreting chemokines and expressing ligands for lymphocyte adhesion molecules. In B cell lymphomas, the tumor cells retain the trafficking and homing ability of their normal counterparts (340-343). Lymphoma cells are directed to supporting stroma by chemokine receptors and adhesion molecules, where they receive survival and drug-resistance signals (344, 345). Stromal cells release chemokines, such as CXCL12 and CXCL13, which provide guidance for localizing B cells within lymph-node compartments (323, 346, 347). Lymphocyte homing requires the cooperation between chemokine receptors and adhesion molecules, such as integrins, CD44 and L-selectins (348). Moreover, accessory cells, including CD68þ macrophages and T cells, in the lymphoma microenvironment can influence the clinical outcome (349-351), indicating that crosstalk between lymphoma and stromal cells plays an important role in lymphoma progression and chemoresistance.

FL patients frequently are initially sensitive to chemotherapy but then relapse. Highly tumorigenic FL cells exhibiting a cancer stem cell-like phenotype (FL-SC) were found to interact with follicular dendritic cells in a CXCL12/CXCR4-dependent manner to resist chemotherapeutics, indicating an important role for FL-SC and niche cell-signaling in maintaining drug resistance in FL (352).

1.2.22 Other

1.2.22.1 Sphingosine kinase

Upregulation of sphingosine kinase 1 (SphK1) frequently occurs in lymphomagenesis. SphK1 is associated with resistance to chemotherapy and radiotherapy (353, 354). SphK1 controls the 'sphingolipid rheostat' by catalyzing the formation of the survival molecule, sphingosine-1-phosphate, at the expense of the proapoptotic molecule, ceramide (355). SphK1 protein and mRNA levels showed increasing expression with increasing clinical grade of NHL (356).

1.2.22.2 Geranylation

Inhibition of protein prenylation (geranylgeranylation) can sensitize DLBCL to chemotherapeutics (357). Prenylation is a post-translational hydrophobic modification of proteins that facilitates the attachment of proteins to membranes. The lipid isoprenoid acts as a lipid anchor, which is essential for proper protein localization and biological function (358-360). Treatment with simvastatin, an inhibitor of protein farnesylation and geranylgeranylation, sensitized CHOP-resistant DLBCL cells to cytotoxic treatment (357). Coadministration of protein geranylgeranylation inhibitors and conventional chemotherapeutics thus may be a strategy for treating patients with CHOP refractory DLBCL.

1.2.22.3 Zinc transporter

Gallium nitrate is a clinically active agent in the treatment of lymphoma (361-365). Gallium binds to transferrin in the circulation, which targets it to transferrin receptors that are expressed on lymphoma cells (366-371). Gallium also acts on zinc metabolism pathways (372). Unfortunately, resistance to gallium can occur, which is caused by the upregulation of metal-responsive transcription factor-1 activity and metallothionein expression (372).

Immunohistochemical staining of lymphomas showed that the metallothionein protein is variably expressed in different lymphomas.

1.2.22.4 PRDM-1

The positive regulatory domain I (PRDM1) protein regulates the differentiation of mature B lymphocytes to plasma cells (373, 374). The PRDM1 gene encodes 2 isoforms, PRDM1α and PRDM1β that are regulated by NFκB (375, 376). Those DLBCL cases that expressed PRDM1 displayed more aggressive behavior and a poorer patient outcome (377). PRDM1β expression thus might serve as a prognostic marker for drug resistance in some types of DLBCL.

1.2.22.5 ALDH

The intracellular enzyme retinaldehyde dehydrogenase (ALDH) promotes resistance of MCL to chemotherapeutics (378-380). ALDH is a cytosolic enzyme required for the biosynthesis of all-trans-retinoic acid and is highly expressed by normal hematopoietic and neural stem cells (381, 382). ALDH is expressed in B cell lymphomas (383, 384) and can induce cyclophosphamide resistance in lymphoma cell lines (385-389).

1.3 Summary and conclusions

Both intrinsic genetic alterations as well as chemoprotective microenvironments can play roles in the cellular response of B cell lymphomas to chemotherapeutics. Given the genetic diversity of B cell lymphomas and differential antigen expression patterns across lymphoma subtypes, it is unlikely that a single small molecule or antibody-based therapeutic will effectively treat all categories of NHL. Overcoming drug resistance to current chemotherapeutic regimes in B-cell

lymphomas will require multitargeted combinatorial therapies to restore apoptotic pathways in tumor cells and inhibit prosurvival signaling from the stroma environment.

With the exception of those patients eligible for allogeneic or autologous stem-cell transplantation, combination chemotherapy offers a potentially curative option for a subset of DLBCL patients (172). However, responses to current combination chemotherapy regimens (e.g. rituximab with cytoxan, hydroxyrubicin, oncovin, and prednisone) vary considerably depending on multiple factors, including disease stage and genetic profile, among others. In particular, patients with the ABC-DLBCL subtype, which is NFκB-dependent (37, 390), appear to have a significantly worse prognosis than other subtypes (391). Collectively, these considerations have motivated the search for more effective combinatorial treatment strategies in DLBCL that are pathway-targeted to specifically target tumor cells without toxicity to nonmalignant cells. Multitargeted combinatorial experimental therapies composed of new targets and conventional chemotherapeutics may provide more immediate hope for relapsed patients who have failed current chemotherapies. For example, preclinical studies have documented synergistic interactions between PIs, such as bortezomib and HDAC inhibitors in diverse malignant cell types (311, 392, 393). Targeting CD40 with dacetuzumab enhanced the antitumor activity of rituximab (CD20) in cell line and xenograft NHL models (394). In MCL, a sequence-dependent synergistic effect was observed with PIs in combination with cytarabine (395). Tipifarnib and bortezomib combination was well-tolerated and produced clinical responses in refractory acute leukemias (396). Multilevel inhibition of the PI3K/Akt/mTOR and cdc2/cdk1 cell-cycle pathways may be more effective in treating DLBCL patients that present with overactive Akt and cdc2/cdk1 (397).

Thus, understanding genotype-response relationships in NHL will be important for the effective use of new targeted therapies in the clinic. Responsiveness to multitargeted therapies will be predicted based on molecular markers to predefine patients who will most likely benefit from these targeted therapies. For instance, 'BH3 profiling' can identify those cells that are sensitive to the Bcl-2 antagonist ABT- 737 (398). Determining the activity of the NFκB pathway in DLBCL tumor biopsies by GEP can predict responsiveness to the IκB kinase inhibitor PS1145. Future approaches to NHL treatment will employ molecular signatures identified through GEP to provide prognostic information and to identify therapeutic targets in patients who relapse or those presenting with high risk disease to guide clinicians in designing a personalized approach to combinatorial molecular therapies.

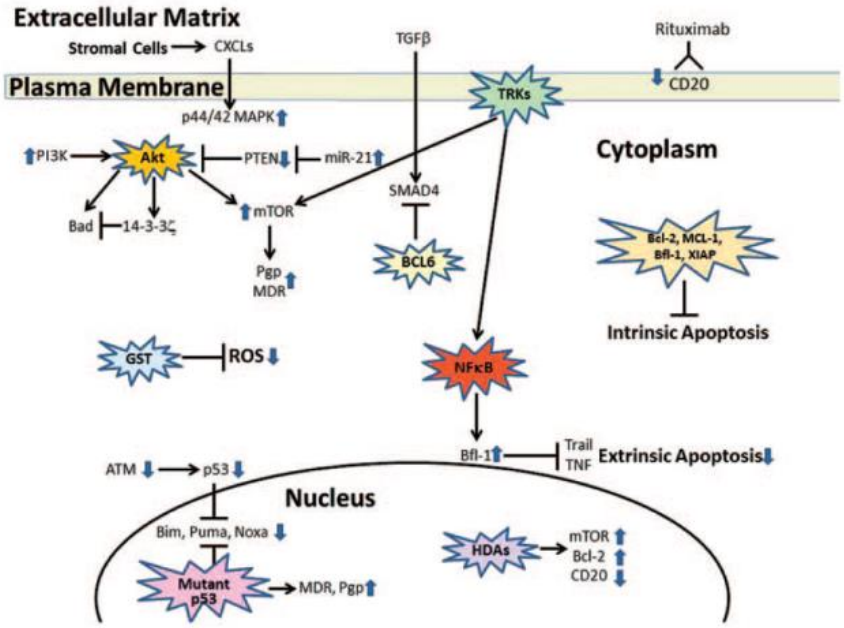

Figure 1.1 Schematic representation of drug resistance pathways in B-cell lymphomas. PI3K/Akt is frequently activated, which leads to increased mTOR activity stimulating upregulation of multidrug resistance pumps (MDR, P-gp). Akt phosphorylates Bad and 14-3-3z, leading to binding and sequestration of the proapoptotic protein Bad and blocking to apoptosis. Upregulation of antiapoptotic proteins (Bcl-2, Mcl-1, XIAP, Bfl-1) can block chemotherapeutic-induced intrinsic apoptosis. The Akt pathway can be activated by upregulation of miR-21, which represses expression of the Akt-negative regulator, PTEN. Activation of tyrosine receptor kinases (TRKs) can induce drug resistance by activating Akt through mTOR. TRKs can also activate NFκB, which upregulates Bfl-1 resulting in blocking of TNF- or Trail-induced extrinsic apoptosis. Upregulation of BCL6 blocks TGFβ-signaling through SMAD4. Glutathione transferases (GSTs) can suppress oxidative stress caused by reactive oxygen species (ROS) that are induced by chemotherapeutics. Histone deacetylases (HDACs) can promote resistance to rituximab combinatorial chemotherapies (R-CHOP) by upregulating mTOR and Bcl-2 and downregulating CD20. Mutation in the p53 gene causes defects in the DNA damage response and upregulation of multidrug resistance pumps (MDR, P-gp). Mutations in Atm can cause deficiencies in the p53-induce DNA damage response, leading to lack of expression of proapoptotic BH3 proteins (Bim, Puma, Noxa) and blocking of intrinsic apoptosis. Downregulation of CD20 through epigenetic silencing can lead to rituximab resistance.

1.4 Nuclear factor erythroid–related factor 2 (Nrf2) regulatory network

The Nrf2, the master regulator of oxidative stress, activates the transcription of over 200 cytoprotective genes (399). Under basal condition, Nrf2 is tightly under regulation of ubiquitin proteasome system. The Kelch-like ECH-associated protein 1 (Keap1)–cullin3 (Cul3)–ring-box1 (Rbx1) E3-ligase is the primary regulator of Nrf2. However, E3 ubiquitin ligases beta-transducin repeat-containing E3 ubiquitin protein ligase (β-TrCP) and synoviolin (Hrd1) are Keap1-independent negative regulators of Nrf2 system (400). Several antioxidant pathways with complementary functions are under control of Nrf2, including glutathione (GSH) production and utilization, thioredoxin (TXN) production and ultilization, and NADPH production. NAD(P)H: quinone oxidoreductase 1 (NQO1) and heme oxygenase (HMOX1) are other antioxidant enzymes that are controlled by Nrf2 (401). Notably, there several other Nrf2 target genes that are not involved in antioxidant functions. Altogether, the Nrf2 regulatory network protects against many diseases including neurodegenerative diseases, aging, cardiovascular disease, inflammation, and even initiation of many types of cancers (400, 402). Despite contribution to the maintenance of cellular homeostasis, uncontrolled Nrf2 hyper-activation is considered as the dark side of Nrf2 that promotes tumor growth and causes resistance to chemotherapeutics (403-405).

Interestingly, there are interactions between pathways involved in drug resistance in B-cell lymphomas (Figure 1.1) and Nrf2 regulation. PI3K/Akt phosphorylates Nrf2, which potentially is an important determinant of Nrf2 activity (406). Several studies demonstrated that PI3K/Akt activity is required for Nrf2 activation in different cancer cell lines (407, 408). Nrf2 upregulates anti-apoptotic protein Bcl-2 expression promoting cancer cell survival and chemoresistance (409). On the other hand, dissociation of Bcl-2 from the Nrf2 inhibitor, Keap1, leads to greater survival and chemoresistance (410). A recent study showed that TGF-β promotes tumor growth

and resistance to radiotherapy in A549 human lung cancer cells via ROS-mediated stimulation of Nrf2 activity (411). Tumor suppressor p53 suppresses the Nrf2-dependent transcription of ARE-containing promoters and is therefore a transcriptional repressor of Nrf2 target genes (412, 413). By contrast, the cyclin-dependent kinase inhibitor p21 which is under control of p53 could upregulate Nrf2 activity. p21 inhibits the degradation of Nrf2 leading to upregulation of antioxidant genes (414). Negative or positive regulation of Nrf2 by p53 may trigger apoptosis or promote survival in cancer cells (412).

Here, we will focus on the role of Nrf2 in metabolic-orientated regulation of oxidative stress in DLBCL. In chapter II, we will explore the regulatory effect of Nrf2 on glucose-6-phosphate dehydrogenase (G6PDH), where during oxidative stress, Nrf2 upregulates G6PDH providing reducing equivalents (NADPH) for the maintenance of a pool of reduced mitochondrial glutathione (GSH) to balance the redox state, which has a crucial role in cellular signaling and antioxidant defenses (415-417). We hypothesized that a Nrf2/G6PDH cascade is dysregulated in drug resistant DLBCL cells and manipulation of this cascade may change the tolerance of those cells to chemotherapy.

In chapter III, we will describe an approach to develop drugs that focus on the cause of chemoresistance. We will define a novel non-toxic rifamycin derivative (RTI-79) as a potent chemosensitizer effective in multiple types of cancer cells. We will explore the mechanisms of action of RTI-79, where inhibition of Nrf2 plays a pivotal role in oxidative stress-mediated reversal of drug resistance in cancer cells.

Finally, in chapter IV we will include the research summary, overall conclusion, and future direction.

CHAPTER II

GLUCOSE-6-PHOSHPHATE DEHYDROGENASE MEDIATES CHEMORESISTANCE IN DIFFUSE LARGE B CELL LYMPHOMA *

2.1 Introduction

Non-Hodgkin's lymphomas (NHLs) are a group of malignancies displaying many different clinical behaviors and thus prognoses (418). The majority (80-85%) of NHL arise from B cells that undergo clonal expansions during different stages of differentiation (419-421). DLBCL is an aggressive subtype of NHL (422, 423). The anthracycline-based CHOP chemotherapy regimen (consisting of cyclophosphamide, doxorubicin, vincristine, and prednisone) in combination with rituximab (anti-CD20) has been the most effective treatment for DLBCL for over two decades (424). Unfortunately, approximately half of DLBCL patients develop a chemoresistant disease with a high mortality rate (425-428).

Thus, characterization of the molecular basis of CHOP resistance is urgently needed to develop a rational strategy to overcome drug resistance (429, 430). Drug-sensitive cancer cells frequently exhibit higher basal ROS levels than their normal counterparts, partly due to oncogenic stimulation, increased metabolic activity, and mitochondrial malfunction (431-433). However, chemoresistant cancer cells frequently display upregulation of antioxidant pathways to antagonize ROS, thus making them resistant to anti-cancer agents that induce oxidative stress (401, 434-436).

* Reprinted from "Glucose-6-phosphate dehydrogenase mediates chemoresistance in diffuse large B cell lymphoma" by Seyed Hossein Mousavi-Fard, Timothy Davis, Deeann Wallis, Jim Sacchettini, and Steve A Maxwell1, 2017. Manuscript submitted for publication to The FASEB Journal.

Nrf2 is an ROS sensor critical in regulating cellular redox status and activates expression of genes encoding for various antioxidant and cytoprotective enzymes (437-439). Normally, Keap1 maintains low levels of Nrf2 by anchoring it within the cytoplasm and directing it for ubiquitination and proteasomal degradation (438, 440). High levels of ROS inhibit the enzymatic activity of Keap1, leading to decreased Nrf2 ubiquitination and degradation, and thus increased Nrf2 stability (441). As a result, Nrf2 migrates into the nucleus and works with other transcription factors to transactivate the antioxidant response elements (AREs) of cytoprotective genes, including G6PDH, to antagonize ROS and reduce oxidative injury (442-445). Constitutive dysregulated activation of Nrf2 can lower ROS levels causing resistance to chemotherapeutic-induced oxidative stress (446).

Activation of Nrf2 results in upregulation of G6PDH expression, indicating a pivotal contribution of Nrf2 in metabolic control of the redox state (442-444). G6PDH is the rate-limiting enzyme of the pentose phosphate shunt (PPP) (447-449), which is an important pathway for recycling of cellular glutathione (GSH), a key scavenger of ROS (450). In the oxidative phase of the PPP, glucose 6-phosphate is irreversibly converted into ribulose 5-phosphate and CO_2, thereby generating NADPH, a redox cofactor for many antioxidant enzymes (451). The NADPH produced is also used by glutathione reductase to reduce glutathione disulfide to glutathione (GSH). Increased G6PDH activity generates more reducing equivalents (NADPH) that can promote increased GSH generation through the PPP. The PPP is activated by Nrf2, thus generating more GSH, which scavenges ROS, thereby promoting reductive stress (decrease in ROS) and resistance to chemotherapeutics (416, 452). Consistent with this model, drug resistance was reversed by suppression of Nrf2 activity combined with depletion of GSH in adenocarcinoma cells (453).

We report here elevated Nrf2 and G6PDH activities in CHOP-resistant DLBCL cells. We hypothesized that a more reduced intracellular state (lower expression of ROS) promotes CHOP resistance in DLBCL cells. We generated CHOP-resistant cells from CHOP-sensitive DLBCL lines as a model to test our hypothesis (82, 83). We report here that CHOP-resistant DLBCL cells have a lower oxidative state (lower ROS) than their more drug-sensitive counterparts. Our data suggest a CHOP-resistance model in DLBCL whereby upregulated Nrf2 and G6PDH activities cause increased GSH levels that scavenge and reduce ROS levels, thus increasing tolerance to CHOP. Moreover, we present evidence that acquisition of CHOP resistance arises from the emergence of a population of $Nrf2^{High}/G6PDH^{High}/ROS^{Low}$ DLBCL cells, which survive repeated exposures to CHOP therapy.

2.2 Materials and methods

2.2.1 Antibodies and reagents

Primary antibodies used were rabbit monoclonal anti-G6PDH (D5D2, Cell Signaling**,** Boston, MA, USA), rabbit monoclonal anti-Nrf2 (ab62352, abcam**,** Cambridge, MA, USA), and mouse monoclonal anti-actin (ab3280, abcam, Cambridge, MA, USA). Secondary antibodies used were polyclonal goat anti-rabbit immunoglobulins /HRP and polyclonal goat anti-mouse immunoglobulins/HRP (Dako, Carpinteria, CA, USA). Trans-Dehydroandrosterone (DHEA) was obtained from Sigma-Aldrich (St. Louis, MO, USA). The components of CHOP (cyclophosphamide, doxorubicin, vincristine, and prednisone) were obtained from Sigma-Aldrich (St. Louis, MO, USA).

2.2.2 Cell lines and culture conditions

Human-derived CRL-2631 and SU-DHL-10 DLBCL cell lines were obtained from the American Type Culture Collection. Variants with relatively more tolerance to CHOP were derived by on and off cycles of CHOP treatment as described (83). The proportion of the four components used in CHOP treatment of DLBCL was consistent with the standard dosage CHOP therapy. The composition of CHOP consisted of cyclophosphamide, doxorubicin, vincristine, and prednisone at the clinical ratio of 80/5.5/0.16/11.1, respectively (424). Similar to patient CHOP regimen, cells were subjected to cycles of 5 days of CHOP treatment followed by 21 days of recovery in the absence of CHOP. Cells were initially selected with several cycles of 80 ng/ml CHOP. Greater than 99.9% of the cells died within 5 days of the first CHOP cycle, but a few cells were able to grow and proliferate. After several on-off cycles in 80 ng/ml CHOP, the viable cells were treated with several on-off cycles of a higher CHOP dose (160 ng/ml). Cycling with CHOP was continued until a cell population emerged that could survive and recover from 5-day exposures to 640 ng/ml CHOP (83). The CHOP-sensitive CRL-2631 (2631) and SU-DHL-10S (10S), and their relatively more CHOP-resistant G3 and SU-DHL-10R (10R) derivatives, respectively, were maintained in RPMI medium 1640 (Gibco; Thermo Fisher Scientific, Waltham, MA, USA) supplemented with 10 mM HEPES, 1.5 g/liter sodium bicarbonate, 1.0 mM sodium pyruvate, 4.5 g/liter D-Glucose, antibiotic-antimycotic and 10% Fetal Bovine Serum (Gibco; Thermo Fisher Scientific, Waltham, MA, USA).

2.2.3 Western Blotting

Whole cell lysates were prepared by disrupting cells in a 2X Laemmli Sample Buffer (Bio-Rad Laboratories, Hercules, CA, USA) supplemented with 2-Mercaptoethanol (Sigma-Aldrich, St. Louis, MO, USA) and Protease/Phosphatase Inhibitor Cocktail (Cell Signaling**,** Boston, MA,

USA) at 95°C for 10 min. Protein concentrations were determined using the Quick Start Bradford protein assay kit (Bio-Rad Laboratories, Hercules, CA, USA). Proteins were loaded (10 µg/lane) onto 10% precast polyacrylamide Mini-PROTEAN Gels (Bio-Rad Laboratories, Hercules, CA, USA) according to the manufacturer's instructions. Proteins were transferred from SDS gels to Immobilon PVDF transfer membranes (EMD Millipore, Billerica, MA, USA). Blots were pre-blocked with TBS-T20 buffer (0.1% Tween-20 and 5% nonfat dried milk in TBS) for 1 hour at room temperature. Blots were then probed with primary antibody (anti-G6PDH; 1:1000, anti-Nrf2; 1:1000, anti-actin; 1:10000) in TBS-T20 buffer overnight at 4°C. Membranes were then washed three times each for 10 min in TBS-T20 and incubated with the appropriate HRP-conjugated secondary antibody (anti-mouse; 1:5000; anti-rabbit; 1:1000) in TBS-T20 buffer for 2 hours. Membranes were washed three times each for 2 hours with TBS-T20 buffer. Membranes were finally treated with Clarity Western ECL substrate (Bio-Rad Laboratories, Hercules, CA, USA) for 5 min and signal detection was performed on Blue Basic Autoradiography Films (GeneMate; Bioexpress, Kaysville, UT, USA).

2.2.4 Measurement of intracellular GSH levels

Intracellular GSH was measured using a monochlorobimane to react with GSH in intact cells to generate a blue fluorescent product (Cayman Chemical Co., Ann Arbor, MI, USA). Cells were treated with DMSO or DHEA and were cultured in a CO_2 incubator overnight at 37 °C. The next day, samples were prepared according to the manufacturer's protocol and 100 µl of Substrate Solution added to 1 million cells. After 30 min incubation at 37 °C, levels of GSH were measured in whole intact cells using the LSRFortessa X-20 flow cytometer (Becton Dickinson, Franklin Lakes, NJ, USA).

2.2.5 Measurement of Intracellular reactive oxygen species' levels

Reactive Oxygen Species detection reagents were purchased from Thermo Fisher Scientific (Waltham, MA, USA). Total ROS levels were measured using CellROX Deep Red Reagent. Superoxide species were detected using MitoSox. Hydrogen peroxide species were detected using Dihydrocalcein AM. Hydroxyl radicals were detected using 3'-(p-Aminophenyl) fluorescein (APF). Cells were treated with drugs and cultured in a CO_2 incubator overnight at 37 °C. The fluorescent ROS indicators were added to cells at a final concentration of 5 μM and samples were incubated for 60 minutes at 37°C. FACS measurements were performed directly on the CellROX-, MitoSox-, Dihydrocalcein AM- or APF-labeled cells in phenol red-free RPMI using a LSRFortessa X-20 flow cytometer (Becton Dickinson, Franklin Lakes, NJ, USA).

2.2.6 G6PDH Assay

G6PDH activity was determined by employing a Glucose-6-Phosphate Dehydrogenase Activity Assay Kit (Cayman Chemical Co., Ann Arbor, MI, USA) based on G6PDH's ability to reduce $NADP^+$ to NADPH, which then reacts with a detector to yield a fluorescent product (excitation: 530-540 nm, emission: 585-595 nm). Assays were performed according to the manufacturer's protocols.

2.2.7 Measurement of intracellular NADPH levels

The levels of cellular NADPH were determined by a NADP/NADPH Quantification Kit (Sigma-Aldrich, St. Louis, MO, USA). Cells were washed with 1X PBS and extracted according to the manufacturer's protocol. A Reaction Mix (containing NADP Cycling Buffer and NADP Cycling Enzyme Mix) was prepared and added to the cell lysates and standards. Finally, NADPH

developer was added to samples and NADPH levels were measured using a colorimetric plate reader at 450 nm.

2.2.8 Cell viability assay

Trypan blue staining was used to assess cell viability. Cells in suspension were mixed with an equal volume of 0.4% trypan blue stain (Gibco; Thermo Fisher Scientific, Waltham, MA, USA), loaded onto a hemocytometer (Bright-Line; Sigma-Aldrich, St. Louis, MO, USA), and cells counted using a microscope (Fisher Micromaster; Fisher Scientific, Pittsburg, PA, USA).

2.2.9 Isolation of low and high oxidative state CRL-2631 DLBCL cells

10 x 10^6 cells were incubated in 5 ml complete cell growth medium containing 5 μM CellROX Deep Red (Life Technologies; Thermo Fisher Scientific, Waltham, MA, USA) for 1 hour and then subjected to flow cytometry. Cells at the lower and higher extremes of the geometric means of the CellROX fluorescence were isolated by FACS sorting and propagated in culture. ROS levels were confirmed as high (2631Hi) or low (2631Lo) in the propagated populations by flow cytometry.

2.2.10 Stable short hairpin RNA (shRNA) knockdown of Nrf2 and G6PDH

Lentiviral particles expressing scrambled (SC-108080) or Nrf2 shRNA (SC-156128-V) or G6PDH shRNA (SC-60667-V) were purchased from Santa Cruz Biotechnology (Santa Cruz, CA, USA). Lentiviral transduction of G3 and 10R (ctrl shRNA or Nrf2 shRNA), and 2631Lo (ctrl shRNA or G6PDH shRNA) cells were performed following the manufacturer's protocol. Briefly, 10^6 cells in 1 ml of complete RPMI medium were plated onto 6-well plates. Next, transduction enhancer polybrene (SC-134220; Santa Cruz, CA, USA) was added to each well at

a concentration of 5 μg/ml, and 30 minutes later viral particles were added to each well at concentrations of 10 μl/ml (containing 50,000 transducing units). The following day, RPMI media containing viral particles were removed from the cells and replaced with fresh media. The day after, the media was removed and replaced with fresh media containing 5 μg /ml Puromycin dihydrochloride (SC-108071; Santa Cruz, CA, USA) to select the stable clones expressing corresponding shRNAs. The transduced cells were selected by puromycin selection, and subjected to Western blot to confirm Nrf2 and G6PDH knockdowns.

2.2.11 Statistical analysis

Data represent the mean ± SEM of results obtained from at least three independent experiments. The statistical package JMP 12 (SAS Institute Inc., Cary, NC, USA) was used for statistical analysis. Data were statistically assessed by paired t test (for conditions in which the same cell line was compared +/- treatments), and unpaired t test (for comparisons between different cell line derivatives). Also, bivariate analysis, and 1-way ANOVA using Tukey's HSD, or Fisher's test were used when appropriate, based on sample size.

2.3 Results

2.3.1 Differential expression of ROS in CHOP-sensitive and –resistant DLBCL cell lines

DLBCL cell lines with acquired resistance to CHOP were derived by repeated "on-off" exposures to increasing concentrations of CHOP as previously described (83). As shown in Figure 2.1A, two variant DLBCL cell lines (G3 and 10R) exhibiting significantly more tolerance to CHOP were generated from the parental CRL-2631 and SU-DHL-10 cell lines. The CHOP concentration of 640 ng/ml composition (see methods) was used in these experiments, which resulted in remarkable cell death in CHOP-sensitive cells after 72 hours of treatment. As shown

in Figure 2.1A, the more CHOP-sensitive 2631 cell line exhibited about 57.25% cell death after 72 hours in the presence of 640 ng/ml CHOP, whereas the more CHOP-resistant variant G3 cells continued to grow in the presence of CHOP for up to 72 hours. Similar to G3, 10R continued to grow under CHOP treatment. However, the rate of growth was slightly slower than G3 cells. In contrast, its parental 10S cell line displayed 94% cell death after 72 hours of CHOP treatment. The CHOP-resistant DLBCL lines consistently exhibited markedly lower levels of ROS than their more CHOP-sensitive parental lines as detected by the CellROX indicator (Figure 2.1B).

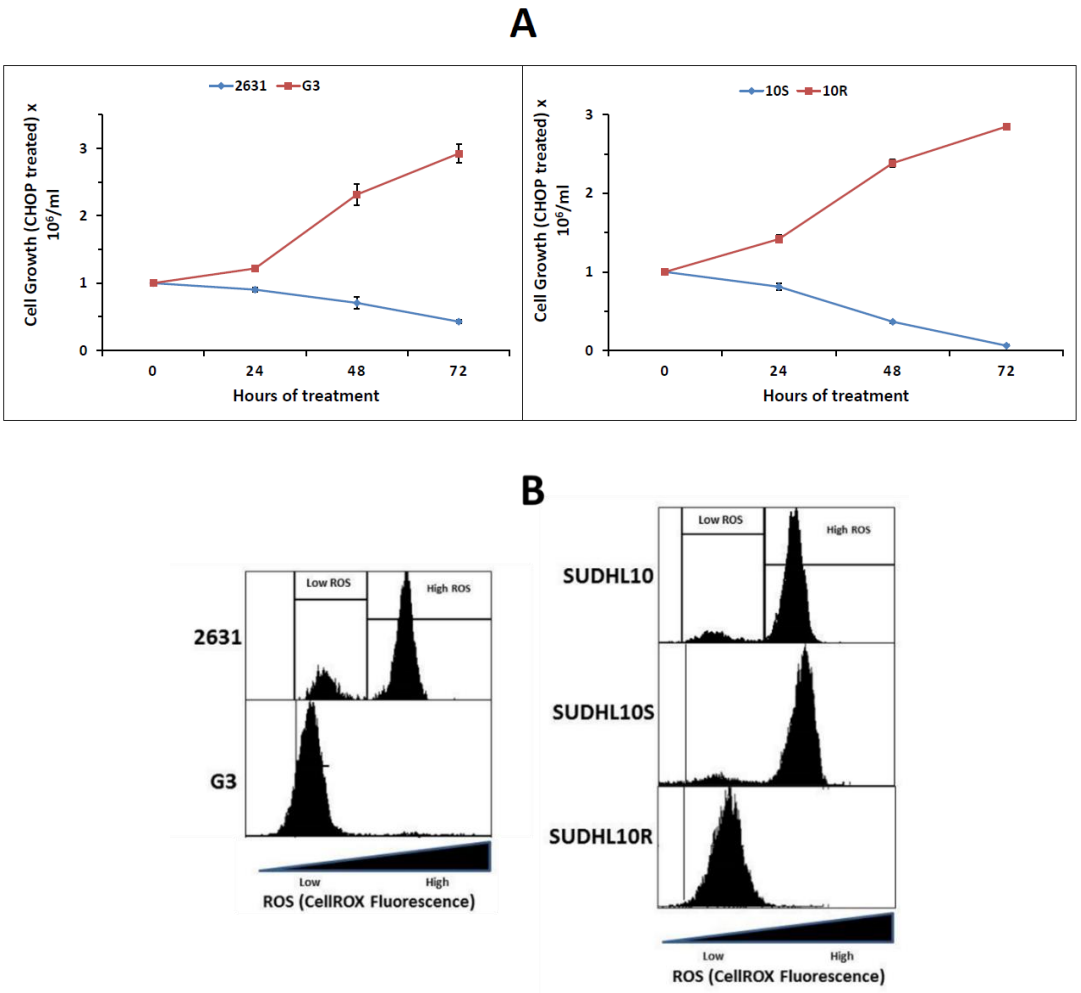

Figure 2.1 Differential expression of ROS in CHOP-sensitive and -resistant DLBCL cells. (A) 1 x 10^6 cells/ml were treated with CHOP (640 ng/ml) from 0 to 72 hours and viable cells quantified by trypan blue staining. G3 and 10R represent the more CHOP-resistant variants derived by repeated on-off CHOP treatment of the 2631 and 10S parental lines. (B) ROS levels were analyzed by FACS (1x 10^6 cells/ml) in the parental CHOP-sensitive (2631, 10S) and the more CHOP-tolerant (G3, 10R) variant DLBCL cells using the CellROX total ROS fluorescent indicator. The CHOP-resistant cell lines exhibited lower ROS levels as indicated by the shift in the geometric mean of the FACS peak toward the left of the FACScan compared to their more CHOP-sensitive parents.

2.3.2 Differential expression of Nrf2 and G6PDH proteins in CHOP-sensitive and resistant lymphoma cells

There are precedents indicating a functional communication between Nrf2 and metabolism. First, Nrf2-dependent protection against oxidative stress relies on an intact PPP, which provides crosstalk between metabolism and ROS detoxification (416). Second, Hepatitis B virus (HBV) upregulates G6PDH expression via HBx-mediated activation of Nrf2, implicating a potential effect of HBV on the reprogramming of the glucose metabolism in hepatocytes, which may be of importance in the development of HBV-associated hepatocarcinoma (454). Moreover, upregulation of the Nrf2/G6PDH pathway has been reported in development of chemoresistance in non-small cell lung carcinoma (455). We therefore conducted Western blotting to compare the expression of Nrf2 and G6PDH proteins in CHOP-sensitive 2631 and 10S lymphoma cells and their resistant derivatives, G3 and 10R, respectively. As shown in Figure 2.2 (top panels), expression of Nrf2 and G6PDH proteins was significantly lower in the CHOP-sensitive 2631 and 10S lines compared to the more CHOP-tolerant G3 and 10R derivatives. More specifically, Nrf2 expression was 92.2% less in 2631 relative to G3, and 95.21% lower in 10S compared to 10R, as normalized to actin. Expression of G6PDH was 68.72% lower in 2631 compared to G3, and 92.8% less in 10S relative to 10R.

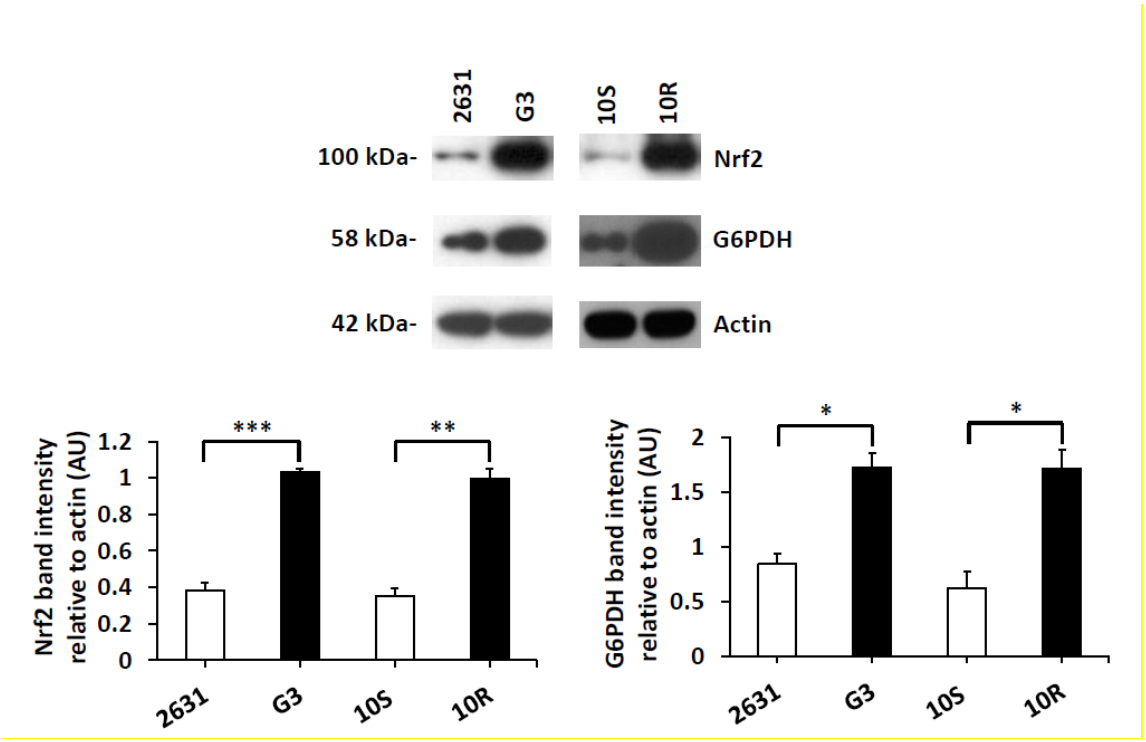

Figure 2.2 Differential expression of Nrf2 and G6PDH in CHOP-sensitive and -resistant

DLBCL cells. (*Upper panels*) Higher expression of Nrf2 and G6PDH proteins was observed by Western blot in CHOP-resistant G3 and 10R lymphoma cells than in the more CHOP-sensitive 2631 and 10S lines. Actin was used as loading control. (*Lower panel*) Quantification of Nrf2 and G6PDH protein expression was conducted by calculating the intensity (pixels) of Nrf2 and G6PDH bands relative to the intensity of actin band. * $p<0.05$, ** $p<0.01$, *** $p<0.001$

2.3.3 Chemosensitization of CHOP-resistant DLBCL via inhibition of G6PDH activity

Since CHOP-resistant DLBCL cell lines expressed markedly higher levels of G6PDH protein, we investigated the role of G6PDH activity in mediating tolerance to CHOP. More G6PDH activity was observed in CHOP-resistant lines G3 and 10R compared with their more CHOP-sensitive parents, 2631 and 10S, respectively (Figure 2.3A; 59.4 and 80.31% more, respectively), which correlated with the increased amounts of G6PDH protein expression in CHOP-resistant lines (Figure 2.2). However, the difference in G6PDH activity between 2631 cells and G3 cells (59.4%) was not as great as the difference in protein expression observed between the two cell lines (68.72%). Similarly, the difference between G6PDH activity and protein level between the 10S and 10R cell lines was 80.31 and 92.8%, respectively.

Cells were treated with the widely-used G6PDH inhibitor, Dehydroepiandrosterone (DHEA) (456-458), and their tolerance to CHOP determined by trypan exclusion viability assay. DHEA reduced the amount of G6PDH activity by 15.61 and 33.44% in G3 and 10R, respectively (Figure 2.3A). In addition, DHEA caused increased sensitivity to CHOP in G3 and 10R, as indicated by the 42.86 and 130.67% lower number of viable cells, respectively, after 72 hours of CHOP treatment compared to CHOP-treated only controls (Figure 2.3B). The growth rate of DMSO-treated control 2631, 10S, G3 and 10R cells were similar over the treatment period. DHEA or CHOP treatment alone did not cause any significant effects on G3 and 10R cell growth.

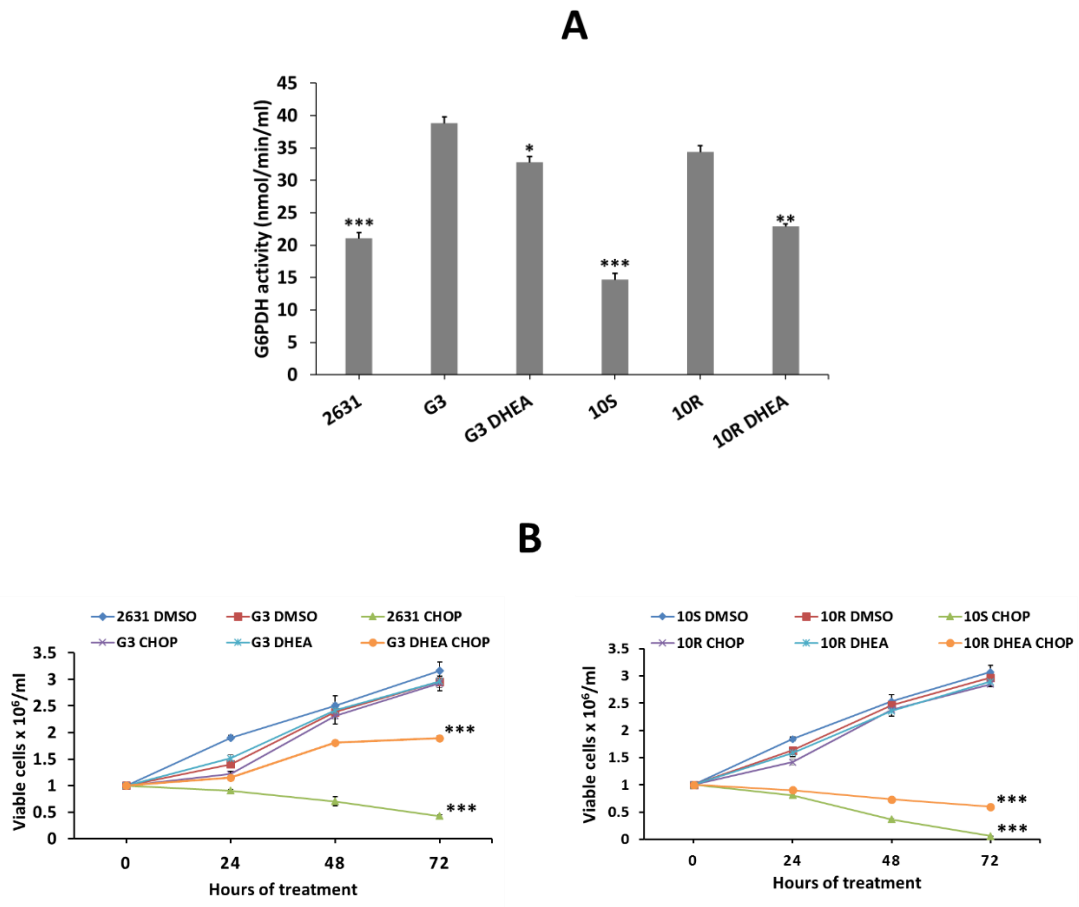

Figure 2.3 Chemosensitization of CHOP-resistant DLBCL cell lines by a G6PDH inhibitor. (A) G6PDH activity was confirmed higher in CHOP-resistant G3 and 10R than in their more sensitive parental cell lines, 2631 and 10S. Treatment of cells with 100 µM DHEA for 4 hours significantly lowered G6PDH activity in CHOP-resistant cell lines. (B) 100 µM DHEA was added to the CHOP cocktail and the growth of cells assayed after 24, 48, and 72 hours by trypan blue exclusion dye to determine whether G6PDH activity is required for tolerance to CHOP. Treatment of CHOP-resistant G3 and 10R cells with a combination of 100 µM DHEA and CHOP resulted in decreased tolerance compared to CHOP alone. * $p<0.05$, ** $p<0.01$, *** $p<0.001$

2.3.4 DHEA promoted oxidative stress in CHOP-resistant DLBCL cell lines

We hypothesized that downregulation of G6PDH activity (by DHEA) in CHOP-resistant cells would cause oxidative stress by decreasing NADPH and GSH levels, resulting in corresponding increases in ROS and increased sensitivity to CHOP. G3 and 10R cells produced 36.72 and 46.50% higher levels of NADPH than their drug-sensitive parental cells, and DHEA significantly decreased NADPH levels in both G3 and 10R cells by 31.46 and 41.65%, respectively, compared to DMSO-treated control cells. Similarly, 70.88 and 72.36% higher levels of GSH were observed in G3 and 10R cells compared to 2631 and 10S, and DHEA significantly decreased GSH levels in both G3 and 10R cells by 11.59 and 37.77%, respectively, compared to DMSO-treated control cells (Figure 2.4B). Interestingly, DHEA brought the NADPH levels down in G3 and 10R cells to the same as their parental 2631 and 10S lines, respectively. As shown in Figure 2.4C, treatment of G3 and 10R cells with DHEA also caused a 0.69- and 2.47-fold increase in intracellular levels of ROS compared to DMSO treated cells, respectively.

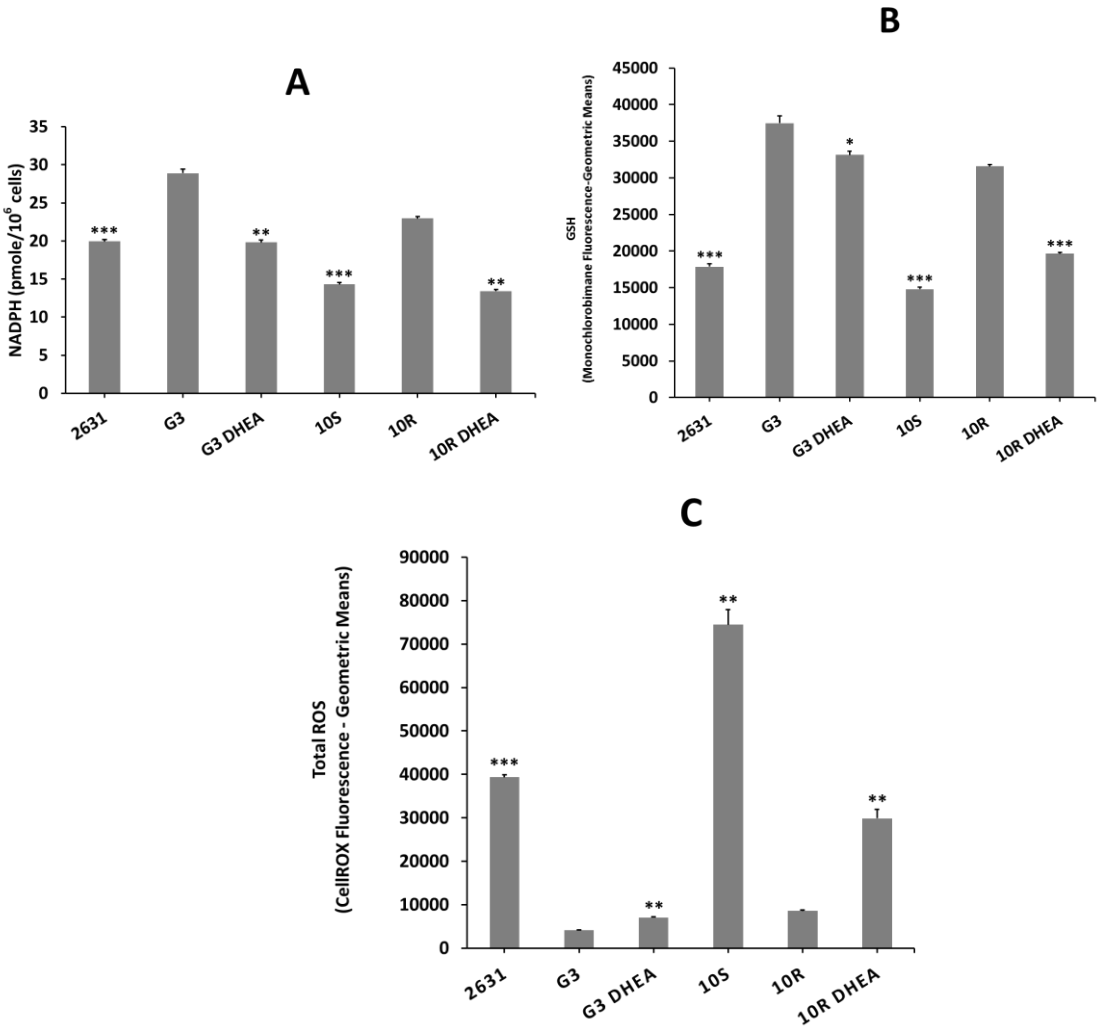

Figure 2.4 DHEA promotes oxidative stress in CHOP-resistant DLBCL cell lines. (A) Inhibition of G6PDH reduced NADPH levels in CHOP-resistant cells. CHOP-sensitive 2631 and 10S showed significantly lower levels of intracellular NADPH levels compared to their respective CHOP-resistant counterparts, G3 and 10R. Treatment of CHOP-resistant cells with 100 μM DHEA for 4 hours significantly reduced the levels of NADPH in both G3 and 10R cells. (B) Inhibition of G6PDH reduced GSH levels in CHOP-resistant cells. CHOP-resistant cells showed higher levels of GSH than CHOP-sensitive cells. The addition of 100 μM DHEA for 16 hours significantly reduced GSH in both G3 and 10R CHOP-resistant cells. (C) Increases in ROS in DHEA-treated CHOP-resistant DLBCL cells. Levels of ROS in CHOP-sensitive cells (2631, 10S) were significantly higher than their respective CHOP-resistant counterparts, G3 and 10R. 16 hours of treatment with 100 μM DHEA produced significant increases in ROS in the CHOP-resistant cells. * $p<0.05$, ** $p<0.01$, *** $p<0.001$

2.3.5 Purification and Characterization of Low and High Oxidative State Cells from CHOP-naïve (sensitive) CRL-2631 Populations

During initial experiments to select for CHOP-resistant DLBCL cells, we observed that 99.9% of the CRL-2631 and SU-DHL-10 cells died after five days of exposure to CHOP. We hypothesized that these few viable cells remaining after the initial CHOP exposures represented a small population of lower ROS-expressing, CHOP-resistant variants that were the ancestors of the CHOP-resistant G3 and 10R cell lines. To test this hypothesis, CHOP-naïve CRL-2631 cell populations were sorted based on CellROX fluorescence (ROS levels). Two distinct lower and higher ROS populations were isolated at the lower and higher 5% fluorescence intensities of the geometric mean, respectively. From these isolated populations, CRL-2631 cell lines expressing either higher (2631Hi) or lower (2631Lo) ROS levels were successfully established in culture (Figure 2.5A and B). These ROS levels in both the 2631Hi and 2631Lo cell populations have been stable for over one hundred cell passages. 2631Hi cells were significantly less tolerant to CHOP than 2631Lo, as indicated by the 76.25% fewer number of trypan-blue viable cells left after 72 hours of CHOP treatment (Figure 2.5C). The inclusion of DHEA (100 μM) to CHOP (640 ng/ml) resulted in increased sensitization of 2631Lo cells to CHOP (Figure 2.6A), as indicated by the 67.18% fewer numbers of viable cells after 72 hours of treatment compared to CHOP alone. Western blot revealed that 2631Lo cells expressed more Nrf2 and G6PDH than 2631Hi cells (Figure 2.6B). Higher G6PDH activity (65.48% more) was observed in 2631Lo cells compared with 2631Hi cells, which correlated with the increased amounts of G6PDH protein expression in 2631Lo cells. Treatment of 2631Lo cells with DHEA caused a significant decrease of 27.44% in G6PDH activity (Figure 2.6C). DHEA also caused significant decreases of 28.30 and 30.71% in both NADPH (Figure 2.7A) and GSH (Figure 2.7B) levels, respectively. On the other hand, treatment of 2631Lo cells with DHEA generated 1.89-fold higher ROS

compared to DMSO-treated cells (Fig 2.7C). The higher expression of NADPH, GSH, and lower generation of ROS in 2631Lo cells compared to 2631Hi cells was a distinctive pattern very similar to that observed in the CHOP-sensitive/resistant 2631/G3 and 10S/10R cell line pairs. However, the G3 and 10R cells were acquired by selection in repeated "on-off" exposures to increasing concentrations of CHOP, whereas the 2631Hi/2631Lo cell pair was isolated from CHOP-naïve populations based on intracellular ROS expression.

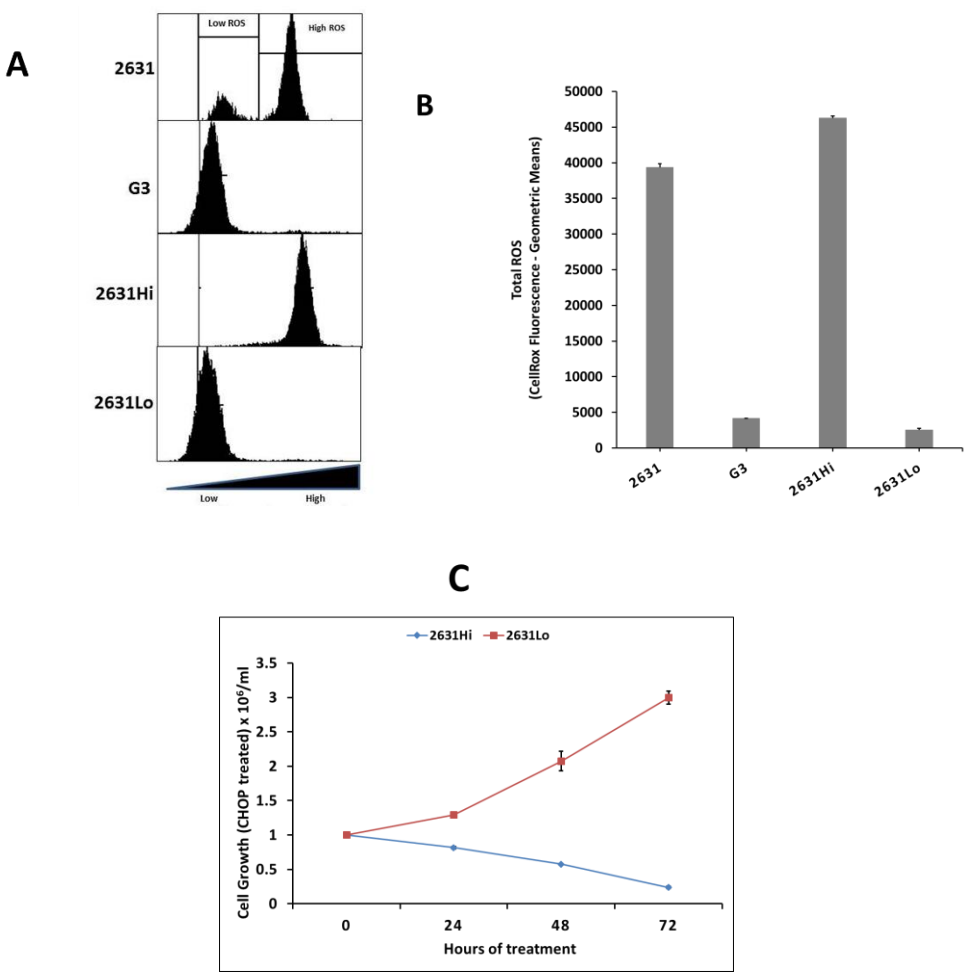

Figure 2.5 Isolation of Relative Higher and Lower Oxidative State CRL-2631 DLBCL Cells. (A) CHOP-naïve CRL-2631 cells were labeled with CellROX for 1 hour and then separated into high and low ROS-expressing populations by FACS as described under Methods. (B) Total ROS levels determined by CellROX in 2631Hi and 2631Lo, which are shown compared with that in the 2631 and G3 cell lines. (C) The lower ROS-expressing 2631Lo cells were markedly more resistant to CHOP than the higher ROS-expressing 2631Hi cells.

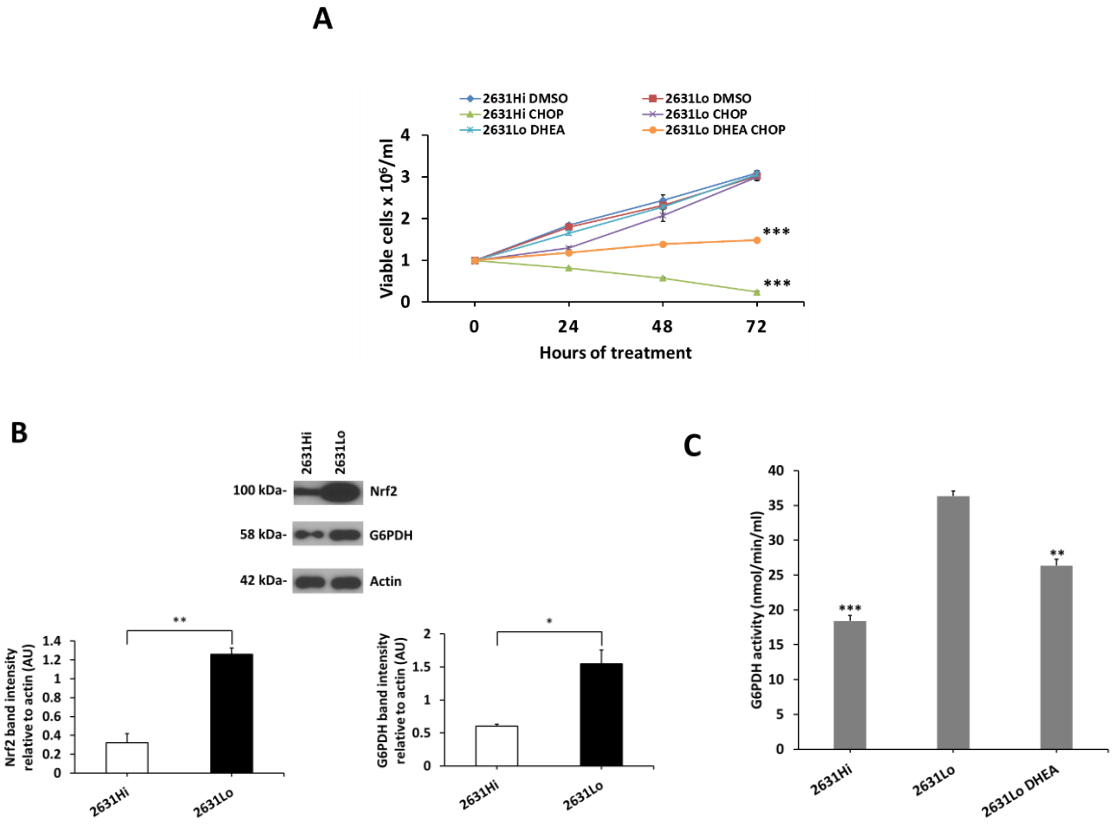

Figure 2.6 Lower-ROS expressing 2631Lo cells are more tolerant to CHOP and have higher levels of Nrf2 and G6PDH than the higher-ROS expressing 2631Hi cells. (A) The growth of 2631Hi and 2631Lo cells was evaluated in absence or presence of CHOP cocktail by trypan blue exclusion dye. Treatment of 2631Lo cells with CHOP revealed that they are relatively more CHOP-resistant than 2631Hi cells. The addition of 100 µM DHEA to CHOP resulted in decreased tolerance to CHOP in 2631Lo cells. (B) Upper panel: Higher expression of Nrf2 and G6PDH protein was observed by western blot in 2631Lo than 2631Hi cells. Actin was used as loading control. Lower panel: Quantification of Nrf2 and G6PDH protein expression determined by calculating the intensity (pixels) of Nrf2 and G6PDH bands relative to the intensity of actin band. (C) Higher G6PDH activity was confirmed in 2631Lo cells than in 2631Hi cells. Treatment of 2631Lo cells with 100 µM DHEA for 4 hours significantly lowered G6PDH activity. * $p<0.05$, ** $p<0.01$, *** $p<0.001$

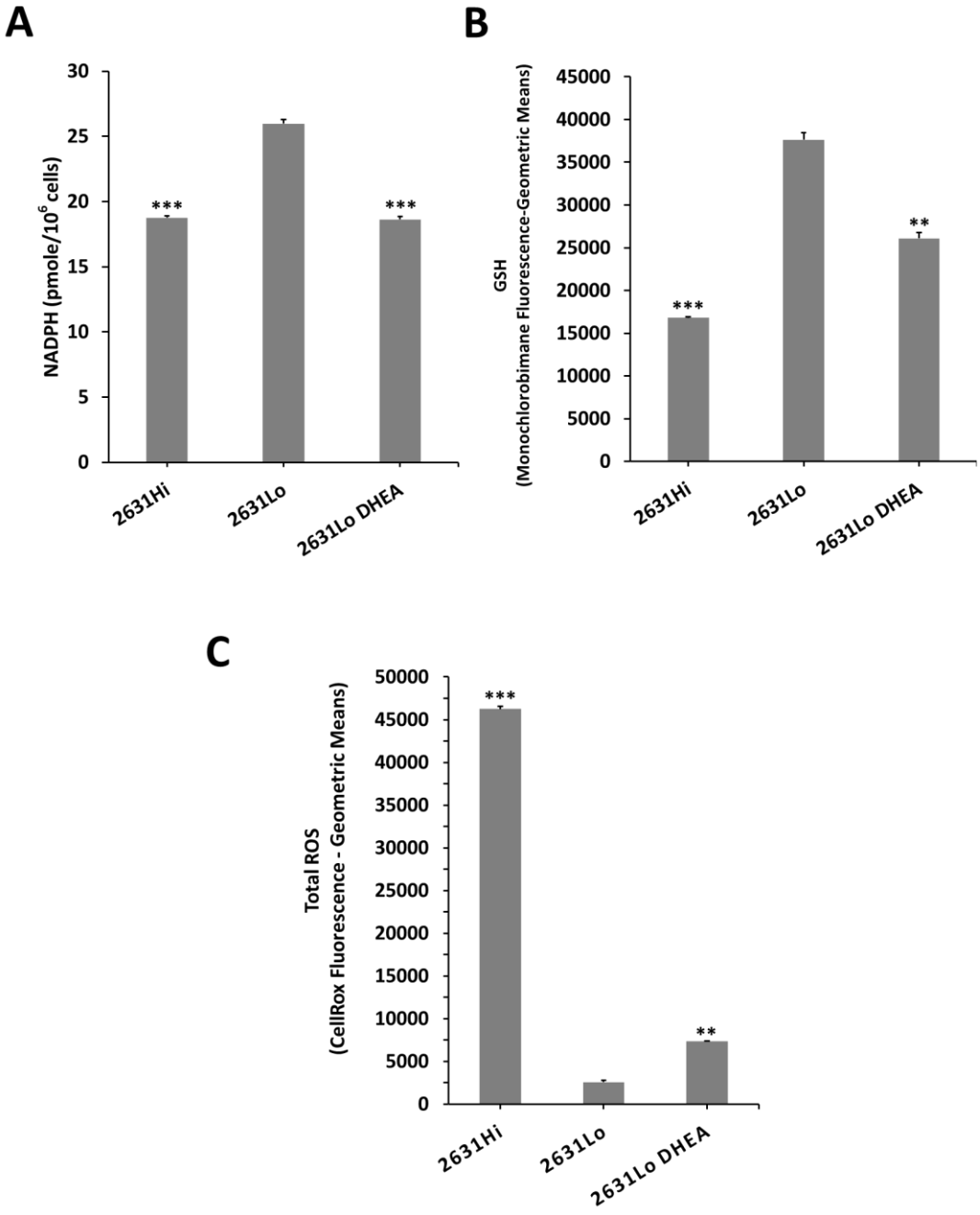

Figure 2.7 Inhibition of G6PDH reduces NADPH and GSH levels in 2631Lo cells. (A) 2631Lo cells showed higher levels of NADPH than 2631Hi cells. A 4 hour incubation with 100 µM DHEA significantly reduced NADPH levels in 2631Lo cells. (B) 2631Lo cells expressed higher levels of GSH than 2631Hi cells. A 16 hour incubation of 2631Lo cells with 100 µM DHEA significantly reduced GSH level in 2631Lo cells. (C) DHEA caused a significant increase in levels of ROS in 2631Lo cells. Levels of ROS in 2631Lo cells after 16 hours of treatment with 100 µM DHEA showed a significant increase compared to DMSO-treated cells. ** $p<0.01$, *** $p<0.001$

2.3.6 shRNA knockdown of Nrf2 promoted oxidative stress-mediated reversal of CHOP resistance in G3 and 10R cells

We investigated the impact of Nrf2 knockdown on the reversal of CHOP-resistance through transduction of the CHOP-resistant G3 and 10R cell lines with lentivirus expressing Nrf2 shRNA. Considering the proposed regulatory role of Nrf2 on G6PDH in our hypothesis, Nrf2 shRNA knock down would be expected to downregulate G6PDH activity with corresponding decreases in NADPH and GSH, and increases in ROS. As shown in Figure 2.8A, Nrf2 shRNA-transduced G3 and 10R cells showed reduced levels of Nrf2 protein compared to the scrambled shRNA controls. Nrf2 shRNA reduced the amount of G6PDH activity by 23.87 and 28.54% in G3 and 10R cells, compared to control shRNA cells, respectively (Figure 2.8B). Moreover, Nrf2 shRNA significantly decreased NADPH levels in both G3 and 10R cells by 19.24 and 21.13%, respectively, compared to control shRNA cells (Figure 2.9A). GSH levels also decreased in G3 Nrf2 shRNA and 10R Nrf2 shRNA cells by 21.88 and 21.08%, compared to G3 control shRNA and 10R ctrl shRNA cells respectively (Figure 2.9B). Correspondingly, Nrf2 knockdown caused a 64.84% and 84.67% increase in intracellular levels of ROS in G3 and 10R cells compared to control cells, respectively (Figure 2.9C). shRNA knockdown of Nrf2 resulted in increased sensitization of G3 Nrf2 shRNA and 10R Nrf2 shRNA cells to CHOP (Figure 2.9D), as indicated by the 64.42 and 81.63% fewer numbers of viable cells after 72 hours of treatment compared to G3 and 10R control shRNA cells respectively.

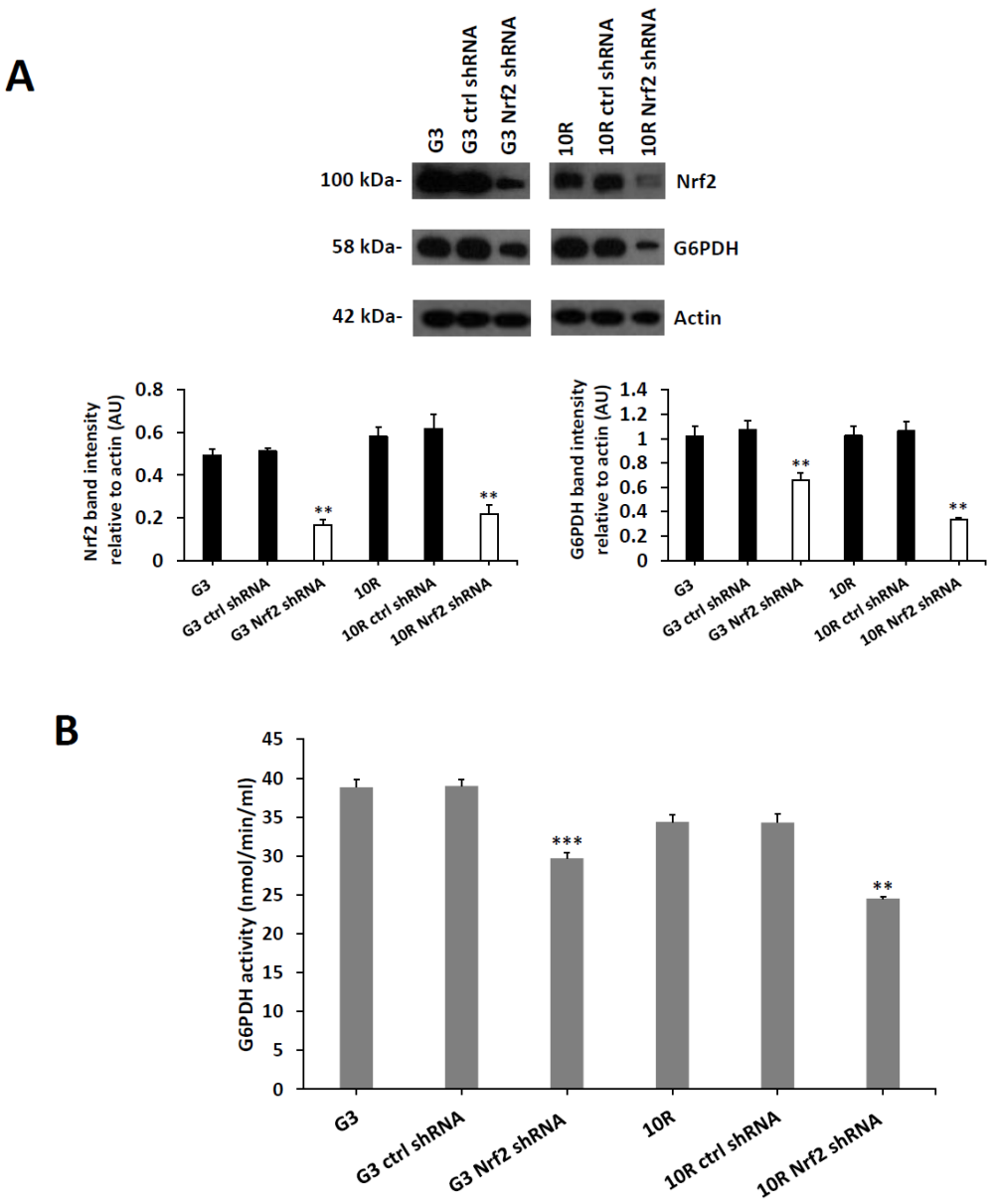

Figure 2.8 Knockdown of Nrf2 reduces G6PDH protein expression and activity in G3 and

10R cells. (A) Nrf2 shRNA transduction downregulated the expression of Nrf2 and G6PDH proteins. (*Upper panel*) Lower levels of Nrf2 and G6PDH proteins in G3 Nrf2 shRNA and 10R Nrf2 shRNA was observed by western blot compared to G3 (control) ctrl shRNA and 10R control (ctrl) shRNA, respectively. Control shRNA did not have any effect on Nrf2 or G6PDH expression in G3 and 10R cells. (*Lower panel*) Quantification of Nrf2 and G6PDH protein expression was determined by calculating the intensity (pixels) of Nrf2 and G6PDH bands relative to the intensity of actin band. (B) Nrf2 shRNA transduction lowered G6PDH activity in G3 and 10R cells. Control shRNA did not affect G6PDH activities in either G3 or 10R cells. ** $p<0.01$, *** $p<0.001$

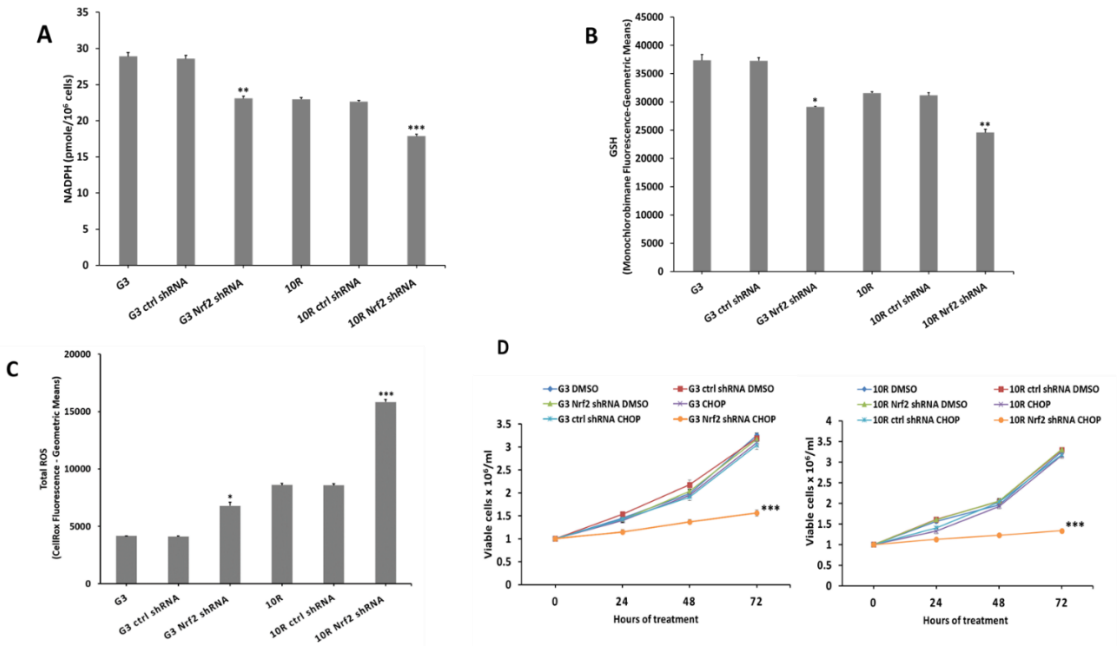

Figure 2.9 Knockdown of Nrf2 promotes oxidative stress and reduced tolerance of G3 and 10R cells to CHOP. (A) Knockdown of Nrf2 reduces NADPH levels in CHOP-resistant cells. G3 and 10R transduced with the control scrambled shRNA showed similar levels of intracellular NADPH levels as the non-transduced G3 and 10R cells, respectively. Knockdown of Nrf2 by shRNA significantly reduced the levels of NADPH in both G3 and 10R cells. (B) Knockdown of Nrf2 reduces GSH levels in CHOP-resistant cells. Both G3 Nrf2 shRNA and 10R Nrf2 shRNA cells showed significantly lower levels of GSH than their respective scrambled shRNA controls. (C) Knockdown of Nrf2 increased ROS production in CHOP-resistant DLBCL cells. Levels of ROS were significantly higher in G3 Nrf2 shRNA and 10R Nrf2 shRNA compared to their respective scrambled shRNA control cells. (D) Knockdown of Nrf2 reduces the tolerance of resistant DLBCL cells to CHOP. Both G3 and 10R cells transduced with Nrf2 shRNA cells were more sensitive to CHOP than control cells as indicated by the significantly decreased the number of viable cells after 72 hours compared to controls. * $p<0.05$, ** $p<0.01$, *** $p<0.001$

2.3.7 shRNA knockdown of G6PDH promoted oxidative stress-mediated reversal of CHOP resistance in 2631Lo cells

We investigated the impact of G6PDH knockdown on CHOP-resistance through transduction of the CHOP-resistant 2631Lo cell line with lentivirus expressing G6PDH shRNA. As shown in Figure 2.10A, G6PDH shRNA-transduced 2631Lo cells showed 58.06% reduced the level of G6PDH protein compared to the scrambled shRNA control. However, G6PDH knockdown didn't show a significant effect on Nrf2 protein in 2631Lo cells. G6PDH shRNA reduced the amount of G6PDH activity by 18.19% in 2631Lo cells, compared to control shRNA cells (Figure 2.10B). Consequently, levels of NADPH and GSH decreased in 2631Lo G6PDH shRNA cells by 18.91 and 18.46%, respectively, compared to 2631Lo ctrl shRNA cells (Figure 2.11A-B). Correspondingly, G6PDH knockdown caused a 57% increase in intracellular levels of ROS in 2631Lo cells compared to control cells (Figure 2.11C). shRNA knockdown of G6PDH resulted in increased sensitization of 2631Lo G6PDH shRNA cells to CHOP (Figure 2.11D), as indicated by the 30.02% fewer numbers of viable cells after 72 hours of treatment compared to 2631Lo ctrl shRNA cells.

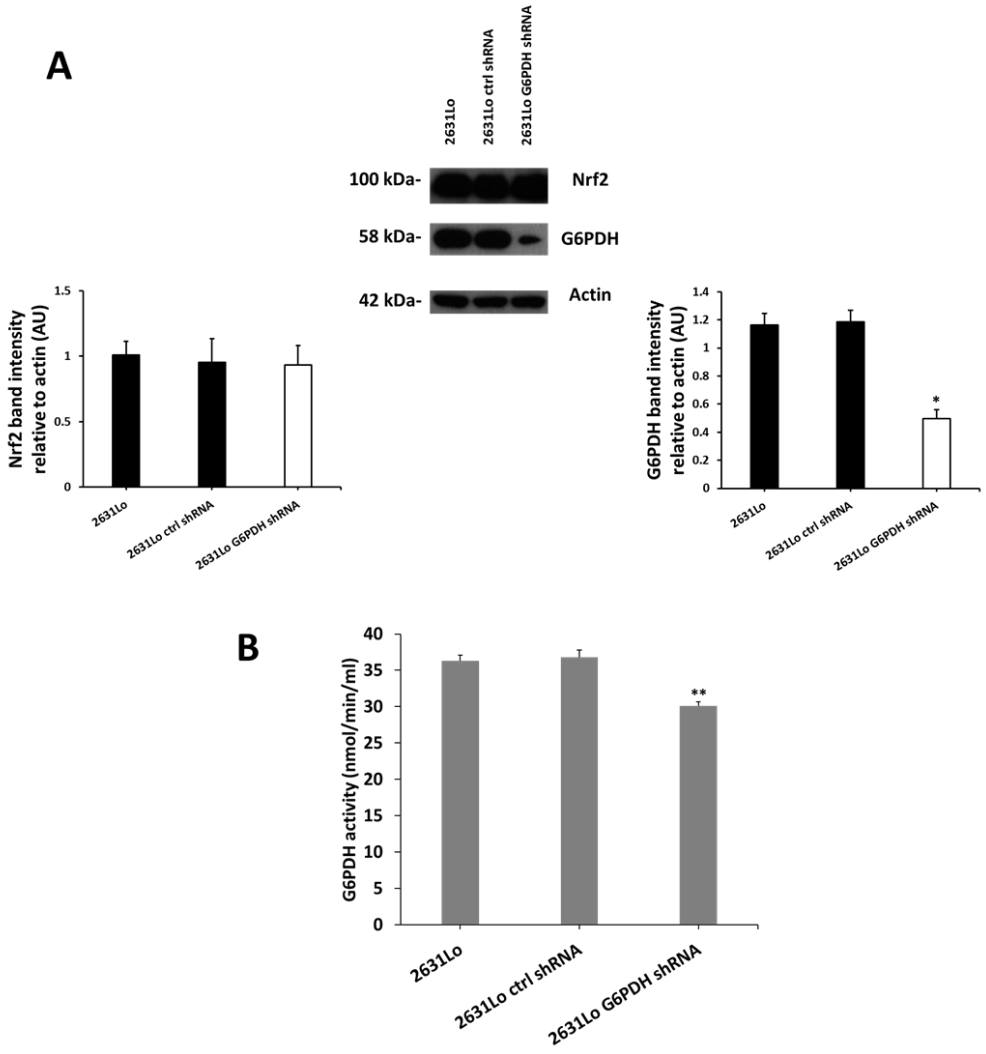

Figure 2.10 G6PDH shRNA transduction downregulated the expression of G6PDH protein. (A) Lower levels of G6PDH protein in 2631Lo G6PDH shRNA was observed by western blot compared to 2631Lo control (ctrl) shRNA. However, no significant difference was observed in Nrf2 expression between samples (Upper panel). Quantification of Nrf2 and G6PDH protein expressions were determined by calculating the intensity (pixels) of Nrf2 and G6PDH bands relative to the intensity of actin bands (Lower panel). (B) G6PDH shRNA transduction lowered G6PDH activity in 2631Lo cells. Control shRNA did not affect G6PDH activities in 2631Lo cells. * $p<0.05$ and ** $p<0.01$

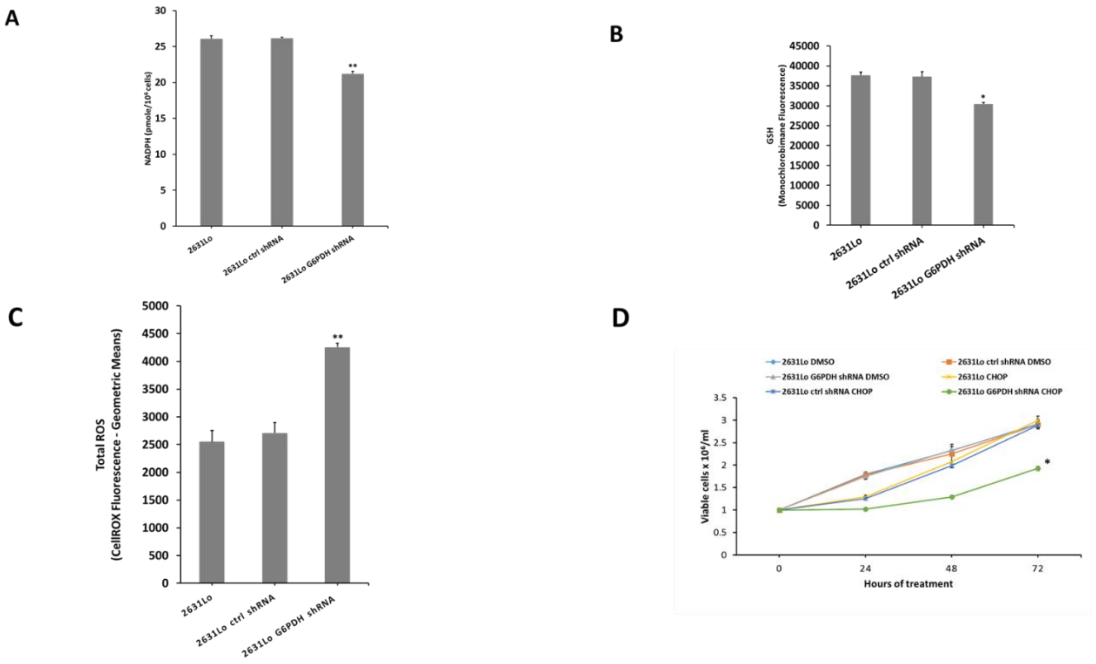

Figure 2.11 Knockdown of G6PDH promotes oxidative stress and reduced tolerance of 2631Lo cells to CHOP. (A) Knockdown of G6PDH reduces NADPH level in CHOP-resistant cells. While knockdown of G6PDH by shRNA significantly reduced the levels of NADPH in 2631Lo G6PDH shRNA cells, 2631Lo ctrl shRNA cells showed similar levels of intracellular NADPH as the non-transduced 2631Lo cells. (B) Knockdown of G6PDH reduces GSH level in CHOP-resistant cells. 2631Lo G6PDH shRNA cells showed significantly lower levels of GSH than their respective scrambled shRNA controls. (C) Knockdown of G6PDH increased ROS production in CHOP-resistant DLBCL cells. Levels of ROS were significantly higher in 2631Lo Nrf2 shRNA cells compared to their shRNA control cells. (D) Knockdown of G6PDH reduces the tolerance of resistant DLBCL cells to CHOP. 2631Lo G6PDH shRNA cells were more sensitive to CHOP than control cells as indicated by the significantly decreased the number of viable cells after 72 hours compared to controls. * $p<0.05$ and ** $p<0.01$

2.3.8 Modulation of Nrf2 and G6PDH affects primarily superoxide/hydrogen peroxide species of ROS

The types of ROS species in sensitive and resistance cells were characterized with fluorescent indicators specific for either superoxide, hydrogen peroxide, or hydroxyl radicals (Figure 2.12). Higher levels of all forms of ROS investigated were detected in sensitive than in resistant cells (Figure 2.12A-C). However, downregulation of either G6PDH (by DHEA or shRNA) or Nrf2 (by shRNA) caused significant increases in superoxide/hydrogen peroxide but not hydroxyl radicals. For instance, while there were significant differences in superoxide levels between 2631vs G3, 10S vs 10R, and 2631Hi vs 2631Lo cells, treatment of G3, 10R, and 2631Lo cells with DHEA caused a 1.89, 3.41-, and 3.19-fold increase in intracellular levels of superoxide compared to DMSO treated cells, respectively. Moreover, G3 Nrf2 shRNA and 10R Nrf2 shRNA cells generated 0.63- and 1.37- fold increases in intracellular levels of superoxide compared to G3 ctrl shRNA and 10R ctrl shRNA cells respectively. In addition, 2631Lo G6PDH shRNA cells generated 1.05- fold increases in intracellular levels of superoxide compared to 2631Lo ctrl shRNA (Figure 2.12A). There also was a significant difference in intracellular hydrogen peroxide levels between resistant vs sensitive lymphoma cells, and treatment with DHEA, and transduction with Nrf2 shRNA and G6PDH shRNA lentiviral particles slightly increased the levels of intracellular hydrogen peroxide (Figure 2.12B). On the other hand, despite the differences in intracellular levels of hydroxyl radicals between resistant vs sensitive lymphoma cells, neither DHEA treatment nor Nrf2/G6PDH shRNA transduction induced hydroxyl radical production in resistant lymphoma cells (Figure 2.12C).

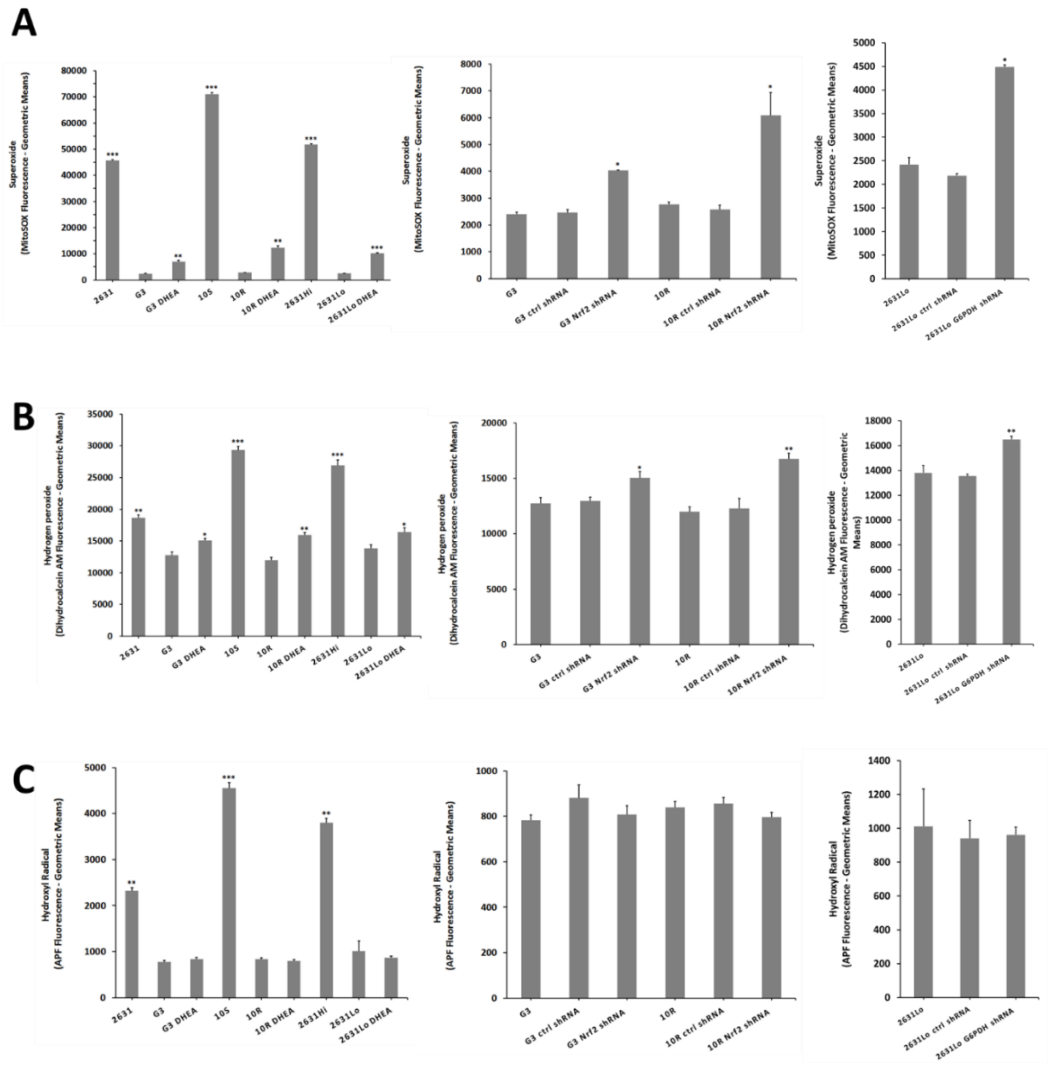

Figure 2.12 Characterization of ROS species in DLBCL cell lines. DHEA, Nrf2 shRNA, and G6PDH shRNA caused primarily increases in superoxide and hydrogen peroxide, but not hydroxyl radicals. (A) Mitosox superoxide indicator revealed higher superoxide in sensitive 2631, 10S, and 2631Hi cells than in their more CHOP-resistant counterparts, G3, 10R, and 2631Lo, respectively. DHEA, Nrf2 shRNA, and G6PDH shRNA induced increases in superoxide in CHOP-resistant cells. (B) The dihydrocalcein-AM indicator revealed higher hydrogen peroxide species levels in CHOP-sensitive cells than in resistant cells. DHEA, Nrf2 knockdown, and G6PDH knockdown caused a slight increase in production of hydrogen peroxide in CHOP-resistant lymphoma cells relative to control cells. (C) The APF indicator revealed markedly higher hydroxyl radicals in CHOP-sensitive cells than in resistant cells. However, DHEA or Nrf2 knockdown or G6PDH knockdown didn't induce increases in hydroxyl radicals in CHOP-resistant lymphoma cells compared to controls. * $p<0.05$, ** $p<0.01$, *** $p<0.001$

2.4 Discussion

In normal cells during oxidative stress, Nrf2 upregulates G6PDH providing reducing equivalents (NADPH) for the maintenance of a pool of reduced mitochondrial glutathione (GSH) to balance the redox state, which has a crucial role in cellular signaling and antioxidant defenses (415-417). We observed that CHOP-resistant DLBCL cell lines expressed a lower oxidative state (ROS) and increased expression of anti-oxidant Nrf2 and G6PDH genes than their more drug-sensitive counterparts. Based on our data, we propose that alterations in the Nrf2/G6PDH pathway can promote a higher reductive (lower oxidative) state that drives resistance to oxidative stress-inducing chemotherapeutics (Figure 2.13).

We utilized DHEA as an adjuvant to the widely used CHOP regimen and transduced G3 and 10R cell lines with Nrf2 shRNA and 2631Lo cell line with G6PDH shRNA to determine a role for the Nrf2/G6PDH cascade in CHOP resistance. The following results indicated a role for the Nrf2/G6PDH pathway in oxidative stress-mediated drug resistance in lymphoma cells. First, we observed increased expression of both Nrf2 and G6PDH in CHOP-resistant variants derived by "on-off" treatments of sensitive cells with increasing concentrations of CHOP. Second, G6PDH protein expression and enzymatic activity were significantly higher in CHOP-resistant lymphoma cells compared with their more CHOP-sensitive parent cells, which also correlated with the lower ROS levels in CHOP-resistant cells. Third, higher expression of G6PDH correlated with higher NADPH and GSH in CHOP-resistant cells. Fourth, the G6PDH inhibitor, DHEA, sensitized CHOP-resistant cells to CHOP. DHEA inhibited G6PDH activity in a time- and dose-dependent manner, which was correlated with declines in NADPH and GSH and increases in ROS (primarily superoxide/hydrogen peroxides).

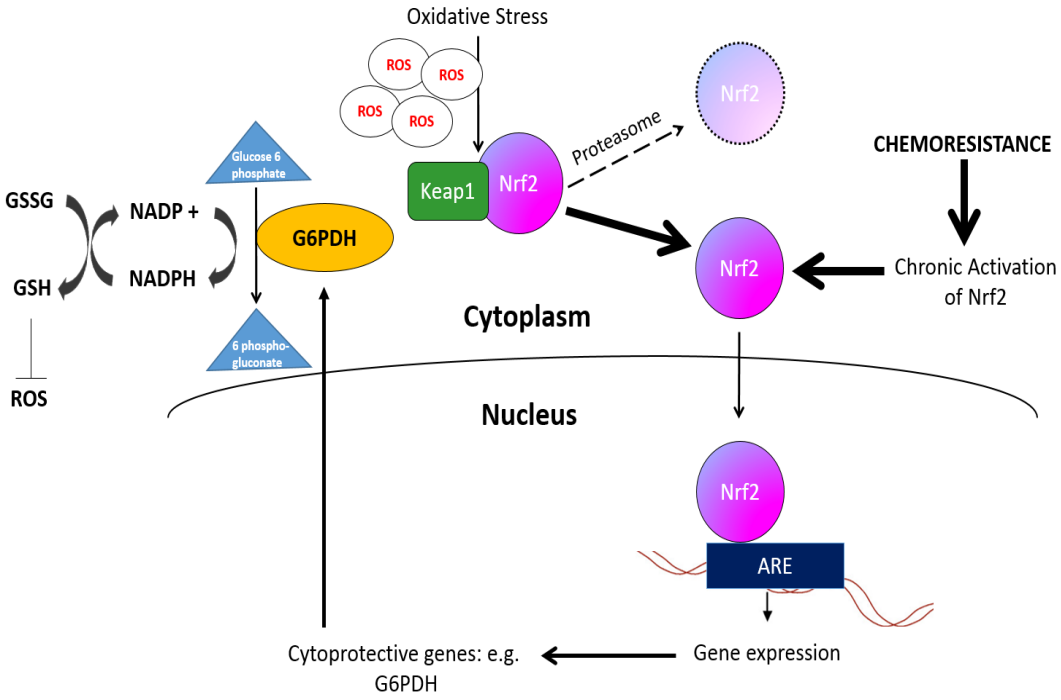

Figure 2.13 A model for the role of the Nrf2/G6PDH pathway in driving lower ROS

expression and CHOP chemoresistance in DLBCL. Repeated exposures to CHOP treatment cause a chronic activation of Nrf2, which constitutively upregulates the G6PDH gene and thus increased G6PDH activity. G6PDH increases NADPH production through the PPP, which leads to increased synthesis of GSH, thus driving down ROS levels in the cell. The resulting increased reductive stress promotes resistance to oxidative stress-inducing chemotherapeutics.

The inhibition of G6PDH activity and consequently NADPH production by DHEA were early events occurring after 4 hours of treatment of CHOP-resistant lymphoma cells with DHEA. On the other hand, the reduction in GSH and induction of ROS generation occurred later after 16 hours of DHEA treatment. This time sequence might be expected if GSH and ROS are downstream to G6PDH and NADPH. Fifth, transduction of G3 and 10R cells with Nrf2 shRNA significantly downregulated the expression of Nrf2, and consequently G6PDH (both protein expression and enzymatic activity). Sixth, transduction of 2631Lo cells with G6PDH shRNA significantly downregulated the expression of G6PDH (both protein expression and enzymatic activity). However, as expected, G6PDH shRNA knockdown didn't affect the expression of Nrf2 protein. Finally, Nrf2 knockdown increased the sensitivity of resistant G3 and 10R cells to CHOP and G6PDH knockdown increased the sensitivity of resistant 2631Lo cells to CHOP. Similar to DHEA, there was a positive correlation between shRNA knockdown of Nrf2/G6PDH with declines in NADPH and GSH, and a high negative correlation with increases in ROS (primarily superoxide/hydrogen peroxides).

Although higher G6PDH activity was clearly associated with higher G6PDH protein expression in CHOP-resistant cell lines, the difference in G6PDH enzyme activity between CHOP-resistant and -sensitive cells was not absolutely correlative with respect to G6PDH protein level. For instance, the difference in enzyme activity of G6PDH between 2631 cells and G3 cells was 59.4% but the difference in expression G6PDH protein level between the two cell lines was 68.83%. For the 10S and 10R lines, the difference between G6PDH activity and protein expression was 80.31 vs 92.8%, respectively. The basis for the discrepancies in G6PDH protein expression and activity is currently not clear. However, G6PDH activity is regulated through phosphorylation by protein kinases. Differential phosphorylation might be responsible for the lack of strict correlation between G6PDH activity and protein levels between the CHOP-

sensitive and –resistant cell lines (459-461). Thus, further work is ongoing to characterize the phosphorylation state of G6PDH in CHOP-sensitive and -resistant cell lines.

We have previously reported the upregulation and roles of the anti-apoptotic 14-3-3zeta and Akt protein kinase in mediating CHOP resistance in DLBCL (82, 83). Of particular interest relevant to this report is the reported interaction of 14-3-3zeta with several redox enzymes and glucose-6-phosphate isomerase (GPI) (462-464). In addition, PI3K/Akt signaling augments the nuclear accumulation of Nrf2 and enables Nrf2 to upregulate G6PDH to promote metabolic activities that support cell proliferation in addition to enhancing cytoprotection (452, 465). We thus plan to investigate potential roles for 14-3-3zeta and PI3K/Akt in Nrf2/G6PDH-mediated CHOP resistance in DLBCL.

We were able to isolate CHOP-resistant variants from CHOP-naïve CRL-2631 cell populations that resembled CHOP-resistant cells ($Nrf2^{High}$, $G6PDH^{High}$, ROS^{Low}) derived by repeated exposures to CHOP (acquired resistance). We propose that a specific type of CHOP-resistant lymphoma cell expressing the $Nrf2^{High}$, $G6PDH^{High}$, ROS^{Low} phenotype may be selected for and amplified during repeated cycles of CHOP regimens, providing one possible explanation of why DLBCL can relapse in patients in clinical remission. We have not observed any differences in the expression of known cancer stem cell markers ($CD44^{+}$, $CD24^{-}$, $CD133^{+}$, Notch) between CHOP-resistant and –sensitive cells or between CRL-2631Hi and CRL-2631Lo cells (data not reported). Moreover, no differences in the expression of the hypothesized lymphoma stem cell marker, ALDH (466), was observed between CHOP–resistant and –sensitive cells. Also, no differences in enzymatic activity of glutathione s-transferases (GST), which mediate ROS detoxification by utilizing GSH as a substrate (467), were observed between CHOP–resistant and –sensitive cells (data not shown). Further work is warranted along these lines and current

studies are thus concerned with applying RNAseq to identify additional specific markers that might characterize 2631Lo, 10R, and G3 cells as a specific type of lymphoma cell with the potential to initiate and propagate a CHOP-resistant disease phenotype.

Based on our data, we propose a Nrf2/G6PDH model (Figure 2.14) for the acquisition of CHOP-resistance in DLBCL. In this model, repeated cycles of on-off treatments with CHOP lead to selective amplification and emergence of a small population of cells expressing higher levels of the Nrf2/G6PDH pathway. An increased reductive state in these cells confers an increased tolerance to oxidative stress-inducing chemotherapeutics such as doxorubicin, a component of the CHOP cocktail. The mechanism driving a lower oxidative state in these resistant cells is upregulation of G6PDH catalyzing the production of NADPH via the PPP. NADPH is a substrate for glutathione reductase that regenerates GSH to detoxify ROS. NADPH is also required for growth and proliferation. Nrf2 directly targets the upregulation of G6PDH in CHOP-resistant cells. Our model proposes that the targeted destruction of these CHOP-resistant $Nrf2^{High}/G6PDH^{High}/ROS^{Low}$ cells with a combination therapy of Nrf2/G6PDH pathway inhibitors and CHOP will reduce the risk for emergence of chemoresistant disease and thus relapse

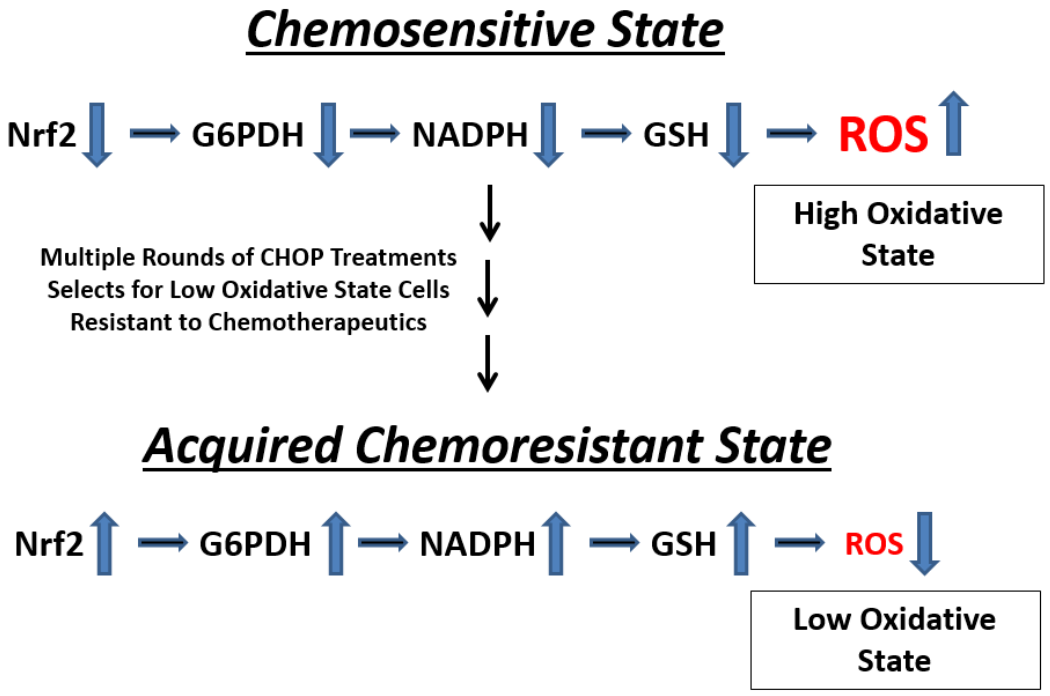

Figure 2.14 Model for the emergence of acquired chemoresistance in DLBCL. We propose that resistance to CHOP is caused by the selected emergence during repeated cycles of CHOP treatment of a small population of CHOP-resistant cells that express high Nrf2 and G6PDH, and low ROS. High Nrf2/G6PDH activity drives increased expression of GSH that drives down ROS, thus giving cells the capacity to resist chemotherapeutics that induce oxidative stress. The $Nrf2^{High}/G6PDH^{High}/ROS^{Low}$ cells outgrow and outlive the more CHOP-sensitive $Nrf2^{Low}/G6PDH^{Low}/ROS^{High}$ cells, thereby leading to relapse and emergence of chemoresistant disease.

CHAPTER III

DEVELOPMENT OF NOVEL, NON-TOXIC RIFAMYCINS THAT REVERSE DRUG RESISTANCE IN CANCER *

3.1 Introduction

The cure rate and progression free survival rate for many cancers have not changed considerably in the past two decades. Ovarian cancer patients have an approximately 70% relapse rate within two years, and most relapse patients do not respond to second line therapeutics (468). Though there have been significant improvements for other cancers due to new drugs, such as Rituximab for NHL, non-responsive tumors remain a significant cause of annual mortality. This is especially true for patients with double and triple hit lymphomas (DHL and THL) due to inherent drug resistance. Pharmacologic resistance in cancer is widespread and not restricted to specific cancer types or drugs. Currently, there are no chemotherapies available that specifically target drug resistant cancer. Therefore, identification of novel strategies and therapeutics to combat resistance is crucial.

Resistance can arise through multiple mechanisms, including the reduction of intracellular ROS (469-473). High intracellular ROS levels in cancer cells is common due to the Warburg effect (401), and it renders neoplastic cells more sensitive to ROS-inducing treatments such as doxorubicin chemotherapy and radiation. Recent evidence shows that many cancers develop altered antioxidant response systems to overcome elevated ROS levels, with a resultant decrease in sensitivity to chemotherapy (402, 474-477). Because higher ROS levels in cancer cells are

* Reprinted from "Development of novel, non-toxic rifamycins that reverse drug resistance in cancers" by Deeann Wallis, Nian Zhou, Dwight Baker, Seyed H. Mousavi-Fard, Kimberly Loesch, Stacy Galaviz, Qingan Sun, Carolina Mantilla Rojas, David W. Threadgill, Maureen T. O'Brien, Fred J. Clubb, Thomas Ioerger, Michael DeJesus, Wen Dong, Gwen Seemann, Theresa Fossum, Steve Maxwell, and James C. Sacchettini, 2017. Manuscript submitted for publication to Nature Medicine.

often a prerequisite for chemotherapy drug efficacy, an agent that forces the production of ROS or inhibits antioxidant response mechanisms would theoretically increase susceptibility to chemotherapy.

Though controversial, the importance of ROS in the action of antibiotics has also been well characterized (478-486). For example, while rifamycins primarily mediate their antibacterial activity through inhibition of bacterial RNA polymerase, they also have additional pharmacological properties including the ability to undergo redox cycling with resultant formation of ROS. This is supported by the finding that ROS may enhance bactericidal activity of rifamycin SV (487). The oxidation of the quinone moiety of rifamycin SV is catalyzed by metal ions resulting in the production of superoxide (488, 489), which damages DNA (490, 491). Moreover, both rifamycin SV and rifabutin have been shown to redox cycle and produce superoxide in rat liver microsomes (492, 493).

3.2 Materials and methods

3.2.1 Cell lines and tissue culture

Cell lines were obtained from the following sources: ATCC –OVCAR-3, SK-OV-3, CRL-2631, MES-Dx5, HL-60, HL-60 Mx, U2-OS, Panc-1, MOLT4 and HDF; the National Cancer Institute Division of Cancer Treatment and Diagnosis Tumor/Cell Line Repository – NCI/ADR-RES, OVCAR-8, and OVCAR-5; Dr. Eric Davis at MD Anderson Cancer Center provided many cell lines as a kind gift – U-2932, SU-DHL-4, SU-DHL-6, SU-DHL-10, OCI-Ly 19, HBL- 1, HT, and WSU-FSCCL; eGFP-ADR-RES were a kind gift from the Michael Gottesman Lab at NCI. All cells were cultured in RPMI 1640 media + 10% FBS except for the SK-OV-3, MES-Dx5, and U2-OS cells which were cultured in McCoy's 5a plus 10% FBS; and Panc-1 and HDF cells

which were cultured in DMEM plus 10% FBS. Cultures were passaged every 3-5 days as necessary.

3.2.2 Creation of G3 drug-resistant NHL cell line

CRL-2631 cells were treated with on/off cycles of CHOP composed of 0.83 μM 4HC; 0.057 μM Dox; 0.01 μM Vincristine; and 0.186 μM Prednisone.

3.2.3 HTS and identification of rifabutin

G3 cells were screened in the presence of CHOP and 5 μM compounds. Importantly, as a counter screen for undesired cytotoxics, compounds were tested alone at 5 μM in the drug sensitive parental CRL-2631 cells; compounds which demonstrated an IC25 or greater in the CRL-2631 cell line were considered cytotoxic and eliminated from further study. Hits were defined as greater than three standard deviation units below the mean of the population, and this resulted in 292 compounds that were identified. The majority of the most potent hits came from the NIH clinical collection; rifabutin, verapamil, lercanidipine, miltefosine, econazole, terfenidine, nefazadone, ketoconazole, and FK-506 (tacrolimus) were some of the most potent identified. Hits were then prioritized for testing in ratio "checkerboard assays", e.g. assay done while varying more than one concentration of drug in order to define the compounds most synergistic with the DOX component of CHOP.

3.2.4 Cell viability assays

We utilized 2 viability assays: resazurin-based and MTT based. For resazurin: 40 μl of cells were plated in appropriate media at various densities based on growth rates into 384-well plates. Suspension cells were treated immediately with compounds, but adherent cells were allowed

several hours to attach prior to compound addition. Cells were cultured for 48 hours at which point 40 ng/ml resazurin was added. After 16-24 hours fluorescent signal was read on a plate reader. Percent control growth was determined by comparing the growth of cells in the presence of the compound to the growth with no compound.

For the MTT assay, we utilized the MTT cell growth Assay kit from Millipore according to the manufacturer's directions.

3.2.5 Drug-like diversity library

Our custom in-house diversity library is designed to offer compounds with drug-like properties but low redundancy for exploring a wide range of chemical space to identify inhibitors with novel structures. This library was constructed such that each compound has a non-redundant chemical structure, minimizing the bias of many existing libraries which often contain many variations of common scaffolds. Thus, we can achieve similar breadth of screening with minimal time and resources compared to a very large ultra-high throughput compound collection. This diversity library was designed by combining structures from over 3 million compounds, and selecting a diverse and representative subset using a clustering algorithm. An incremental algorithm was then used to select a representative subset that covered the entire space, while guaranteeing that no pair of compounds had a chemical similarity greater than 0.7.

3.2.6 Calculation of combination index

Constant ratio dose response assays were conducted in triplicate on G3 and ADR-RES cell lines to determine the extent of synergy between the drugs. Normalized inhibition data were analyzed using CompuSyn software.

3.2.7 Statistical analysis – Determination of IC_{50} for chemotherapeutics with and without RTI-79

Cell lines were treated with chemotherapeutics in dose response both with and without RTI-79. All assays were performed in triplicate. We utilized Graph Pad Prism and began by transforming the X values (compound concentration) to X=Log(X). Next, we performed a nonlinear regression curve fit of the transform; log (inhibitor) vs. dose response (three parameter) to determine IC_{50}. Individual fitted midpoints within each cell line were compared using the extra sum-of-squares F test to determine if the best-fit values of selected unshared parameters differed. Significance was set at $p<0.05$.

3.2.8 Mouse xenografts

10^7 cells were injected sc into the left and right flanks of 6-8 week old female mice. SCID mice were used for NHL xenografts and nude mice were used for ovarian cancer xenografts. Once tumors were established and growing mice were assigned to treatment arms and treatments were begun. Tumor volume was monitored every other day, three times per week by caliper and calculated as (L*W*W)/2. Data are plotted as percent change in tumor volume according to: $((V_{Day\ X}-V_{Day\ 0})/(V_{Day\ 0}))*100$; where V= volume; Day 0 is the day of treatment initiation, Day X is any subsequent day. In the first study, WSU xenografts were implanted into SCID mice and treated 12 days later when tumor volume was approximately 375 mm^3 with saline (once per week), 3.3 mg/kg DOX iv (once per week), 25 mg/kg oral RTI-79 (twice weekly on Days 1 and 2) or a simultaneous combination of iv DOX once weekly (Day 1) and oral RTI-79 (twice weekly on Day 1 and 2). Mice received two cycles of treatment. In the second study, WSU xenografts were implanted into SCID mice and treated 11 days later when tumor volume was approximately 165 mm^3 weekly with saline, 12 mg/kg etoposide given on days 1, 2, and 3 of

each week, 25 mg/kg RTI-79 given on days 1, 2, and 3 of each week, or etoposide plus RTI-79 given on days 1, 2, and 3. Mice received three cycles of treatment. In the third study, nude mice were injected with ADR-RES cells and treated 9 days later when tumor volume was approximately 90 mm^3 with once weekly saline, 7 mg/kg DOXIL iv, 25 mg/kg oral RTI-79 given on days 2 and 3, or a combination of iv DOXIL on Day 1 and oral RTI-79 on days 2 and 3. Mice received 6 rounds of treatment. In the fourth study, SK-OV-3 cells were injected into nude mice and treated 3 weeks later when tumor volume was approximately 100 mm^3 once weekly with saline, 3mg/kg DOXIL on Day 1, 25 mg/kg oral RTI-79 on days 2 and 3, iv DOXIL on Day 1 and 25 mg/kg oral RTI-79 on days 2 and 3, or iv DOXIL on Day 1 and 25 mg/kg oral rifabutin on days 2 and 3. Mice received 3 rounds of treatment.

Tumor growth delay was evaluated and percent change in tumor growth based on the starting volume on the day prior to the first treatment i.e. $((V_{t=X}-V_{t=0})/V_{t=0}))*100$. Student's t-test was run to evaluate statistical significance between groups.

3.2.9 ROS quantitation and FACS: CellROX, MitoSOX, dihydrocalcein-AM, and APF

Cells (1×10^6) were incubated with 1 µl of the ROS indicators CellROX, MitoSOX, dihydrocalcein-AM, or APF (Life Technologies) in 1 ml complete RPMI for 0-1 hour. Cells were then analyzed directly by flow cytometry at appropriate absorption/emission maxima. CellROX detects total ROS, whereas MitoSOX detects specifically superoxide, dihydrocalcein-AM labels hydrogen peroxide, and aminophenyl fluorescein (APF) labels hydroxyl radicals. ROS and superoxide levels were quantitated as the geometric mean of fluorescence.

3.2.10 CellROX imaging

Cells were plated at 20,000 - 50,000 cells per well in 96-well optical imaging plates. CellROX (5 µM) (Invitrogen Cat # C10422) and compounds were added simultaneously in fresh media to triplicate wells and imaged on a GE INCell Analyzer after 30-60 minutes to detect fluorescent signal. As necessary cells were then fixed in 4% PFA and stained with DAPI and the same fields were reimaged to obtain a cell count. Images were analyzed using the INCell Developer software to determine cell count and CellROX intensity. Values were averaged over the triplicates and SEM calculated.

3.2.11 Oxidation sensitive GFP construct

Ratiometric rhoGFP fluorescence detectors were used to examine RTI-induced redox changes in real-time in cells. The reduction-oxidation sensitive green fluorescent protein (roGFP) is a redox biosensor that is retained in the cytoplasm (494). The resulting redox-sensitive protein has excitation maxima at 400 and 484 nm, with emission at 525 nm. In response to changes in redox conditions, roGFP exhibits reciprocal changes in intensity at the two excitation maxima (494), and its ratiometric characteristics render it insensitive to expression levels (495-497). RoGFP-2 (Cyto roGFP) localizes primarily to the cytoplasm. RoGFP-1 (Mito-roGFP) was engineered to express GFP containing the pyruvate dehydrogenase E1subunit leader sequence for targeting to mitochondria (494). ADR-RES cells transfected with roGFPs were treated with 10 µM RTI-79 and immediately analyzed by FACS with 400 nm and 488 nm lasers for excitation and 515 nm for emission. Oxidized and reduced roGFP assays were conducted by incubating cells in the presence of 25 µM H2O2 and 1 mM DTT, respectively. The oxidation state of roGFP was determined by the ratio of 400 ex/480 ex, which was monitored in real-time from 0 to 12 min.

3.2.12 Confocal microscopy for subcellular localization of ROS

ADR-RES ovarian carcinoma cells were infected with a baculovirus expressing a GFP-tagged recombinant protein (Bacman; Life Technologies) localizing to the mitochondria for 24 hours in the presence of RTI-79. Cells were then co-stained with CellROX (ROS indicator) and DAPI (nuclear stain) for 1 hour. Viable cells were immediately imaged under a confocal microscope. CellRox does not enter into organelles but remains in the cytoplasm and will react with ROS in the vicinity of their origin.

3.2.13 Q-RT-PCR

RNA was extracted from cells using Qiagen RNeasy Mini kit, catalog number 74106 and quantitated by Nanodrop fluorimeter. We utilized QuantiTect SYBR Green RT-PCR Master Mix (Mat. number 1026225) to perform RT and PCR on the same reaction.

Commercially available QuantiTect Primer Assay gene specific primers were used on a Stratagene Mx3005P System that ran the following cycling parameters: Reverse transcription for 30 min 50 C; PCR initial activation 15 min 95 C; followed by 40 cycles of denaturation 15 sec at 94 C, annealing 30 sec 55 C, and extension 30 sec 72 C. Each RNA sample was amplified in triplicate and cycle thresholds (Ct) were determined automatically and delta Ct for each cell line were determined by subtracting the gene of interest Ct from the GAPDH Ct. Differences in delta Ct were determined between cell lines or treatment groups and converted to fold change.

3.2.14 Western blots and antibodies

For protein extraction, cells were solubilized in RIPA lysis buffer (Sigma Aldrich), supplemented with protease inhibitors (Sigma Aldrich), on ice for 20 min.

The detergent extracts were collected and centrifuged at 20,000 × g for 15 min at 4 C and then electrophoresed under reducing conditions by addition of Laemmli SDS-PAGE sample buffer and resolved by SDS-PAGE (BioRad). Western transfer of proteins and blocking of Hybond-ECL (Amersham Biosciences) with 2% BSA were performed following manufacturers' protocol. Immunoblotting with primary antibodies (1:1000) was followed by horseradish peroxidase conjugated anti-rabbit (1:1000) and detection using SuperSignal West Pico chemiluminescent substrate (Pierce, Rockford, IL). Antibodies: Actin: abcam cat#ab3280, Nrf2 (Nrf2): abcam cat# ab62352, NQO1: Cell Signaling Cat#3187, HMOX: Cell Signaling Cat #5853, BiP: Cell Signalling Cat#3177, Total IRE1alpha: Cell Signalling cat#3294, Total PERK: Cell Signaling cat# 5683, CHOP: Cell Signaling cat#2895, XBP-1s: Cell Signaling cat#12782, SYVN: Cell Signaling 14773, Phosph-PERK (1:500): Santa Cruz Biotechnology Cat#sc-32577, and Phospo-IRE1 alpha pSer724: ThermoFisher cat# PA1-16923.

3.2.15 Caspase 3/7 activity

The assay was performed using Promega's Caspase 3/7 Glo kits as per manufacturer's instructions and imaged on a GE INCell Analyzer to detect fluorescent signal. Images were analyzed using the INCell Developer software to determine cell count. Values were averaged over the triplicates and SEM calculated.

3.2.16 RNAseq

RNA was extracted using Qiagen RNeasy miniprep kit from 1ml of cultures containing ~1,000,000 cells. The samples were then depleted of ribosomal RNAs using the RiboZero kit from Epicenter. Adapters were the applied using the Illumina RNA-Seq kit. The samples were sequenced on an Illumina 2500 in single-end mode, collecting 10-15 million reads per sample.

3.2.17 Analysis of RNAseq data

The reads were aligned to the human genome (build GRCh37.69) using Bowtie2 to produce SAM files (498). Cufflinks 2.2.1 (499) was used to calculate normalized FPKM values (Fragments Per thousand (K) nucleotides per Million reads) for each transcript in the annotation. Statistical analysis of differential expression was done using Cuffdiff 2.2.1 (499), which uses the Negative Binomial distribution to assess the significance of fold-changes between samples and assign p-values. The Benjamini-Hochberg procedure for multiple-tests correction was applied to calculate adjusted p-values.

3.3 Results

3.3.1 High throughput screening strategy and identification of rifabutin

We found that rifabutin was highly synergistic with CHOP (cyclophosphamide, doxorubicin, vincristine, and prednisone) in drug-resistant NHL cells. This synergy was discovered by screening a highly diverse collection of approximately 50,000 drug-like molecules including the NIH Clinical Collection (www.nihclinicalcollection.com) against a CHOP-resistant NHL cell line (referred to as G3) in the presence of normally cytotoxic levels of CHOP and then counter screening the library against its CHOP sensitive parental line, ATCC CRL-2631 cells. The resistant G3 sub-cell line was derived from CRL-2631 through repeated on-off cycles of CHOP treatment, analogous to clinical therapy (83). The G3 cells were over 25 times more resistant to doxorubicin (DOX) (IC_{50} 3.1 μM) compared to the parental CRL-2631 cells (IC_{50} 0.12 μM). Following validation of screening hits, we prioritized the natural product-derived antibiotic, rifabutin, because of its potent synergy with CHOP and its lack of inherent cytotoxicity. Additionally, rifabutin has been used clinically for almost 25 years, is orally bioavailable, crosses the blood-brain barrier, and has excellent toxicological and pharmacological profiles.

3.3.2 Development of RTI-79

We determined that the key structural characteristic for rifamycin synergizing activity and low cytotoxicity is the 3,4-[2-spiro-(isobutylpiperidinyl)-(1H)-imidazo] substitution at the 3,4 position of the quinone (Figure 3.1A). For example, rifampicin with its hydroxyquinone (a hydroxy at the 4-position) and (4-methylpiperazin-1-yl)iminomethyl at the 3-position did not show appreciable synergy with DOX in the G3 cells (Figure 3.1B), nor was it cytotoxic on its own in primary human dermal fibroblasts (HDF cells) up to 80 µM (Figure 3.1C), though rifamycin SV with a hydrogen at the 3-position and a hydroxyl at the 4-position and rifamycin B with a hydrogen at the 3-position and carboxymethyloxy at the 4-position were cytotoxic alone (IC_{50} ~ 20 µM and 8 µM, respectively on HDF cells (Figure 3.1C)). This initial SAR pointed to the importance of the hydroxyquinonimine core of rifabutin for the synergy with DOX. A series of substitutions made to the hydroxyquinonimine, such as alkyl, aryl, amide, urea, or carbamate groups (Figure 3.1A) showed considerable variability in the DOX synergizing activity of the analogs (Figure 3.1A); with the substitution of a carbamate being the most potent. Improvements in solubility without losing activity were made by modifications at the ketone group at the 11-position through conversion to a hydroxyl (RTI-175), amine (RTI-176), and imine (RTI-81). Hydroxyl or amine substitutions at the 11-position slightly decreased activity, as measured by the increase of the IC_{50} of DOX against G3 cells, compared to the ketone (RTI-79 vs RTI-175 and RTI-176). Although imine substitution (RTI-81) showed good activity, it was unstable and converted to RTI-79 with a ketone group at the 11-position. The more stable imine derivative ketoxime (RTI-197) was also prepared but had decreased sensitizing activity. RTI-79, in particular, outperformed rifabutin by more than 6-fold in DOX-sensitization on G3 cells (Figure 3.1B). Further, the in vivo toxicity and pharmacokinetics (PK) of RTI-79 were indistinguishable from rifabutin (see below).While the degree of synergy is impressive between rifabutin and

DOX, ratio checkerboard assays and combination index plots demonstrated that RTI-79 showed substantially more synergy with DOX as indicated by increased fractional activity at the ratios tested in G3 cells (between 5:1 and 10:1) (Figure 3.1D). As both DOX and rifamycins are known to use ROS as part of their mechanism of action, we continued to focus on understanding the relationship between ROS production and drug sensitivity for the DOX and rifamycin combination.

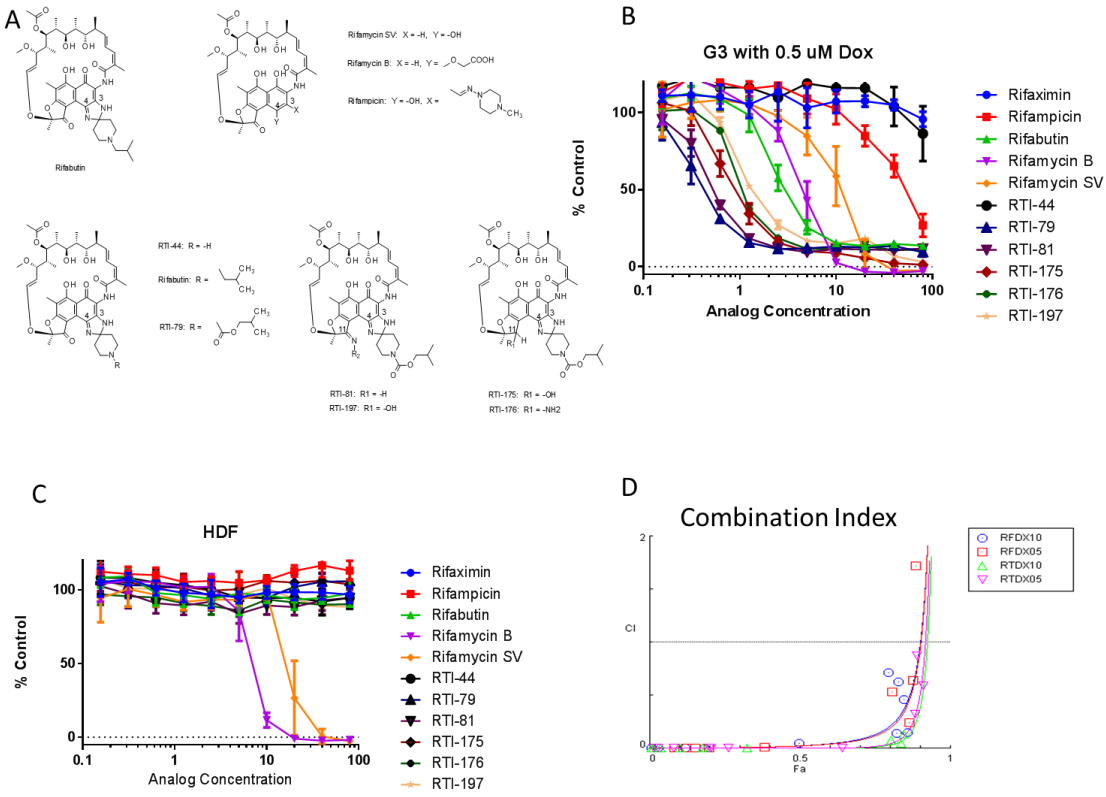

Figure 3.1 Medicinal Chemistry is used to define SAR and discover RTI-79. (A) Chemical structures of rifabutin, and other commercially available rifamycins including rifampicin, and comparison with analog structures of RTI-44, RTI-79, RTI-81, RTI-175, RTI-176, and RTI-197. (B) Relative potency of rifamycin structures and analogs in combination with 0.5 µM DOX on G3 cells as determined by resazurin-based cytotoxicity assay at analog concentrations up to 80 µM. (C) The relative lack of toxicity of rifamycin structures and analogs on primary human dermal fibroblast cells (HDF) as determined by resazurin-based cytotoxicity assay at analog concentrations up to 80 µM. Only rifamycin B and rifamycin SV show toxicity with IC_{50}'s below 20 µM. (D) The combination index plot (also known as the Chou-Talalay plot) generated via Compusyn software showing the resulting combination index (CI) which offers a quantitative definition for synergism when CI < 1. Data for G3 cells and constant-ratio drug combinations of rifabutin: DOX at 10:1 or 5:1 (RFDX10 and RFDX5 respectively) and RTI-79: DOX at 10:1 or 5:1 (RTDX10 and RTDX5 respectively) are plotted and virtually all data points indicate synergy as synergism (CI < 1).

3.3.3 RTI-79 has a broad in vitro spectrum of action

When we evaluated the effects of RTI-79 on 10 NHL cell lines with variable degrees of DOX resistance (Table 3.1 and Figure 3.2a-j), we observed that the potency of DOX against these resistant cells was restored to levels active against sensitive NHL cell lines. For example, 10 μM RTI-79 reduced the DOX IC_{50} for the laboratory-derived G3 cells greater than 8-fold from 3.08 μM to 0.44 μM (Table 1 and Supplementary 1a). Improvements in DOX susceptibility were also observed for patient-derived resistant NHL cell lines (500, 501); RTI-79 shifted the DOX IC_{50} of U-2932 cells from 1 μM to 0.22 μM. Of particular clinical importance is that DHL (WSU-FSCCL, SU-DHL-6, SU-DHL10, and OCI-Ly19) and even THL (SU-DHL-4) (500, 502) cells responded to RTI-79, shifting their sensitivity to DOX to that observed for drug-sensitive NHL cells (Table 1 and Figure 3.2b-e). While all of the resistant NHL cell lines tested responded to RTI-79, only the relatively drug-sensitive cell lines HT and CRL-2631 did not show any statistically significant differences in sensitivity to DOX after the addition of RTI-79 (Table 1 and Figure 3.2g, j).

The liposome formulation of doxorubicin (DOXIL) is widely used as a second-line therapeutic for ovarian cancer. Unfortunately, irrespective of the selected treatment, ovarian cancer recurrence is very common and incurable for most patients (503); hence, any improvements in therapy would be extremely beneficial. We thus tested RTI-79 in combination with DOX in 5 drug-resistant ovarian cancer cell lines including NCI/ADR-RES, the most well-studied and highly drug resistant ovarian cancer cell line ever reported (Table 1 and Figure 3.2k-o). RTI-79 (10μM) shifted the NCI/ADR-RES DOX IC_{50} from over 187μM (504) to 0.23 μM (over 800-fold improvement in potency) (Table 1 and Figure 3.2k). RTI-79 shifted the IC_{50} in resistant cell lines back to what is typically observed in sensitive cell lines. For example, the SK-OV-3 IC_{50} shifted from 1.3 μM to 0.37 μM (3.5-fold) (Table 1 and Figure 3.2l), and the OVCAR-8 IC_{50}

shifted from 0.38 μM to 0.14 μM (Figure 3.2m). Similar to what was observed for NHL, RTI-79 showed the most potent effect in drug-resistant ovarian cancer cell lines. Furthermore, as with G3 NHL cells described above, ratio checkerboard assays and combination index plots indicated that both rifabutin and RTI-79 synergize with DOX in ADR-RES cells (Figure 3.2p).

We found that RTI-79 is also effective in many other types of drug-resistant cancers, including uterine sarcoma, osteosarcoma, pancreatic cancer, and leukemia (Table 1 and Figure 3.2q-t). Moreover, RTI-79 is able to potentiate the activity of a variety of chemotherapeutics, including daunorubicin, epirubicin, vinblastine, etoposide, paclitaxel, and topotecan (Table 1 and Supplementary Fig 3.1w-c´). Indeed, RTI-79 was effective at enhancing the cytotoxicity of a broad range of anti-cancer agents that are typically associated with multi-drug resistance (505).

Table 3.1 RTI-79 spectrum of action

	Cell Line	Drug	IC_{50}	IC_{50} + RTI-79 *p<0.05	Fold Change
NHL	G3	Doxorubicin	3.08	0.44*	6.9
	U-2932	Doxorubicin	1.01	0.22*	4.5
	WSU-FSCCL	Doxorubicin	0.54	0.18*	3.1
	SU-DHL-4	Doxorubicin	0.38	0.12*	3.3
	SU-DHL-10	Doxorubicin	0.19	0.05*	3.6
	OCI-Ly19	Doxorubicin	1.30	0.43*	3.0
	HT	Doxorubicin	0.28	0.24	1.2
	HBL- 1	Doxorubicin	0.60	0.27*	2.2
	SU-DHL-6	Doxorubicin	0.24	0.15*	1.6
	CRL-2631	Doxorubicin	0.12	0.10	1.2
Ovarian	NCI/ADR-RES	Doxorubicin	187.00	0.23*	813.0
	SK-OV-3	Doxorubicin	1.29	0.37*	3.5
	OVCAR-8	Doxorubicin	0.38	0.14*	2.7
	OVCAR-3	Doxorubicin	1.97	1.12	1.8
	OVCAR-5	Doxorubicin	1.31	0.14*	9.7
Uterine sarcoma	MES-Dx5	Doxorubicin	>10	0.24*	>42
Osteosarcoma	U2-OS	Doxorubicin	0.29	0.07*	4.1
Pancreatic	Panc-1	Doxorubicin	1.15	0.27*	4.3
Leukemia	HL-60 Mx	Doxorubicin	0.62	0.19*	3.3
	HL-60	Doxorubicin	0.15	0.10*	1.6
	MOLT4	Doxorubicin	0.08	0.06	1.3
NHL	G3	Dauorubicin	2.01	<0.16*	>12.9
	G3	Epirubicin	7.30	0.16*	45.9
	G3	Vinblastine	2.13	0.13*	16.6
	WSU-FSCCL	ICE	5.42	1.06*	5.1
	WSU-FSCCL	Etoposide	6.06	1.71*	3.5
Ovarian	NCI/ADR-RES	Paclitaxel	>100	0.21*	>480
	NCI/ADR-RES	Topotecan	2.80	0.17*	16.1

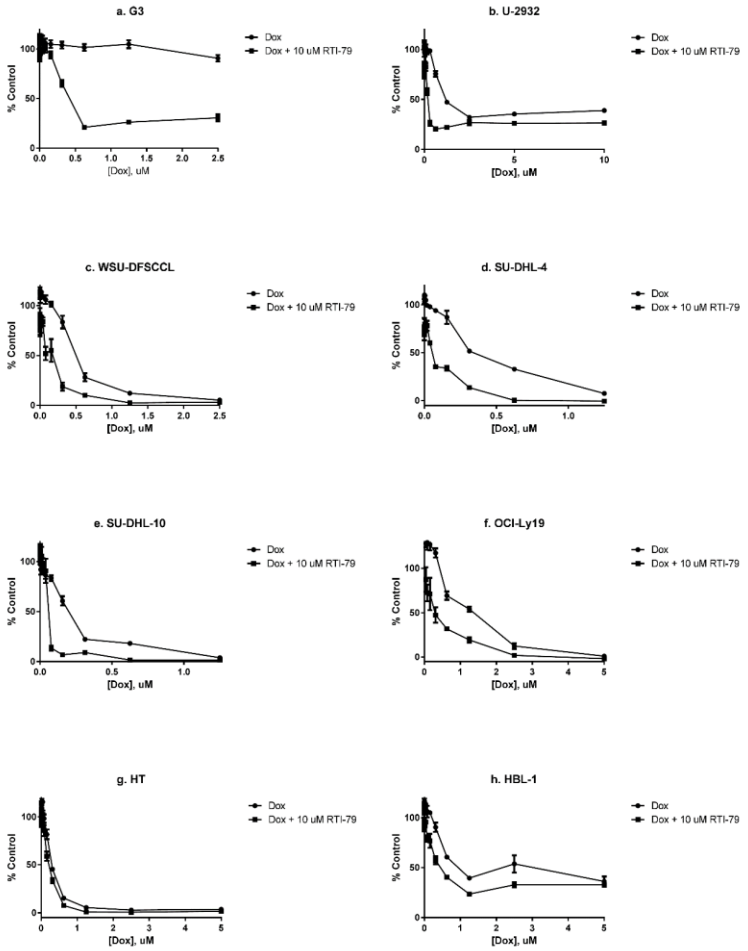

Figure 3.2 Spectrum of RTI-79 activity on various types of cancer cells lines and with multiple chemotherapeutics. (a-o, q-c´) Dose response curves visually depict all data summarized in Table 1. Cell lines are listed in the same order and show cell's dose response to chemotherapy alone or chemotherapy plus RTI-79 as determined by resazurin blue cytotoxicity assay. Error bars represent SEM. (p) The combination index plot (also known as the Chou- Talalay plot) generated via Compusyn software showing the resulting combination index (CI) which offers a quantitative definition for synergism when CI < 1. Data for ADR-RES cells and constant-ratio drug combinations of hifalutin: DOX at 10:1 or 5:1 (RFDX10 and RFDX5 respectively) and RTI-79: DOX at 10:1 or 5:1 (RTDX10 and RTDX5 respectively) are plotted and all data points indicate synergy as synergism (CI < 1).

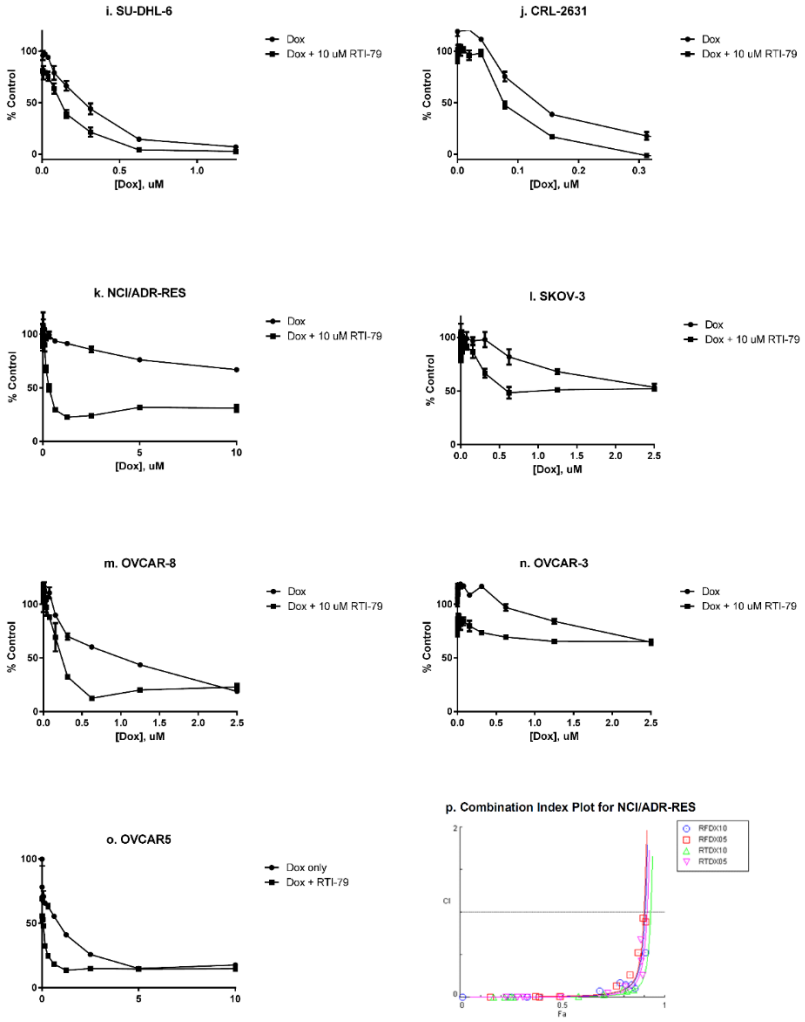

Figure 3.2 Continued

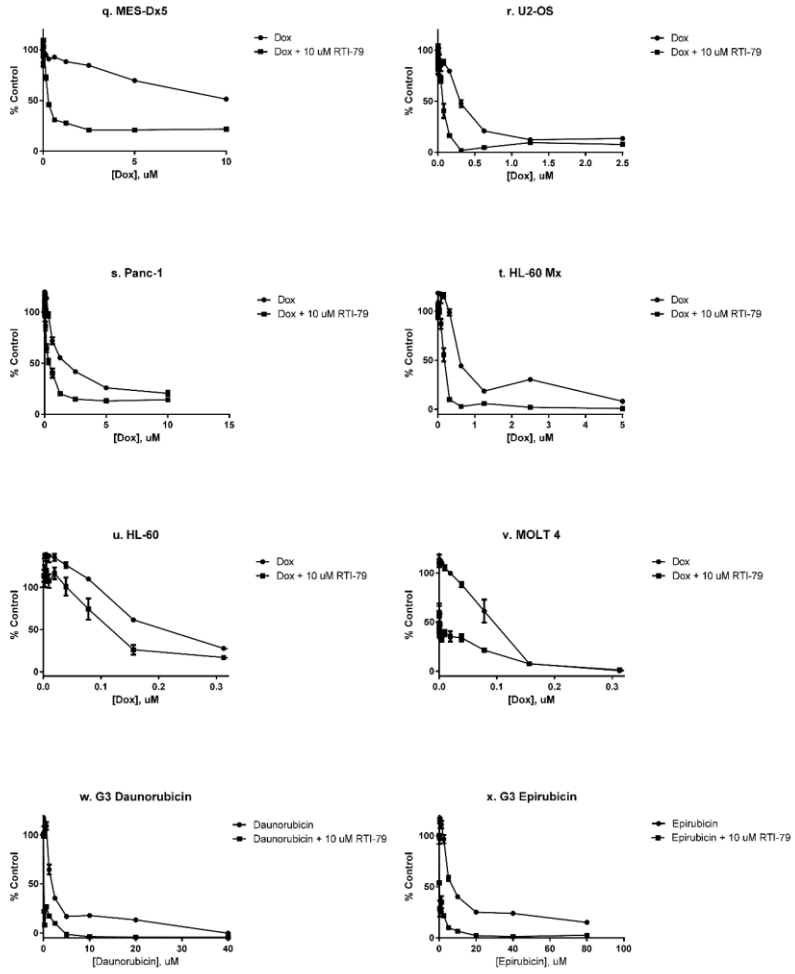

Figure 3.2 Continued

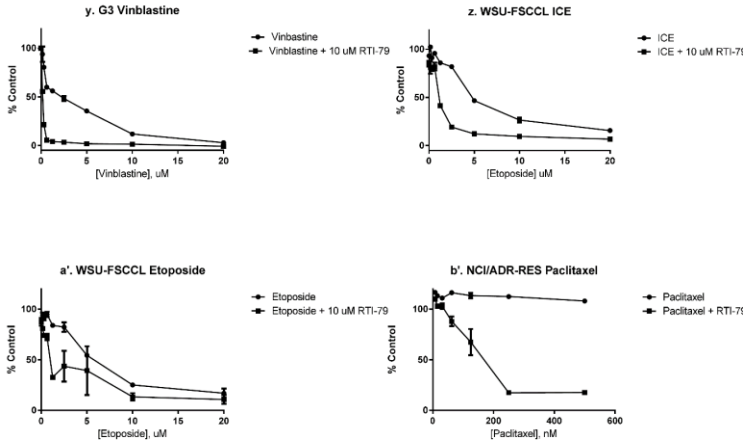

Figure 3.2 Continued

3.3.4 RTI-79 PK and toxicity profiles are equivalent to rifabutin

To evaluate the PK of RTI-79 in comparison to rifabutin, both were given individually via oral administration to dogs at 9 mg/kg and plasma samples were collected over 48-hours. A maximum concentration (Cmax) of 1350 ± 450 ng/mL and 1182 ± 434 ng/mL was reached at 1.7 ± 0.6 and 1.3 ± 0.6 hours post dose with an average half-life of 26.3 ± 5.1 and 19.7 ± 0.8 hours for RTI-79 or rifabutin, respectively (Figure 3.3A). These data indicated that RTI-79's PK characteristics are similar to rifabutin and thus sufficient for clinical use. RTI-79 has no overt toxicity in mice at high doses (250 mg/kg; 10-fold the dose used in efficacy studies [see below] or 5 times the human equivalent dose based on body surface area; BSA). After 3 weekly oral doses of RTI-79, all mice gained weight and no significant differences were observed after analysis of blood and serum for complete blood count (CBC) and manual differentials (Figure 3.3B). Further, rats were given two daily doses of 500 mg/kg RTI-79 and there were no detectible differences in blood chemistry, CBC, or manual differential (data not shown). Finally, we determined that RTI-79 does not appear to exacerbate the known cardiotoxicity associated with DOX by giving both drugs in combination and evaluating body weight and CBCs in one study and heart function via echocardiograms, the most sensitive measure for cardiotoxicity, in a second study (Figure 3.3C-D). Histology was performed on all hearts that received echocardiograms (Figure 3.3E). We saw no significant differences between DOX-alone and DOX plus RTI-79 treatments at therapeutically-relevant doses in any of the measures. The ejection fraction and global and longitudinal strain showed no differences between the two regimens. Statistical differences in body weight, platelet counts, and heart rate ($p<0.5$) were detected between groups treated with DOX and DOX plus RTI-79 in comparison to saline-treated mice (Figure 3.3C-D). Mild histologic changes were also present in both DOX-treated groups (Figure 3.3E). Together these data indicated that while the DOX dosing regimen caused

mild cardiotoxicity, RTI-79 does not worsen mild DOX cardiotoxicity when given concurrently in vivo. Thus, RTI-79 has desirable PK characteristics and is safe in vivo. The low toxicity observed for RTI-79 is consistent with its parent rifabutin molecule, which has an oral LD50 of 3322 mg/kg in mice and a repeated dose toxicity (LOAEL) over 13 weeks in mice of 100 mg/kg/day.

A

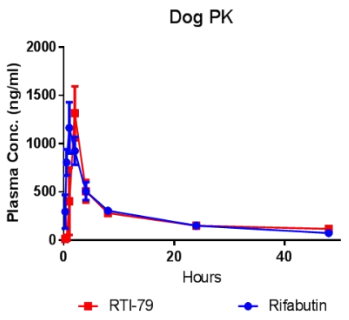

B

Assay	3weekly doses 250 mg/kg		
Complete Blood Count			
	(Reference)	Mean RTI-79	SEM RTI-79
WBC	1.0-12.2	14.4	0.72
RBC	7.14-9.71	9.71	0.26
HGB	11.3-15.6	14.95	0.26
HCT	36.5-47.3	45.6	0.89
MCV	43.6-55.9	47.12	0.45
MCH	14.0-18.0	15.86	0.11
MCHC	28.4-35.3	33.68	0.21
PLT	625-2241	1015	67.84
Manual Differential			
NEUT ABS	0.0-2.5	1.02	0.09
LYMPHS ABS	2.4-10.2	13.55	0.28
MONOS ABS	0.0-0.4	0.27	0.07
EOS ABS	0.0-0.2	0.05	0.04
SEGS	0-38	6.4	0.24
LYMPHS	4-100	89.8	0.37
MONOS	0-6	2.6	0.51
EOS	0-4	0.6	0.40

C

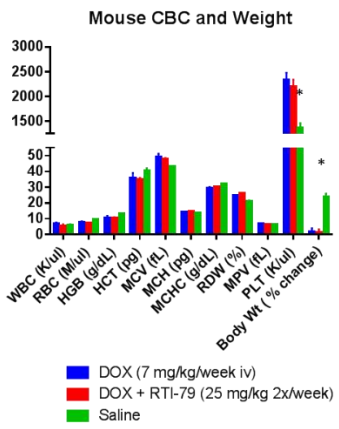

D

Post-treatment Echocardiogram Summary						
	Saline (n=8)		Dox (n=8)		Dox + RTI-79 (n=8)	
	Mean	SEM	Mean	SEM	Mean	SEM
LVEDD	2.83	0.12	2.85	0.06	2.70	0.05
LVESD	1.02	0.07	1.15	0.07	1.02	0.08
IVS;d (mm)	1.36	0.06	1.21	0.07	1.16	0.04
LVPW;d (mm)	1.18	0.08	1.07	0.07	1.17	0.08
FS (%)	63.94	1.83	59.74	2.10	62.51	2.48
EF (%)	92.54	0.89	89.92	1.44	91.54	1.41
Heart Rate (bpm)*	732.36	9.14	691.14	11.34	675.83	20.87
GLS (%)	-15.08	1.80	-12.97	2.37	-16.23	1.61

LVEDD	left ventricular end diastolic dimension
LVESD	left ventricular end systolic dimension
IVS,d	interventricular septal wall thickness at end diastole
LVPW,d	left ventricular posterior wall thickness at end diastole
FS	fractional shortening
EF	ejection fraction

E

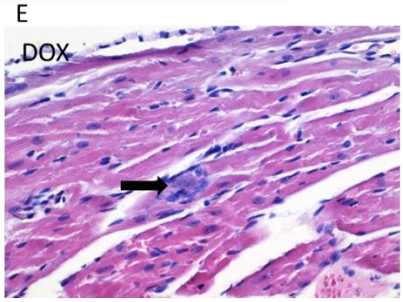

Figure 3.3 PK and toxicity data for RTI-79. Data indicate that it has PK characteristics similar to rifabutin, is not toxic at high doses, and does not exacerbate or add to the known cardiotoxicity of DOX. (A) Plasma concentration of rifabutin and RTI-79 over time in male beagle dogs after oral administration of 9 mg/kg compound over a 48 hour time period. (B) Table of CBCs and manual differentials after administration of 3 weekly doses of high concentration (250 mg/kg) RTI-79 in mice indicating little change and lack of toxicity. Error bars represent SEM. (C) Mouse CBCs and weights after 6 weekly treatments of: saline, 7 mg/kg iv DOX given once weekly, or combination 7 mg/kg iv DOX given once weekly with 25 mg/kg RTI-79 given orally the same day and 24 hours post-DOX treatment. Error bars represent SEM. * indicates $p<0.05$ for saline treatment in comparison to both DOX and DOX+ 79. (D) Echocardiogram measurements after five weekly treatments of: saline, 7 mg/kg iv DOX, or combination 7 mg/kg iv DOX with 25 mg/kg oral RTI-79 given on the same day and 24 hours post-DOX treatment. Only heart rate is significantly affected ($p<0.5$) as indicated with "*". (E) H&E stain of histological section of hearts from echocardiogram study. Analysis of sections show that 2 of 8 hearts that received DOX only treatment have single necrotic fibers with surrounding inflammation and macrophage (as indicated by the arrow); however, only 1 of 8 hearts treated with DOX+RTI-79 show this feature. Necrotic fibers were not detected in saline treated or RTI-79 only treated hearts.

3.3.5 RTI-79 efficacy in in vivo xenograft models of NHL and ovarian cancer

We performed efficacy studies in mouse xenograft models of human DLBCL and ovarian cancer cells. Tumors were treated with saline, RTI-79 alone, chemotherapeutic alone (DOX, etoposide, or DOXIL), or RTI-79 in combination with drug. In all cases, there was a dramatic reduction in tumor growth when combination therapy was given. For example, in mice with tumors derived from the DHL cell line WSU-FSCCL, clinically relevant levels of DOX had little effect on tumor growth. However, DOX + RTI-79 (25 mg/kg po) stopped tumor growth ($p=0.0034$ for DOX vs DOX+ RTI-79) (Figure 3.4a-b). Similarly, there was a significant reduction in growth of WSU-FSCCL tumors with the combination of etoposide (a component of ICE salvage chemotherapy) and RTI-79 compared to etoposide alone ($p = 0.02$) (Figure 3.4c-d). Mice harboring ovarian cancer xenografts derived from NCI/ADR-RES and SK-OV-3 (another well-studied drug-resistant ovarian cancer cell line) cells were given weekly DOXIL cycles with and without RTI-79 treatment at 24 and 48 hours post DOXIL. Both ovarian cancer xenograft models showed efficacy of RTI-79 + DOXIL over DOXIL alone ($p= 0.0004$ and 0.0002 respectively) (Figures 3.4e-h). Again, DOXIL-alone treatment had minimal effect on tumor growth for ADR-RES xenografts and no effect on SK-OV-3 xenografts. However, the addition of RTI-79 to DOXIL therapy stopped tumor growth in ADR-RES xenografts and severely limited it for SK-OV-3 xenografts. Furthermore, the activity of rifabutin against xenografts is statistically inferior to the addition of RTI-79 ($p=0.01$), and rifabutin treatment is not significantly better than saline treatment.

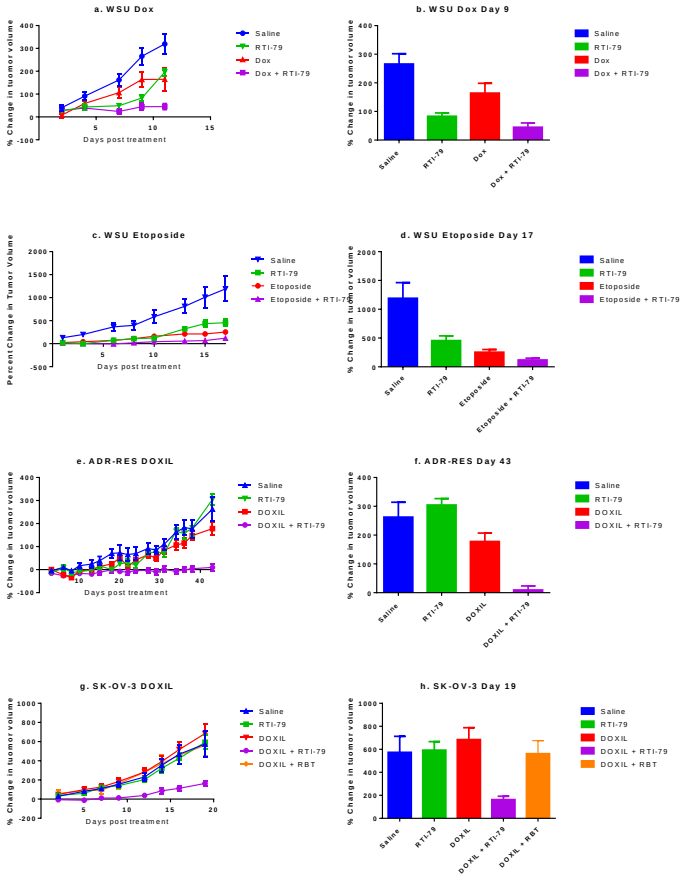

Figure 3.4 RTI-79 in combination with standard chemotherapies is effective in treating mouse xenograft models of NHL and ovarian cancer in 6-8 week old female mice. Two-tailed Student's t-test was run to evaluate statistical significance between groups. Samples were unpaired. (a-b) SCID mice were injected with 1 X 10^7 WSU-FSCCL cells. After one week tumors were an average size of 370 mm^3 and treatments began. Arms included saline (Day 0 and Day7), i.v. 3.3 mg/kg DOX (Day 0 and Day7), oral 25 mg/kg RTI-79 (Day 0, 1, 7, and 8), and combination DOX (Day 0 and 7) with RTI-79 (Day 0, 1, 7, and 8). C d.) WSU-FSCCL xenografts were implanted into SCID mice and treated 11 days later when tumor volume was approximately 165 mm^3. Three total treatments were given weekly starting at Day1. Arms included: saline, 12 mg/kg etoposide given on days 1, 2, and 3 of each week, 25 mg/kg RTI-79 given on days 1, 2, and 3 of each week, or etoposide plus RTI-79. (e-h) In the third and fourth study, nude mice were injected with either 1 X 10^7 ADR-RES cells and treated 9 days later when tumor volume was approximately 90 mm^3 (e, f) or 1 X 10^7 SK-OV-3 cells and treated 3 weeks later when tumor volume was approximately 100 mm^3 (g, h). Arms included: saline, 7 mg/kg DOXIL iv given on Day 1 of each week, 25 mg/kg oral RTI-79 given on days 2 and 3 of each week, a combination of DOXIL and RTI-79, or a combination of DOXIL and rifabutin. Error bars represent SEM.

3.3.6 RTI-79 overcomes drug-resistance through a rapid increase in superoxide and hydrogen peroxide

Many different approaches were used to determine the mechanism of action (MOA) of rifabutin and RTI-79 in sensitizing drug resistant cancer cells to standard chemotherapy. First, we performed RNAseq to evaluate the transcriptome changes in resistant (G3 and ADR-RES) and sensitive (CRL2631 and OVCAR8) cell lines with and without treatment with RTI-79 for 1 hour and 6 hours. We found that at these time points, there were few transcripts that showed large changes due to treatment (Figure 3.5A). We found that overexpression of the drug pump ABCB1 (P-gp) was associated with chemoresistance in NCI/ADR-RES and G3 cells. P-gp was upregulated over 9.3-fold in the resistant G3 cells as compared to the more sensitive CRL-2631cells, and P-gp was upregulated 89-fold in the resistant NCI/ADR-RES cells as compared to the more sensitive OVCAR-8 cells (Figure 3.5B). Indeed, the overexpression of P-gp in the NCI/ADR-RES cell line is already well-documented (506). Second, we determined that RTI-79 and rifabutin are substrates for P-gp (Figure 3.5C), and they can prevent calcein-AM efflux from ADR-RES cells, a measure of drug pump activity (Figure 3.5D). In addition, RTI-79 caused increased DOX accumulation in G3 and ADR-RES cells (Figure 3.5E-F). However, inhibition of the P-gp drug pump is unlikely to be a primary mechanism, as P-gp levels were not elevated in all cell lines where we observed RTI-79 chemosensitizing activity (Figure 3.5G).

Finally, other ansamycins such as geldanamycin are known to inhibit HSP90 and prevent expression of HSP90 targets such as RAF-1, but we did not detect any changes in RAF-1 expression in rifabutin-treated cells. Moreover, rifabutin and RTI-79 did not bind to purified recombinant HSP90 (Figure 3.6).

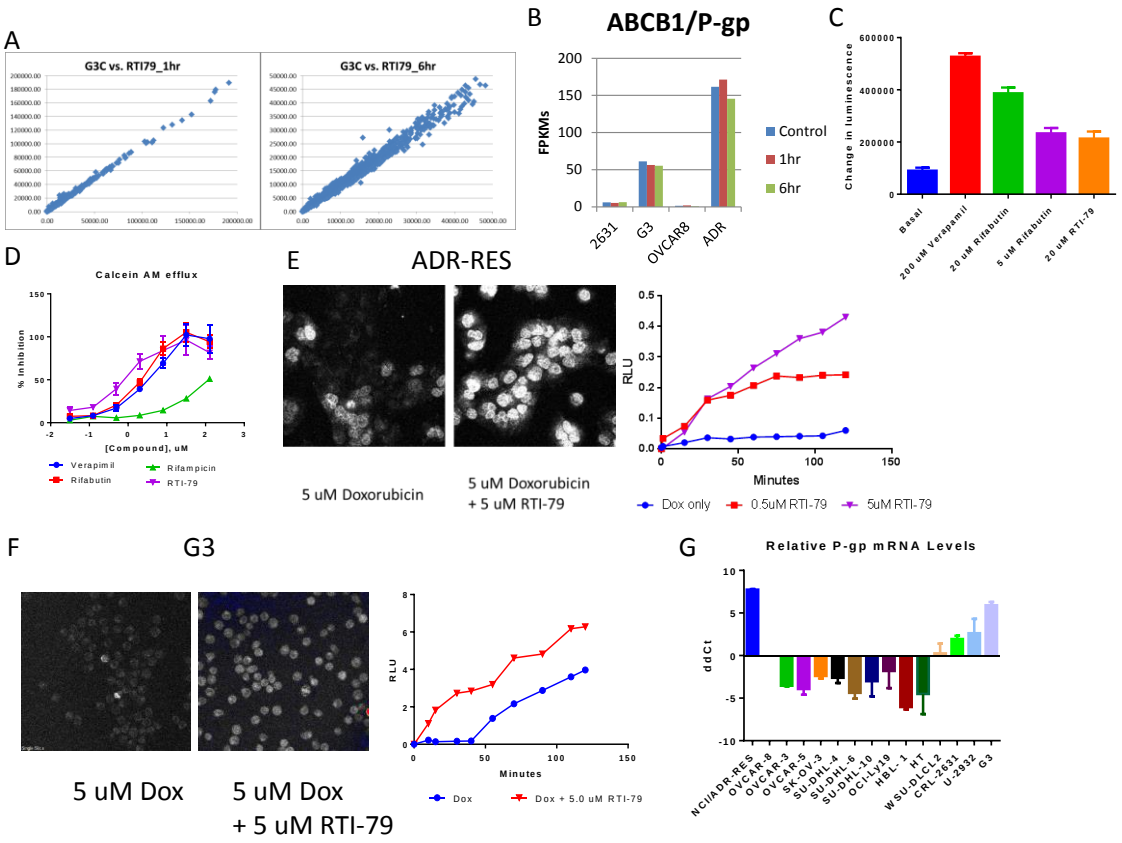

Figure 3.5 RTI-79 overcomes chemoresistance associated with overexpression of drug pumps and results in elevated intracellular drug concentrations. (A) RTI-79 induces a little change in the transcriptome after 1 and 6 hours of treatment in G3 cells based on RNA-Seq analysis. (B) ABCB1/MDR1/P-glycoprotein mRNA expression in drug sensitive (CRL-2631 and OVCAR-8) and resistant (G3 and NCI/ADR-RES) cell lines indicates its overexpression is associated with resistance. (C) Stimulation of P-gp ATPase activity in P-gp Glo assay by rifabutin, RTI-79, and known Pg-p substrate verapamil indicates that RTI-79 is a substrate for P-gp. (D) Inhibition of Calcein AM efflux by RTI-79, rifabutin, rifampicin, and known inhibitor verapamil indicates that RTI-79 inhibits efflux. (E, F) Increased intracellular DOX fluorescence inside ADR-RES cells (E) or G3 cells (F) after treatment with RTI-79. From left to right: live micrograph of cells treated with 5 µM DOX for 2 hours; live micrograph of cells treated with 5 µM DOX in combination with 5 µM RTI-79 for 2 hours; quantitation of relative light units of intracellular DOX fluorescence over 2 hours live imaging time for cells treated with DOX only, or DOX plus RTI-79. (G) Relative P-gp mRNA levels in various cancer cell lines compared to OVCAR8 ovarian cancer cells as determined by q-RT-PCR. Note that y-axis represents ddCt values for visualization purposes. Error bars represent SEM.

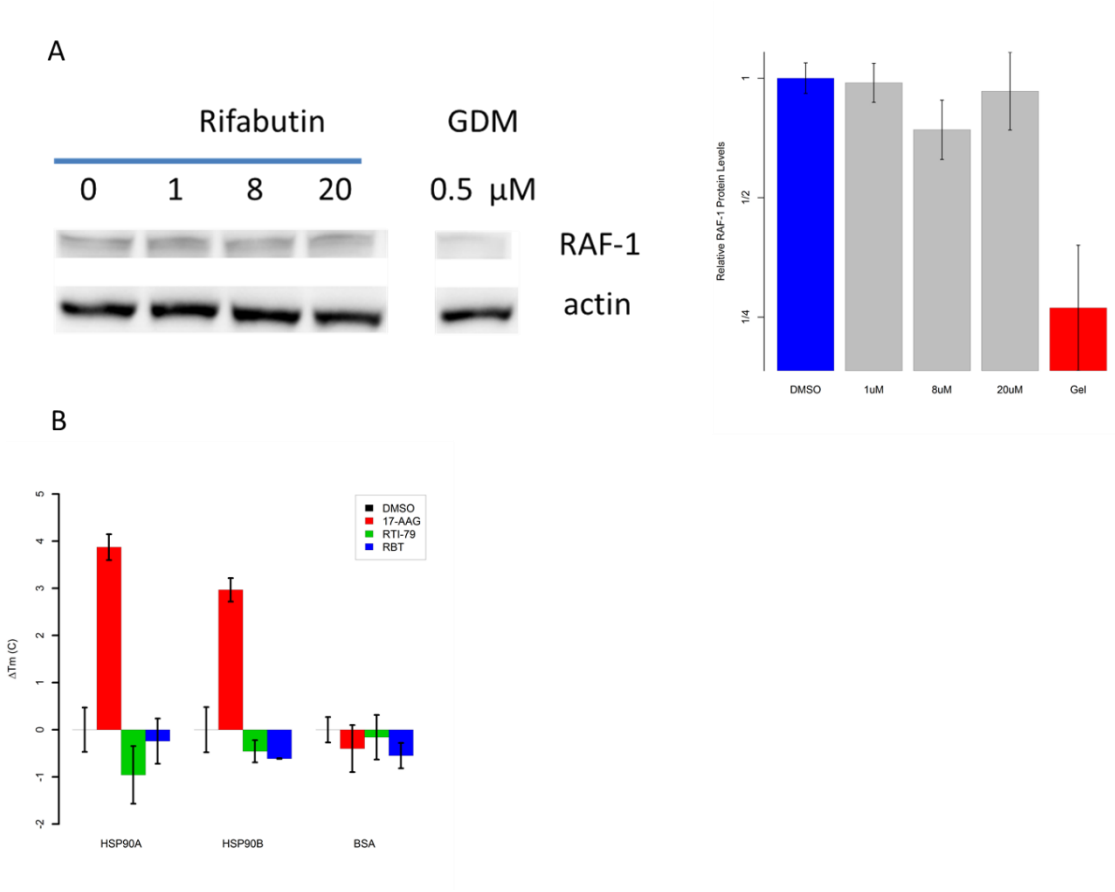

Figure 3.6 Rifabutin and RTI-79 are not effective inhibitors of HSP90. (A) Inhibition of HSP90 by known inhibitor geldanamycin (0.5 µM) leads to reduced RAF-1 protein as detected by western blot and densitometry, but up to 20µM rifabutin does not. (B) Inhibition of HSP90A and HSP90B refolding by known inhibitor 17-AAG causes changes in Tm, but rifabutin and RTI-79 do not. BSA was included as a control to show specificity of 17-AGG for HSP90. Error bars represent SEM. Further, the tip of the geldanamycin ansa ring, which has a carbamate, binds near the bottom of the Hsp90 pocket and makes a high density of van der Waals contacts [1]. The carbamate amino group makes a critical hydrogen bond to one of the Asp93 side chain oxygen atoms. Note that RBT and RTI-79 have no carbamate at this position to make these intimate contacts and have a larger ring structure making it less likely to fit in the active site of Hsp90.

Consistent with other studies that report the association of low ROS levels with resistance, basal ROS levels in the drug-resistant G3 and NCI/ADR-RES cells were much lower (13 and 3.3-fold respectively) than basal ROS levels of their respective drug-sensitive parental lines, CRL-2631 and OVCAR-8 (Figure 3.7A). Treatment of the cells with RTI-79 dramatically increased ROS in all cancer cells tested, but paradoxically not in primary fibroblasts (HDF cells). For instance, RTI-79 increased ROS over 23-fold in G3 cells and 12.7-fold in NCI/ADR-RES cells, as measured with the CellROX ROS indicator (Figure 3.7B). RTI-79 also increased intracellular ROS as measured by an oxidation sensitive GFP construct, as treatment resulted in increases of emission spectra ratios for both cytoplasmic and mitochondrial GFP (Figure 3.7D). Further, ROS-oxidized CellROX primarily co-localized to mitochondria based on confocal microscopy, which showed that the red CellROX fluorescence co-localized with a mitochondrial GFP-tagged recombinant protein (Figure 3.7C). Induction of ROS was rapid, e.g. in as little as 10 minutes in G3 cells (Figure 3.7D). Such rapid induction indicates that this initial response does not involve transcription or translation which would likely require hours. As determined by ROS species-specific dyes, we observed a greater than 12-fold increase in intracellular superoxide levels in RTI-79 treated G3 cells, a two fold increase in hydrogen peroxide, and no changes in hydroxyl radicals (Figure 3.7E). This is consistent with redox cycling of quinone-containing compounds (such as rifamycins) that are known to generate primarily superoxides (507, 508). We found that either by dose-response or by comparing compounds within the series, ROS induction was highly correlated to synergy with DOX. For example, RTI-79 generated higher levels of ROS compared to rifabutin. Moreover, rifampicin does not produce ROS and does not synergize with DOX to reverse drug resistance (compare Figure 3.7F with Figure 3.1B). RTI-79 was the most potent synergizer and produced up to 10 fold more ROS, compared to rifabutin at the same dose. To further demonstrate the correlation between synergy and ROS levels, when the anti-oxidants

quercetin and luteolin (509) were added they were able to reduce RTI-79-induced ROS by over 17-fold with quercetin and up to 3-fold with luteolin (Figure 3.7G-H). Most importantly, altering ROS levels with these compounds concomitantly alters RTI-79 + DOX induced cytotoxicity; quercetin and luteolin are protective against RTI-79 + DOX induced cytotoxicity in G3 and ADR-RES cells (Figure 3.7I-G). For example, the addition of 1 μM RTI-79 to DOX in G3 cells kills virtually all cells, but the addition of quercetin rescues up to 60% of the cells (Figure 3.7I). Quercetin and luteolin decreased ROS correlated directly to the degree to which they decreased drug sensitivity.

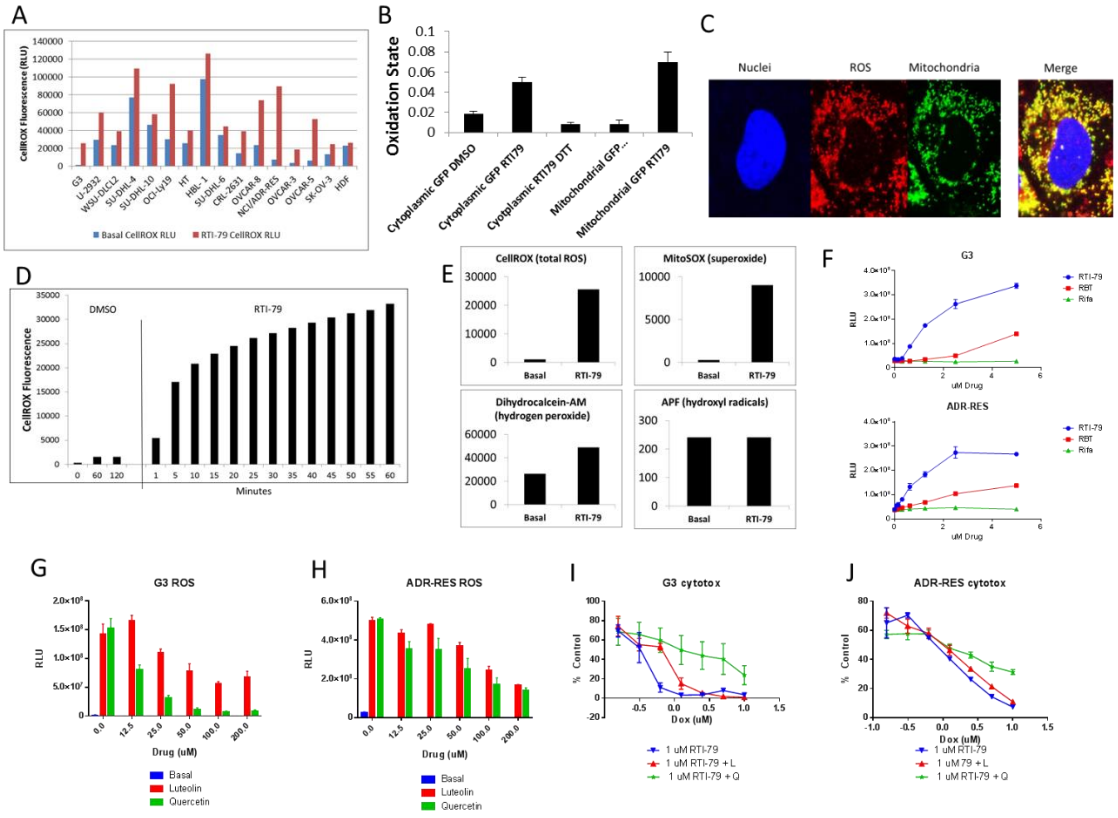

Figure 3.7 RTI-79 overcomes chemoresistance associated with low ROS by inducing a rapid increase in superoxide and hydrogen peroxide, but can be quenched with antioxidants luteolin and quercetin. (A) Basal and RTI-79 (10 µM) induced ROS in NHL, ovarian cell lines, and primary fibroblasts as determined by CellROX and FACs. (B) Confirmation that ROS are indeed generated by RTI-79 by utilizing an assay independent of fluorescent dye up-take e.g. a GFP Biosensor. The GFP Biosensor changes oxidation state after encountering ROS and/or RTI-79 (10 µM) both in the cytoplasm and the mitochondria. DMSO was utilized as a no treatment control. DTT (100 µM), a known ROS scavenger was utilized to antagonize RTI-79. (C) Confocal analysis indicates that ROS originates primarily at the mitochondria in NCI/ADR-RES cells. (D) RTI-79 (10 µM) induces ROS in as little as 5 minutes and ROS remains sustained over 60 minutes in G3 cells. (E) ROS species specific dyes for superoxide, hydrogen peroxide, and hydroxyl radicals indicate that RTI-79 primarily produces superoxide in G3 cells. (F) Dose-dependent quantitation of ROS (as measured by CellROX imaging) with RTI-79, rifabutin, and rifampicin in G3 and ADR-RES cells. (G-H) The addition of anti-oxidants quercetin and luteolin reduce RTI-79-induced ROS levels in G3 cells (G) and ADR-RES cells (H). (I-J) The addition of antioxidants quercetin (100 µM) and luteolin (50 µM in G3 cells and 100 µM on ADR-RES cells) reduce RTI-79 (1 µM) + DOX induced cytotoxicity. Error bars represent SEM.

3.3.7 Cancer cells cannot respond to RTI-79-induced ROS because of the inhibition of Nrf2 Activity

Normally, ROS production is controlled by the induction of the antioxidant response system regulated by Nrf2 (510). Review of our transcriptome data indicated that there was no antioxidant response as a set of 38 well-studied Nrf2 targets and their FPKMs were evaluated with statistical comparisons of p-values and adjusted q-values in CRL-2631, G3, OVCAR-8, and ADR-RES cells (Figure 3.8A). While, we saw induction of the Nrf2 targets NQO1 and HMOX1 by q-RT-PCR in as little as 6 hours when cells were treated with tBHQ or Menadione (known antioxidant response generators), this response was not seen in cells treated with RTI-79 (Figure 3.8B), despite the very large increases in ROS that we observe following RTI-79 treatment. Further, we saw a reduction in Nrf2 protein levels after treatment of G3 and ADR-RES cells with RTI-79 by 78% and 61%, respectively (based on Student's t-test, p=0.007 and 0.03); tBHQ led to a 2-fold increase in Nrf2 protein levels (Figure 3.8C-D). We also saw a reduction in the downstream Nrf2 targets, HMOX, by 18% in G3 cells and 87% in ADR-RES cells, and NQO1 by 64% in ADR-RES cells by Western blot (Figure 3.8C-D). When ROS levels are low, Nrf2 homeostasis is maintained in the cytoplasm via KEAP1 and ubiquitin-mediated degradation (511, 512). In efforts to understand the observed loss of Nrf2, we investigated SYVN1 (Hrd1) as it is an E3 ubiquitin ligase that interacts directly with Nrf2. Activation of the IRE1a-XBP1 arm, one of the 3 major pathways of the unfolded protein response (UPR), transcriptionally upregulates SYVN1 by approximately 2-fold in liver cirrhosis, resulting in enhanced Nrf2 ubiquitination, degradation, and attenuation of the Nrf2 signaling pathway (513). We find that RTI-79 increases SYVN1 expression by approximately 2 to 4-fold over time in both G3 and ADR-RES cells (Figure 3.8E). Again, the addition of quercetin and luteolin antagonized RTI-79-induced expression of SYVN1 at the 8 hour time point by up to 4-fold.

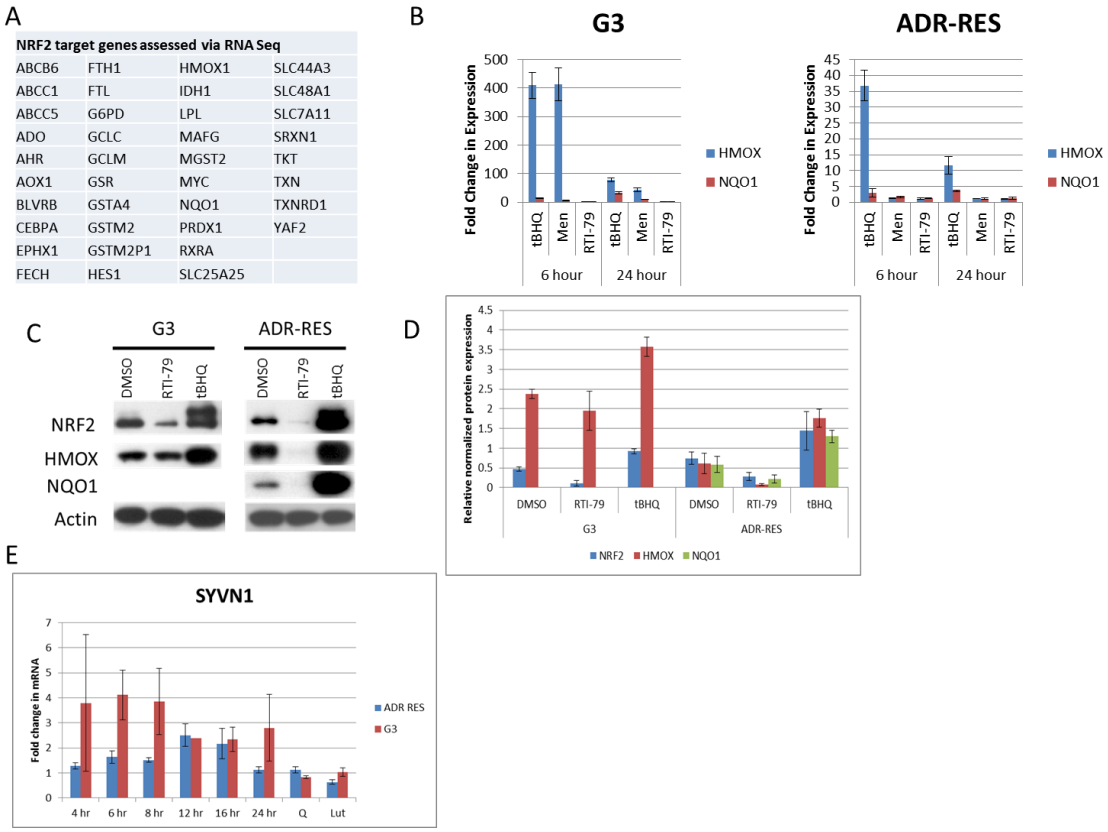

Figure 3.8 RTI-79 does not induce antioxidant response and inhibits Nrf2 activity. (A) Table of 38-known Nrf2 target genes evaluated by RNA-Seq after 1 and 6 hours treatment with RTI-79. (B) q-RT-PCR confirms the lack of antioxidant response with RTI-79 treatment: fold change in HMOX and NQO1 mRNA at 6 and 24 hours in G3 and ADR-RES cells after treatment with RTI-79 (10 µM) and known anti-oxidant response inducers tBHQ (50 µM) and menadione (50 µM). (C) Representative blots showing that treatment of G3 and ADR-RES cells with 10 µM RTI-79 for 16 hours results in decreased Nrf2 and HMOX protein levels by western blot analysis. ADR-RES cells also show decreased NQO1 protein levels after RTI-79 treatment. (G3 cells did not have detectable NQO1 protein levels by Western blot). The known Nrf2 stabilizer, tBHQ (50 µM) was used as a control (D) Average densitometric quantification of western blots for each cell line and treatment group normalized to actin concentration. The graph represents the average of 3 independent experiments. (E) Treatment of G3 and ADR-RES cells with 10 µM RTI-79 increases the mRNA expression of SYVN1 a known E3 ubiquitin ligase that interacts directly with Nrf2. The addition of antioxidants quercetin (100 µM) and luteolin (200 µM) antagonizes RTI-79 induced SYVN1 expression at 8 hours. Error bars represent SEM.

3.3.8 RTI-79 induces UPR in drug resistant cancer cells

Sustained ROS production has been linked to ER stress and the UPR (514). We utilized our transcriptome data and performed Generally Applicable Gene-set Enrichment (GAGE) and evaluated the GO term "response to unfolded protein" (GO:0006986) representing 157 genes. It was significantly enriched for differential expression ($p<0.05$) in all the cells (2631, G3, OVCAR8, and ADR-RES) at both 1 and 6 hour time points (data not shown). We tested this concept further by evaluating transcripts by q-RT-PCR. The addition of 10 µM RTI-79 results in increased expression of DDIT3/CHOP (up to 5-fold) and HSPA5A/BiP (up to 4-fold), and minimally increased expression of ATF4 mRNAs in both G3 and ADR-RES cells at various time points between 4 and 24 hours (Figure 3.9A-B). Dynamic and temporal changes in expression are known to occur based on the duration of stress (515). The addition of quercetin or luteolin antagonized the increased expression levels in ADR-RES cells at 8 hours of RTI-79 treatment but not necessarily in G3 cells (Figure 3.9C) indicating that reduction of RTI-79-induced ROS dampens the UPR response. RTI-79 treatment also resulted in increased protein expression of the IRE1a-UPR associated proteins (p-IRE1a, HSPA5A/BiP, and XBP1-s) at 8 and 16 hours (Figure 3.9D-E), but not p-PERK (Figure 3.9E). As might be anticipated with the activation of the p-IREa and XBP1-s arm of the UPR pathway, SYVN protein expression was also increased with the addition of RTI-79. RTI-79-induced expression of these proteins was also antagonized by the addition of quercetin or luteolin in ADR-RES cells (Figure 3.9D-E), again indicating that reduction of ROS dampens the UPR response. In addition, we observed that RTI-79 treatment resulted in increased total cellular ubiquitination of proteins, as would be anticipated for compounds that induce UPR (Figure 3.9F). However, RTI-79-induced UPR does not trigger apoptosis as it is not toxic when used alone. Indeed, CASP3 cleavage in G3 cells is not induced by RTI-79 alone (Figure 3.9G). When both RTI-79 and DOX are used together, we observe

CASP3 cleavage (Figure 3.9G) and cytotoxicity (Figure 3.1B). We propose that RTI-79 + chemotherapeutic induces chronic UPR and apoptosis. Hence, we propose a model (Figure 3.9H) in which ROS is rapidly induced by direct redox cycling of RTI-79, which results in UPR and SYVN1 induction. SYVN1, in turn, downregulates the Nrf2 pathway causing a state of oxidative stress, which sensitizes the chemoresistant cells to DOX and other chemotherapeutics.

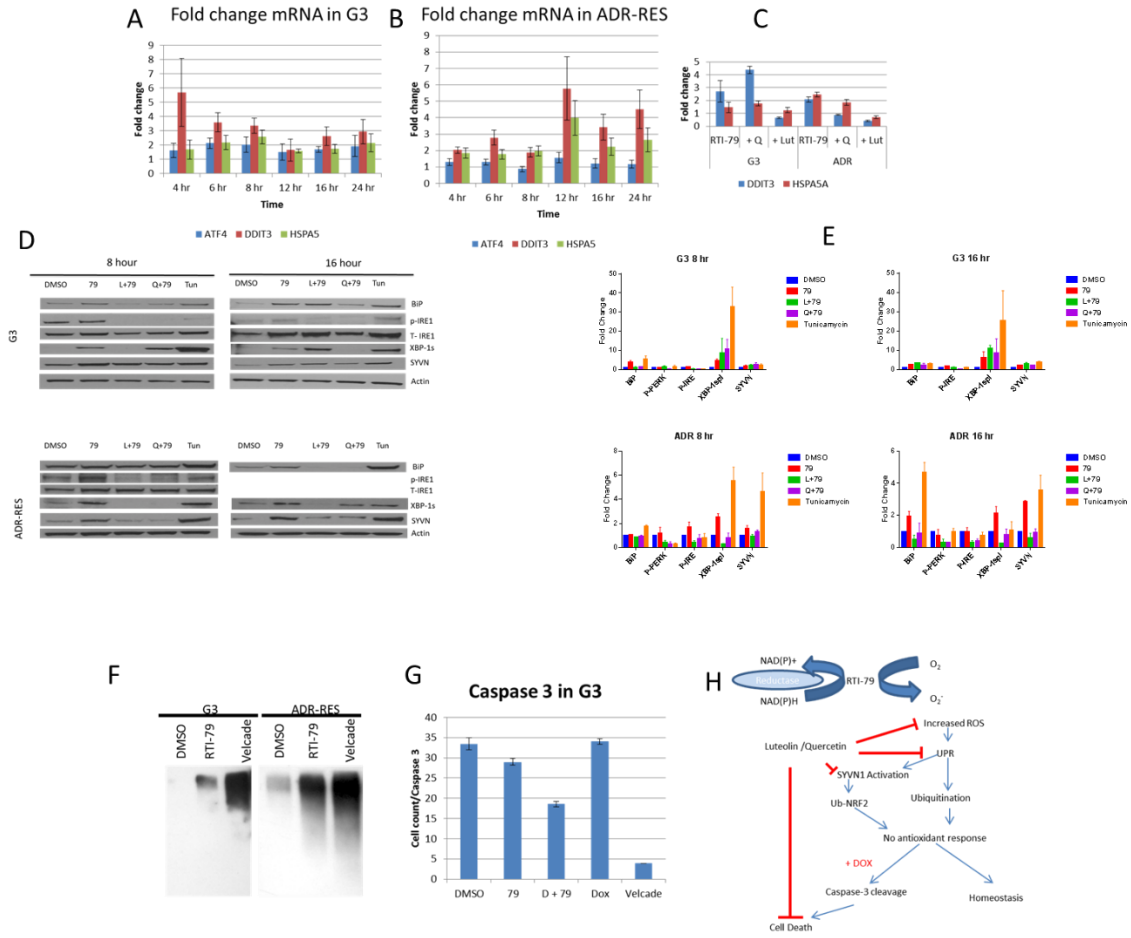

Figure 3.9 RTI-79 induces UPR. (A-C) The addition of 10 µM RTI-79 induces the expression of genes associated with UPR in both G3 (A, C) and ADR-RES cells (B-C) over 4-24 hours. (C) The addition of antioxidants quercetin (100 µM) and luteolin (200 µM) antagonizes RTI-79 induced gene expression at 8 hours. (D-E) Addition of RTI-79 induces the expression of proteins associated with UPR in both G3 and ADR-RES cells. Addition quercetin (100 µM) and luteolin (50 µM) antagonizes RTI-79 induced protein expression. (F) The addition of 10 µM RTI-79 to G3 and ADR cells results in increased total cellular ubiquitination after 4 hours. 100 nM Velcade was used as an inhibitor of the proteasome and a control for increased ubiquitination. (G) RTI-79 alone does not increase caspase-3 activity (a measure of apoptosis) as determined by Caspase Glo 3/7 assay. G3 Cells were treated with compounds and then imaged to determine the ratio of the total number of cells over the number that are positive for Caspase 3 activity. (H) Model for RTI-79 mechanism of action. RTI-79 undergoes redox cycling to produce superoxide. Increased ROS induces UPR and activation of SYVN1 which in turn lead to increased ubiquitination of total cellular proteins and Nrf2. Loss of Nrf2 leads to the absence of the antioxidant response. When only RTI-79 is present the cell is able to reach homeostasis, but when DOX or another chemotherapeutic is present in combination, the cells become sensitized, activate Caspase 3 and undergo cell death. Error bars represent SEM.

3.4 Discussion

Today, most cancer deaths are the result of recurrence, a situation where a cancer returns after remission. Often recurrent cancer will have either reduced or completely lost sensitivity to chemotherapy. There are currently no drugs that specifically target drug-resistant cancers. We have developed a novel and potent compound that reverses drug resistance for a number of cancers. RTI-79 is not designed to be a cancer drug, per se, but a versatile new compound that sensitizes cancer cells to existing approved cancer drugs without adding any new toxicity. Here we are able to demonstrate that low (10 μM), non-toxic concentrations of rifabutin and RTI-79 are very effective at synergizing with chemotherapeutics by generating high levels of intracellular ROS in resistant cancer cells.

Elevated levels of ROS are common in cancer cells, and many chemotherapeutics, including DOX, increase the levels of ROS as part of their mode of action. We show, in agreement with other studies, that a number of drug-resistant cancer cells have significantly lower levels of ROS. Figure 3.7A shows that basal ROS levels in the drug-resistant G3 and NCI/ADR-RES cells were much lower than basal ROS levels in their respective drug-sensitive parental lines, CRL-2631, and OVCAR-8. This is believed to occur through modifications of their complex, and not entirely understood, antioxidant response systems. Low ROS likely gives cancer cells a selective advantage for survival in the face of chemotherapy. We have demonstrated that for many cancers there is a direct correlation between ROS levels in the cell, and sensitivity to chemotherapy (Table 3.1 and Figure 3.7A, G-J). The higher the ROS levels, the more sensitive the cancer cell is to chemotherapy. As examples, CRL-2631 have about 13-fold higher ROS and are about 25-times more sensitive to DOX than G3 cells, and OVCAR-8 have about 3.3-fold higher ROS and are about 490 times more sensitive than NCI/ADR-RES cells.

When we increase ROS levels with small molecules that generate ROS, we see significant increases in their sensitivity (Figure 3.7A). RTI-79 increased ROS over 23-fold in G3 cells and 12.7-fold in NCI/ADR-RES cells. However, this can be reversed with common antioxidants albeit at relatively high levels (Figure 3.7G-H). Importantly, the changes in ROS correlate with RTI-79-induced sensitivity to chemotherapy (Figure 3.7I-J). Rifabutin and RTI-79 are members of a class of quinones that are known to be producers of ROS through redox cycling performed by reductases. What distinguishes RTI-79 from the other quinones, and makes it more potent and effective, is the fact that it also triggers the UPR (Figure 3.9A-E), which leads to increased ubiquitination (Figure 3.9F) and ultimately to the dysregulation of Nrf2 in the resistant cancer cells (Figure 3.8). Consequently, the cancer cells can no longer respond to increases in ROS by augmenting their antioxidant response. In contrast to other ROS generators (like tBHQ and menadione), RTI-79 displays a combination of high levels of ROS (Figure 3.7), reduction of Nrf2 levels (Figure 3.8), and potent ability to synergize with DOX (Figure 3.1, Table 3.1, and Supplementary Figure 3.1).

One major concern was that increased ROS would also lead to toxicity in normal cells. That was not the case, as we did not see elevated ROS or cytotoxicity in primary fibroblasts (Figure 3.1C and 3.3A). In addition, we tested whether RTI-79 would increase DOX-induced cardiotoxicity. Mice treated either with DOX alone or with a combination of RTI-79 and DOX were evaluated by a number of different tests, including echocardiograms. Although mice in the DOX-only group demonstrated minimal histologic changes following administration of DOX, our results indicated no additional cardiotoxicity when RTI-79 was added to DOX (Supplementary Figure 3.4c-e).

RTI-79 has essentially the same desirable pharmacology as rifabutin. For example, dog PK studies show similar plasma concentration (1350 ± 450 mg/mL) and half-life (26.3 ± 5.1 hours) at 9 mg/kg (Supplementary Figure 3.4a). In vivo efficacy studies with drug-resistant double-hit lymphoma and ovarian cancer xenograft tumors showed that RTI-79 was able to re-sensitize both of these cancers to the standard of care therapeutics including DOX, DOXIL, and etoposide (Figure 3.4). Most significant was the potent efficacy at relatively low doses (25 mg/kg) of RTI-79.

Further, our in vivo efficacy studies with RTI-79 predict a positive clinical outcome. First, we began treatment on actively growing tumors as this approach is more predictive of clinical potential compared to beginning treatment before tumor growth (516, 517). We also clearly surpass the 40% threshold of tumor reduction to indicate predictive clinical outcome (518). Finally, we show efficacy in xenograft models with multiple cancers (518). Hence, these preclinical models highly suggest that our observations will translate to clinical efficacy, and indicate that RTI-79 would be successful in trials of drug-resistant ovarian cancer and NHL, including DHL and THL.

RTI-79's utility in treating DHL and THL is particularly exciting and significant. Up to 78% of Burkitt's and 12% of all DLBCL patients have DHL or THL (519). These patients often present with poor prognostic parameters despite aggressive treatments (520). It is remarkable that many DHL and THL have overexpression of BCL6. BCL6 overexpression is able to inhibit the normal increases in ROS levels and apoptosis that occur in response to chemotherapeutic agents, most likely by enhancing the antioxidant response (521). Hence it is tempting to speculate that RTI-79 might be able to override the ability of BCL6 to inhibit increases in ROS as RTI-79 would overcome the enhanced activity of the antioxidant response system by degrading Nrf2. The

combination of RTI-79-induced increases in ROS and antagonism of anti-oxidant systems would cause the cell to become sensitized to oxidative stress-inducing chemotherapeutics. Thus, it might be efficacious to treat cancers that overexpress BCL6 as part of their resistance mechanism. Interestingly, BCL6 is also a negative prognostic indicator for ovarian cancer (522). Such a wide spectrum of action indicates that RTI-79 might be used clinically in multiple drug resistant cancer types and with a variety of chemotherapeutics.

CHAPTER IV

OVERALL CONCLUSION AND FUTURE DIRECTION

4.1 Research summary

We have discovered that drug-resistant lymphoma and ovarian carcinoma cell lines have a lower oxidative state (ROS; reactive oxygen species) and increased expression of anti-oxidant Nrf2 than their drug-sensitive counterparts. In normal cells during oxidative stress, Nrf2 upregulates G6PDH providing reducing equivalents (NADPH) for the maintenance of a pool of reduced mitochondrial glutathione (GSH) to balance the redox state, which has a crucial role in cellular signaling and antioxidant defenses (415-417, 442, 443, 523-525). Evidence emerging from diverse systems indicates that oxidative stress activation of Nrf2 upregulates G6PDH expression (442, 443), which generates reducing equivalents (NADPH) to increase glutathione (GSH) production through the pentose phosphate shunt. GSH scavenges ROS, thus reducing the redox state. (415, 442, 443, 446, 526-536). We showed that a more reduced intracellular state promotes resistance to chemotherapeutics. Based on published literature and our studies, we propose that a lower oxidative state in drug-resistant cells is caused by higher expression of anti-oxidant Nrf2 and glucose-6-phosphate dehydrogenase (G6PDH) activities.

To study drug resistance, acquired chemoresistant cell line models were generated by repeated on-off exposures of chemosensitive diffuse large B-cell lymphoma cells to increasing concentrations of doxorubicin-based chemotherapeutics (82, 83), similar to clinical CHOP chemotherapy protocols in patients. Employing the chemoresistant lymphoma cells in a high-throughput screen, we discovered that a rifamycin (Rifabutin) reversed resistance to the chemotherapy cocktail, CHOP. Rifabutin on its own had no cytotoxicity but in the presence of CHOP caused cytotoxicity in resistant cells. Rifabutin acted to increase superoxide (O_2^-) and decrease Nrf2 expression in multiple drug-resistant cancer cell types.

We have created a novel non-toxic rifamycin derivative (RTI-79) from the parent rifabutin molecule that acts as a potent chemosensitizer in multiple types of cancer cells. RTI-79 reverses drug resistance in multiple types of cancers, including lymphoma and ovarian, breast, and prostate carcinomas. RTI-79 has little or no toxicity on its own but increases the sensitivity of chemoresistant cancers to a broad range of chemotherapeutics. RTI-79 has also shown great success in animals; in combination with doxorubicin-based chemotherapies, it neither significantly repressed lymphoma and ovarian carcinoma growth without increasing the side effects of medications nor adversely affect healthy cells. RTI-79 acts to increase the oxidative state in chemoresistant cancer cells by generating superoxide (O_2^-) and downregulating the Nrf2 signaling pathway. The source of the rapid induction of O_2^- could be the direct oxidation of RTI-79 as rifamycins have been reported to cause ROS production (493).

4.2 Role of the mitochondrial unfolded protein response (UPRmt) in drug resistance

In chapter III we showed that RTI-79 treatment results in increased total cellular ubiquitination of proteins. Our Protein mass spectrometry (MS sequence) data from a gel prep also revealed that RTI-79 increases the ubiquitination state of several mitochondrial-associated proteins (Table 4.1). The mitochondrial unfolded protein response (UPRmt) has been recognized as a regulator of a mitochondrial retrograde signaling cascade that affects gene expression in the nucleus in mammals (537-539). UPRmt retrograde signaling has recently been implicated in cell survival and drug resistance, potentially by upregulating Nrf2 antioxidant defenses (538, 540). However, unlike the ER-associated UPR, the mechanisms behind the signal transduction cascade leading to mitochondrial UPR are not as well understood. One hypothetical chemoresistance mechanism is that the stress caused by repeated exposures to chemotherapeutics may select for cancer cells that have activated UPRmt caused by upregulated expression of the mitochondrial chaperones,

mtHSP70[mortalin], HSP60, and HSP40[DnaJ] (537, 541). It was of our interest that RTI-79 increased the ubiquitination state of HSP70mt (mortalin) known to play role in the UPRmt (Table 4.1). The UPRmt chaperone, mtHSP70 [mortalin], is a key player in mitochondrial stress response, aging, and programmed cell death (542-544). Overexpression of mortalin extends lifespan in human cells and the nematode C. elegans, indicating a protective function in vitro and in vivo (545-547). Reduction of mortalin results in alterations in mitochondrial morphology, impaired mitochondrial membrane potential, and increased cellular levels of ROS (545). Indeed, we have detected increased expression of canonical UPRmt chaperones and Nrf2 in chemoresistant cells, and RTI-79 increased the ubiquitination state and decreased expression of UPRmt chaperones, along with increased ROS and sensitivity to chemotherapeutics. We believe that RTI-79 affects one or more ubiquitin-conjugating enzymes in mitochondria to increase the ubiquitination state of UPRmt chaperones thus destabilizing and decreasing mitochondrial retrograde signaling that drives upregulation of Nrf2/G6PDH/GSH.

We believe this is significant since activation of the UPRmt mediates retrograde signaling, in which mitochondria have the ability to alter nuclear gene expression (548, 549). UPRmt is unique from the better understood UPR of the endoplasmic reticulum and has a potential impact on chemoresistant disease (550). The UPRmt is believed to compensate for metabolic dysfunction by stimulating retrograde communication through transcriptional regulators, such as NFκB, cAMP response element-binding protein (CREB), CCAAT-enhancer-binding protein homologous protein (CHOP), and nuclear factor of activated T cells (NFAT), to modulate gene expression to adapt mitochondria function to promote recovery and function to resolve the stress (539, 551, 552). In yeast, an optimal redox defense system appears to be an important outcome of mitochondrial retrograde signaling activation (553).

Table 4.1 RTI-79 increases the ubiquitination state of several mitochondrial-associated proteins.

Protein	Function
ATP synthase, O subunit	H^+ transporting, mitochondrial F1 complex, (oligomycin sensitivity conferring protein)
ATP synthase, alpha subunit	H+ transporting, mitochondrial F1 complex
Solute carrier family 25	Mitochondrial carrier; adenine nucleotide translocator, member 5
Glyceraldehyde-3-phosphate dehydrogenase	Maintains the redox potential across the inner mitochondrial membrane in glycolysis
Voltage-dependent anion-selective channel protein 1 (VDAC1)	A protein of the outer mitochondrial membrane of eukaryotes forms a voltage-dependent anion-selective channel (VDAC) that behaves as a general diffusion pore for small hydrophilic molecules
Voltage-dependent anion-selective channel protein 3 (VDAC3)	A protein of the outer mitochondrial membrane of eukaryotes forms a voltage-dependent anion-selective channel (VDAC) that behaves as a general diffusion pore for small hydrophilic molecules
Heterogeneous nuclear ribonucleoprotein A2/B1	Mitochondrial stress-mediated transcription activation of nuclear target genes
Heterogeneous nuclear ribonucleoproteins C1/C2	Play a role in the early steps of spliceosome assembly and pre-mRNA splicing.
Heterogeneous nuclear ribonucleoprotein H1	This protein is a component of the heterogeneous nuclear ribonucleoprotein (hnRNP) complexes which provide the substrate for the processing events
Heterogeneous nuclear ribonucleoprotein K	Regulates expression of uncoupling protein 2, UCP2, a member of a family of inner mitochondrial membrane ion carriers involved in a host of metabolic processes
Heterogeneous nuclear ribonucleoprotein M	interaction with mitochondrial ribosomal protein S12, functions in mitochondrial mRNA localization for binding to ribosomal proteins
Heterogeneous nuclear ribonucleoprotein U	Promotes MYC mRNA stabilization. Binds to pre-mRNA. Binds to double- and single-stranded DNA and RNA

Table 4.1 Continued

Heat shock 70kDa protein 9 (mortalin)	Anti-oxidant (grp75, mtHSP70) functions ranging from stress response, control of cell proliferation, and inhibition/prevention of apoptosis
Peptidyl-prolyl cis-trans isomerase A	Protein folding
Prohibitin	Anti-oxidant mitochondrial membrane protein – mitochondrial ubiquitin-proteasome pathway
Elongation factor Tu (EFTu)	Mitochondrial protein translation
Cofilin-1	Regulation of mitochondrial apoptosis
Peroxiredoxin 1	Antioxidant – H202 detoxification – binds to p66Shc, preventing it from inducing mitochondrial H2O2 (ROS burst)

Mitochondrial dysfunctions are an important determinant in conferring cancer cell resistance to certain chemotherapeutic drugs. However, the presence of mitochondrial dysfunctions involving the UPRmt retrograde signaling pathway may represent the "Achilles' heel" for cancer cells, providing a basis for rationale development of therapeutic strategies to selectively kill cancer cells. Increases in the UPRmt canonical chaperones, HSP40, HSP60, and mtHSP70, that activate retrograde signaling is a new emerging paradigm driving chemoresistance. Thus, mitochondrial retrograde inhibitors may provide a new therapeutic opportunity in drug-resistant tumors with mitochondrial dysfunction. Along with this line, we have evidence (Figure 4.1) that RTI-79 is a novel chemosensitizing drug that targets mitochondrial UPRmt chaperones to downgrade retrograde signaling and promote oxidative stress.

Based on our studies, we propose that drug-resistance is caused, in part, by activated mitochondrial retrograde signaling, which upregulates Nrf2 and its downstream antioxidant cascade, G6PDH/GSH (Figure 4.2).

RTI-79 promotes chemosensitization by downregulating the Nrf2/G6PDH/GSH cascade via repression of the mitochondrial unfolded protein response (UPRmt) (Figure 4.3).

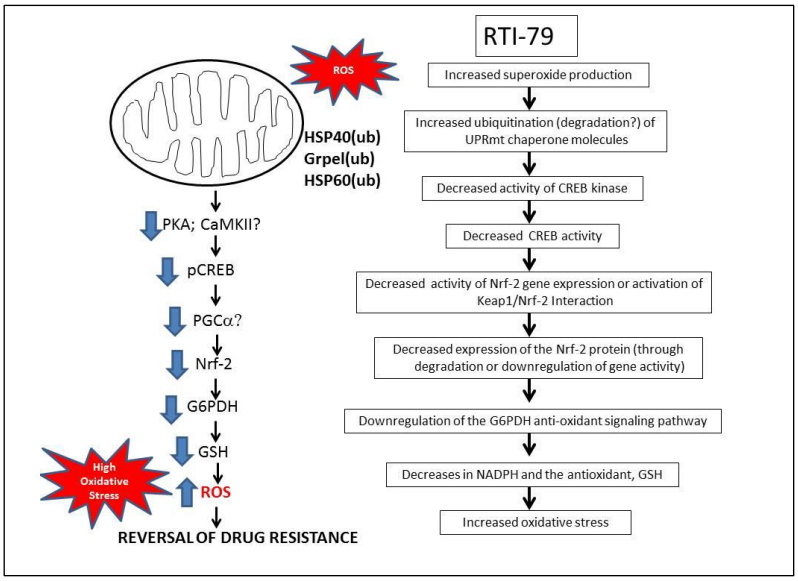

Figure 4.1 The hypothetical model in which RTI-79 targets mitochondrial UPRmt chaperones to downgrade retrograde signaling and promote oxidative stress. RTI-79 reverses drug resistance by downregulating the UPRmt, resulting in loss of CREB activity and repression of the Nrf2/G6PDH/GSH antioxidant cascade.

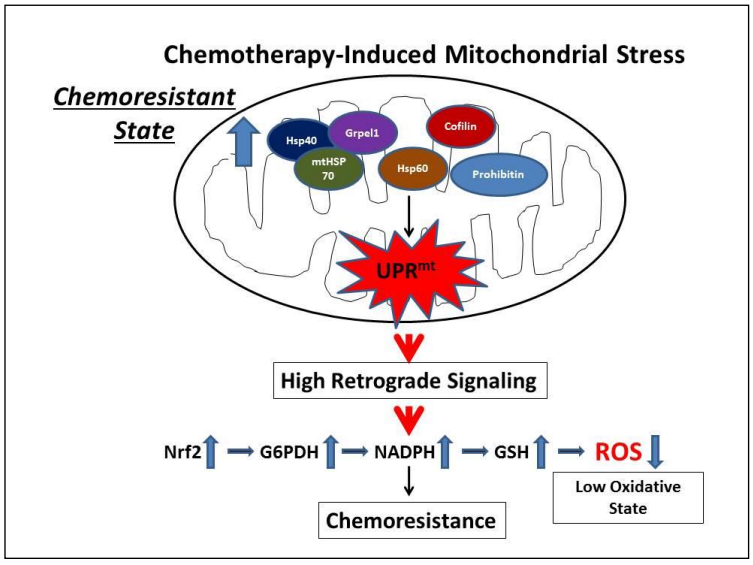

Figure 4.2 The hypothetical model in which UPRmt retrograde signaling drives the Nrf2/G6PDH/NADPH/GSH pathway in drug-resistant cancer cells.

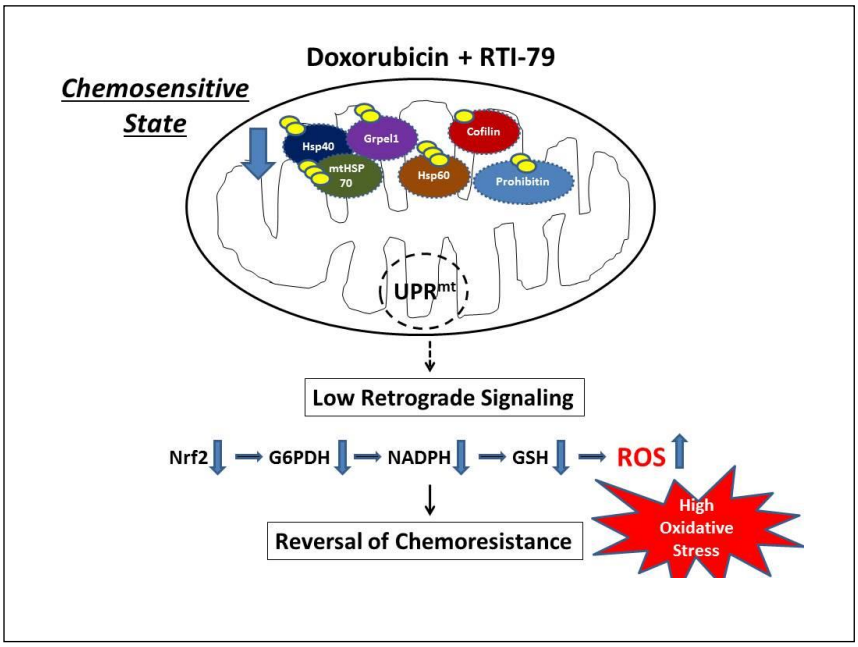

Figure 4.3 The hypothetical model in which RTI-79 targets downregulation of the UPRmt retrograde signal to reverse drug-resistance. RTI-79 induces ubiquitination/degradation of proteins involved in UPRmt retrograde signaling.

The UPRmt can cause activation of retrograde signaling that drives upregulation of Nrf2 and G6PDH (Figure 4.2). More specifically, our preliminary data demonstrate that RTI-79 causes the following events in chemoresistant cells: (1) increased superoxide; (2) an increased ubiquitination state in canonical UPRmt chaperone proteins; (3) decreased expression of UPRmt chaperones; (4) decreased activation (ser133 phosphorylation) of the CREB mitochondrial retrograde signal mediator; (5) decreased Nrf2, G6PDH, and GSH (higher oxidative stress); and (6) increased sensitivity to multiple chemotherapeutics, including doxorubicin, etoposide, and cisplatin.

Moreover, activated UPRmt retrograde signaling has been reported in the literature to upregulate MDR pumps (i.e., P-gp), and RTI-79 downregulated P-gp activity in drug-resistant cells. Additional support for our chemosensitization model, as we showed in chapter II, is that a G6PDH inhibitor (i.e. DHEA) induced O2- and increased the sensitivity of chemoresistant cells to CHOP.

Our discovery that RTI-79 increased the ubiquitination state of canonical UPRmt chaperones is significant since several reports indicate a role for ubiquitination in regulating chaperone activities (554-556). First, the E3 ubiquitin ligase, CHIP, ubiquitinates the HSP70 chaperone (557). When HSP70 carries no client proteins, CHIP catalyzes its polyubiquitination and subsequent proteasomal degradation. Second, ubiquitination upon oxidative stress is not a random process to degrade the mass of oxidized proteins but concerns specific targeted ubiquitination of functional proteins, including chaperones (558). Third, the Ubiquitin-like protein 5 positively regulates chaperone gene expression in the UPRmt (559). Moreover, the ubiquitin-proteasome (UPS) and mitochondria systems are highly interdependent (Mitochondrion-UPS Axis) (560). The UPS is not only involved in the degradation of proteins

present in the mitochondrial outer membrane, but also of substrates derived from the inner membrane and matrix (561-563).

Therefore, we hypothesize that RTI-79 targets the repression of UPRmt through the increased ubiquitination state/degradation of mitochondrial chaperones, which represses retrograde signaling and causes decreases in Nrf2/G6PDH/GSH antioxidant activities in chemoresistant cells leading to reversal of drug resistance (Figure 4.3). Downstream signaling steps and transcriptional regulation of the mammalian UPRmt remain not well understood. Although we have gathered substantial preliminary data implicating a role for UPRmt in reversal of drug resistance, more study is needed to more fully understand the regulation of the UPRmt and how downstream retrograde signals promote drug resistance. Along these lines, we believe RTI-79 is a novel anti-cancer agent that targets the UPRmt and can be a useful tool to probe the mechanism of action of the UPRmt in cancer chemoresistance.

4.3 RTI-79-mediated chemosensitization in drug-resistant cancer cells

In Chapter III, we showed that that low (10 μM), non-toxic concentrations of RTI-79 synergizes with chemotherapeutics by generating high levels of intracellular ROS (predominantly superoxide) in resistant cancer cells. RTI-79 acts to increase the oxidative state in chemoresistant cancer cells by generating superoxide. RTI-79 also triggers the UPR, which leads to increased ubiquitination and ultimately to the dysregulation of Nrf2 in the resistant cancer cells. Consequently, the cancer cells can no longer respond to increases in ROS by augmenting their antioxidant response. In contrast to other ROS generators (like tBHQ and menadione), RTI-79 displays a combination of high levels of ROS, reduction of Nrf2 levels, and potent ability to synergize with DOX.

Employing affinity chromatography to purify whole-cell polyubiquitinated proteins, we discovered that RTI-79 increased the polyubiquitination state of several UPRmt proteins (Figure 4.4; DNAJ[mtHSP40], HSP60, and mtHSP70[mortalin]) on lys48, a ubiquitin mark that targets proteins for proteasomal degradation (564). Velcade (a proteasome inhibitor) did not change the ubiquitination state of UPRmt proteins. Velcade does not exhibit the ability to potentiate Doxorubicin like RTI-79 and is cytotoxic to lymphoma cells on its own (Data are not shown). In addition, RTI-79 increased the polyubiquitination state of GrpE1, which controls the nucleotide-dependent binding of mitochondrial HSP70 (mtHSP70 [mortalin]) to substrate proteins, and can stimulate its ATPase activity. GrpE1 also interacts with DNAJ [mtHSP40]. The expression levels of UPRmt chaperones was lower in RTI-79-chemosensitized cells relative to chemoresistant cells (Figure 4.4, in particular HSP40), indicating that increases in polyubiquitination was likely not the result of reduced proteasomal degradation activity. Moreover, one published report indicates that Nrf2 can upregulate HSP40 and mtHSP70 expression (565). Thus, altered ubiquitination/stability of UPRmt proteins may be a mechanism driving chemoresistance in cancer cells.

RTI-79 reduced phosphorylation (activity) of CREB at Ser133 (Figure 4.5). A potential mechanism would be modulation of Ca^{+2}/calmodulin-dependent protein kinase II (CaMKII) or protein kinase A (PKA), which are known to target phosphorylation of Ser133 on CREB, which activates it to mediate nuclear gene expression. We hypothesize that UPRmt-mediated phosphorylation at Ser133 on CREB by CaMKII activates retrograde signaling, which upregulates Nrf2 and G6PDH. In support of this model, activation of CREB has been reported to induce the G6PDH gene (566, 567), as we detected Ca^{+2} fluxing about 5-10 minutes after the initial ROS burst in RTI-79-treated cells (Figure 4.6), which might activate CaMKII to phosphorylate CREB. Once activated by CaMKII-mediated phosphorylation at Ser133, CREB

could then activate transcription of the Nrf2 gene indirectly through activation of the PGC-1 transcription factor (568). Nrf2 would then activate transcription of the G6PDH gene (442) thus increasing NADPH via the pentose phosphate shunt, which is used to increase GSH production. In support of this model, the G6PDH gene promoter has an antioxidant response element and the Keap1/Nrf2 system stimulates G6PDH transcription under stressed conditions (444). Moreover, we showed increased Nrf2, G6PDH, NADPH, and GSH in chemoresistant cells (chapter II), and RTI-79 decreased Nrf2, G6PDH, NADPH, and GSH in chemoresistant cells to levels more similar to those observed in chemosensitive cells (Figure 4.7).

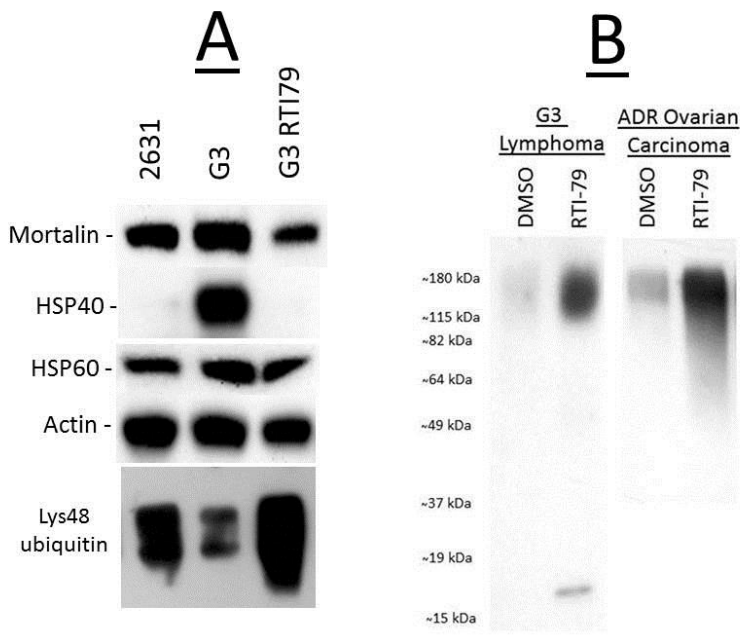

Figure 4.4 Drug-resistant cancer cells have higher UPRmt proteins than their more sensitive counterparts. (Panel A) Drug-resistant G3 lymphoma cells had higher UPRmt proteins than their more sensitive 2631 counterparts. RTI-79 caused decreases in UPRmt expression in G3 cells. (Panel B) RTI-79 also increased polyubiquitination in doxorubicin-resistant ADR-RES ovarian carcinoma cells.

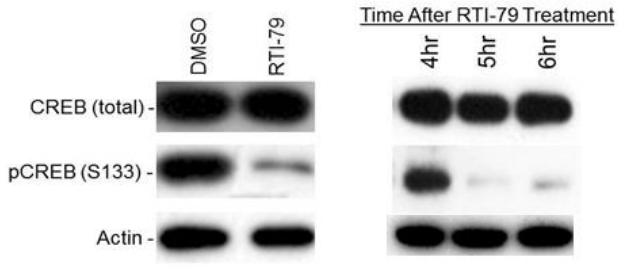

Figure 4.5 RTI-79 decreases CREB phosphorylation in G3 cells. RTI-79 decreased CREB phosphorylation at Ser133 indicating inactivation of CREB in drug-resistant G3 lymphoma cells. The decreases in CREB phosphorylation occurred between 4 to 5 hours after RTI-79 treatment.

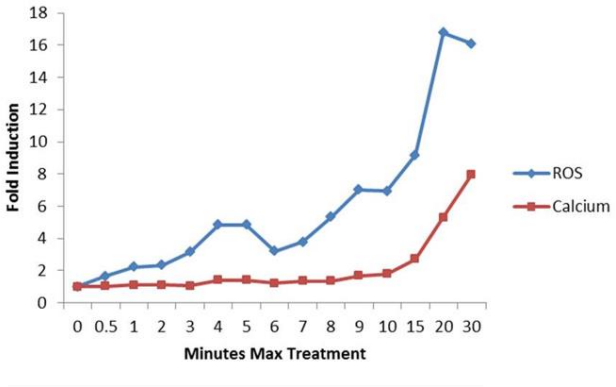

Figure 4.6 RTI-79 increases Ca^{+2} fluxing after the initial ROS burst. The rate of ROS and Calcium fluxes increases in CHOP-resistant G3 lymphoma cells after RTI-79 treatment.

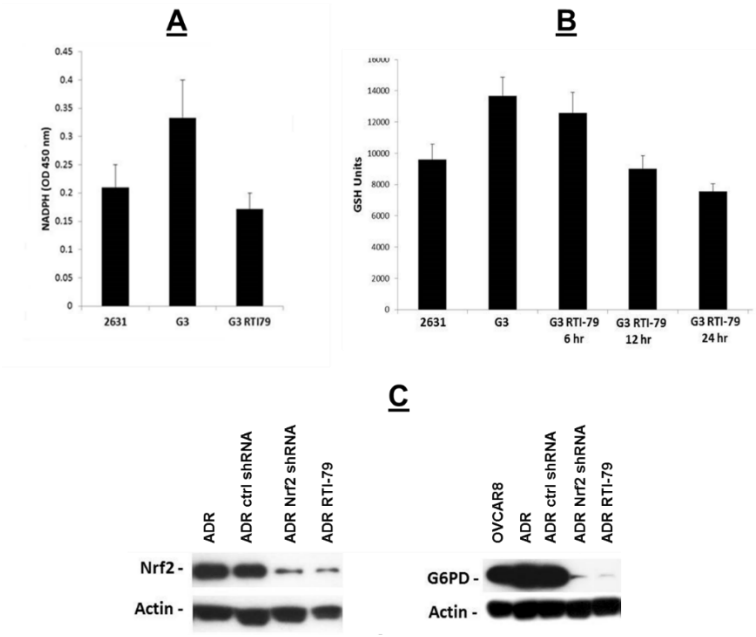

Figure 4.7 RTI-79 downregulates the Nrf2/G6PDH cascade in chemoresistant cells. (A) RTI-79 reduced NADPH levels in drug-resistant G3 lymphoma cells to that observed in the more sensitive 2631 line. (B) 10 µM RTI-79 decreased GSH levels in drug-resistant G3 levels to similar levels observed in their more sensitive counterparts after 12 hours of exposure. (C) Knocking down Nrf2 or treatment with RTI-79 resulted in decreases in the expression of G6PDH.

4.4 Characterize UPRmt ubiquitin-conjugating enzymes in chemoresistant and RTI-79-chemosensitized cells.

The polyubiquitination at lysine 48 is a tag for the proteasome pathway, one of the main processes of cellular protein degradation (569). In this respect, the ability of deubiquitinating enzymes (DUBs) to edit the ubiquitination state of a protein or to cleave polyubiquitin chains from substrates is a key step in the correct definition of tags for subcellular localization and intracellular trafficking of the target protein (570). The differences in ubiquitination in mitochondrial chaperones between chemosensitive and chemoresistant cells, as well as RTI-79-induced changes in ubiquitination, occur on lysine 48, indicating changes in the degradative proteasomal signal.

Mitochondrial-specific E3 ubiquitin ligases (MITOL, GIDE, RNF185, and Parkin) (571-574) and deubiquitylases (DUBs; USP30 and USP35) (575) are known to regulate mitochondrial function through the UPRmt. We thus plan to identify and characterize ubiquitin-conjugating enzymes in mitochondria of chemosensitive, chemoresistant, and RTI-79-treated lymphoma and ovarian cells. The goals are to (1) identify an ubiquitin-conjugating modifier that is differentially expressed/activated in chemosensitive and chemoresistant cells, and (2) identify a specific ubiquitin-conjugating modifier in chemoresistant cells that we believe is targeted by RTI-79. The next approach will be to modulate this ubiquitin-conjugating modifier to confirm its role in chemoresistance. Initial studies will employ our chemosensitive/chemoresistant cell line models (CRL2631/G3 – diffuse large B-cell lymphoma; OVCAR8/ADR-RES – ovarian carcinoma) (82). Follow-up studies will be expanded to include other chemosensitive/chemoresistant lymphoma and ovarian carcinoma cell line pairs that we have generated in the laboratory. Western blotting of purified mitochondria lysates using an anti-ubiquitin antibody detected markedly increased polyubiquitination of proteins in RTI-79-treated chemoresistant lymphoma

cells compared to DMSO-treated controls (see arrow in Figure 4.8). Based on our preliminary studies, we believe this high molecular weight species is the result of increases in the polyubiquitination state of specific UPRmt proteins. We believe it is feasible to conduct characterization of ubiquitin-conjugating enzymes targeted by RTI-79 in an in vitro ubiquitination assay of purified whole-mitochondria. We hypothesize that the lower polyubiquitinated state of UPRmt chaperones in chemoresistant cells is caused by decreased E3 ligase or increased deubiquitinase activity. RTI-79 targets a specific ubiquitin-conjugating modifier to increase the lys48 ubiquitination state of UPRmt chaperones, marking them for proteosomal degradation.

Therefore, whole-mitochondria or mitochondrial lysates from chemosensitive, chemoresistant, and RTI-79-chemosensitized cells will be subjected to in vitro ubiquitination assays. Ubiquitin ligases and DUBs can be tagged in the in vitro assays with HA-ubiquitin and purified by affinity chromatography on anti-HA agarose or by the UBI-QAPTURE-Q® kit (Enzo Life Sciences). Eluted ubiquitinated proteins from chemoresistant and chemosensitized cells will be compared by mass spectrometry (MS). We will focus on differentially-expressed sequences using the same approach that successfully identified polyubiquitinated UPRmt chaperones in the Preliminary Data (Figure 4.4). However, this study will include a more expansive analysis of ubiquitin-modified proteins ranging from mono- to poly-ubiquitination forms.

De-ubiquitinating (DUB) activities will be assayed in whole-mitochondrial lysates subjected to ubiquitination reactions containing or lacking RTI-79 in the presence of biotin- or HA-ubiquitin, and the ubiquitinated proteins probed by western using avidin or anti-HA, respectively, as described (562, 563). If RTI-79 inhibits a DUB, then the level of HA-ubiquitination would be expected to increase in RTI-79-treated assays compared to controls.

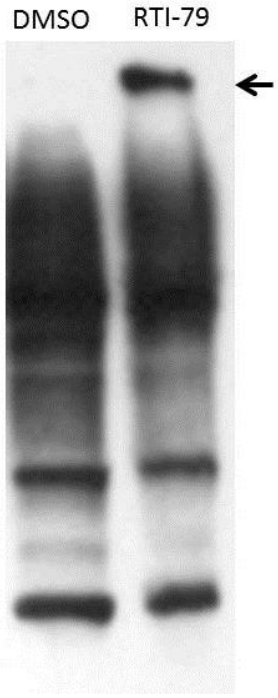

Figure 4.8 RTI-79 increases polyubiquitination of proteins in mitochondria lysates. G3 lymphoma cells were treated with DMSO or RTI-79 (10 μM) for 4 hours. Mitochondria were purified and subjected to western blot using an anti-ubiquitin antibody.

If a DUB is involved in RTI-79-mediated chemosensitization, then we would expect to see increased amounts of biotin-ubiquitin tag in whole-mitochondrial proteins isolated from RTI-79-chemosensitized cells treated with biotin-ubiquitin compared to control cells. These biotin-ubiquitin-tagged candidates will be affinity-purified with avidin-conjugated agarose and subjected to MS sequencing for identification.

Alternatively, we could purify ubiquitin-conjugating activities in mitochondrial lysates using classical hydrophobic, anion-exchange, and gel-filtration chromatography and an in vitro ubiquitination assay (Enzo Life Sciences, Inc.), which can tag E3 ligases and DUBs with HA-ubiquitin or biotin-ubiquitin. We expect that an ubiquitin conjugation-modifying enzyme will be identified as differentially activated/regulated between drug-sensitive and –resistant cells. RTI-79 will be shown to bind to the ubiquitin-conjugation modifier (E3 ligase or DUB) and modulate its activity. Downregulation (siRNA knockdown) or upregulation (recombinant lentivirus expression) of the candidate ubiquitin-conjugation modifier will influence the drug tolerance of chemoresistant and chemosensitive cells. Our studies will be expanded to include other paired chemosensitive/chemoresistant lymphoma and ovarian carcinoma cells available in the laboratory. Moreover, the effect of modulating the ubiquitin-conjugating modifier on CREB phosphorylation, Nrf2, and G6PDH/GSH will be investigated as described below under sections 4.5 and 4.6.

4.5 Modulate UPRmt chaperone expression and CREB (phosphoSer133) activity and determine the effect on chemoresistance.

Here we hypothesize that activation or upregulation of the UPRmt activates CaMKII, which phosphorylates and activates CREB to transactivate the Nrf2 and G6PDH genes. The role of CREB signaling in chemoresistance and chemosensitization will be investigated using siRNA

knockdown and cell-permeable CREB inhibitors (Calbiochem; Santa Cruz). CaMKII activity will be modulated using siRNA, and chemical inhibitor (KN-93) and activator (Oleic acid, Santa Cruz; Tocris). PKA activity will be modulated using siRNA, and chemical inhibitor (H89, Santa Cruz) and activator (8-bromo-cAMP, Santa Cruz). UPRmt chaperone proteins will be modulated by siRNA knockdown (576), lentivirus overexpression (Vigene Biosciences, Inc), and induction by paraquat (577) or ethidium bromide-induced depletion of mtDNA (576), and the effect on CREB activity (Ser133 phosphorylation) will be determined. Ubiquitin-conjugating modifiers interacting with RTI-79 identified in section 4.4 will be modulated by siRNA and the effect on CaMKII, CREB, and chemoresistance determined. We would expect to see that inhibition of CREB or CaMKII will decrease tolerance to chemotherapeutics (doxorubicin. etoposide, cisplatin). Downregulation of UPRmt proteins (HSP40, HSP60, and mtHSP70), inhibition of CREB, and inhibition of CaMKII will result in decreases in both Nrf2 and G6PDH, decreases in both NADPH and GSH, and increases in ROS (oxidative state) expression, thereby sensitizing chemoresistant cells to chemotherapeutics. Upregulation of UPRmt proteins (by paraquat or recombinant lentivirus) or activation (phosphorylation at ser133) of CREB will have the opposite effect, increasing Nrf2/G6PDH and drug tolerance in drug-sensitive cells. However, if CREB is acting directly to regulate the G6PDH gene, then modulation of CREB may affect G6PDH but not Nrf2 expression.

Alternatively, if CREB is ruled out, other molecules that mediate retrograde signaling will be investigated. For instance, UPRmt retrograde signaling is also mediated by the bZip transcription factor ATFS-1 (578), which is normally efficiently imported into mitochondria and degraded. The expression and localization of ATFS-1 by cell fractionation and western blot could be studied by using anti-ATFS-1 antibody (Biocompare, Inc.). If a role for ATFS-1 is eliminated,

we would examine still other transcription factors implicated in retrograde signaling, such as CHOP and NFκB (579).

4.6 Determine the role of the Nrf2/G6PDH/GSH pathway in UPRmt-mediated drug resistance.

Mitochondrial retrograde signaling activates the Nrf2/HO-1 cascade during oxidative stress (580-582). Thus, constitutive activation of UPRmt might promote stabilization, and thus upregulation, of Nrf2, which then upregulates G6PDH. Nrf2 is anchored in the cytoplasm through binding to Keap1, which, in turn, facilitates the ubiquitination and subsequent proteolysis of Nrf2. Such sequestration and degradation of Nrf2 in the cytoplasm is a mechanism for the repressive effects of Keap1 on Nrf2. We suspect that RTI-79 downgrades UPRmt retrograde signaling, resulting in destabilization and downregulation of Nrf2 protein since increases in cytoplasmic Nrf2 relative to nuclear Nrf2 protein were observed in RTI-79-treated cells (Figure 4.9). We thus will investigate whether either UPRmt or RTI-79 alone modulates Nrf2-Keap1 interactions.

Here we hypothesize that UPRmt activates retrograde signaling, which stabilizes Nrf2 and upregulates G6PDH, thus lowering the oxidative state and increasing tolerance to chemotherapeutics. Therefore we plan to modulate the expression of UPRmt chaperones to influence the Nrf2/G6PDH/GSH cascade and chemoresistance.

Overexpression of an aggregation-prone mutant mitochondrial protein, ornithine transcarbamylase (ΔOTC), results in UPRmt activation and efficient clearance of misfolded ΔOTC (538). Chemosensitive CRL2631 lymphoma and OVCAR8 ovarian carcinoma cells will be transfected with recombinant ΔOTC to activate the UPRmt. Alternatively, the UPRmt can be

upregulated by paraquat. The effect of upregulation of UPRmt on chemosensitivity will be investigated along with the determination of CREB, Nrf2, and G6PDH activities and ROS levels.

Also, Keap1/Nrf2 interactions and Nrf2 activity will be determined using three independent assays: (1) PathHunter NRF2 assay (DiscoverRX, Inc), (2) Keap1/Nrf2 Screening Assay Kit designed for study of Keap1/Nrf2 binding (BPS Bioscience, Inc), and (3) Antioxidant Response Reporter System (ARRS; Qiagen). The effect of knocking down UPRmt retrograde signaling (described in section 4.4) (HSP40, mtHSP70, and HSP60 siRNAs) on Keap/Nrf2 interactions will be investigated in drug-sensitive and -resistant cells. If we do not see changes in Nrf2/Keap interactions, we could explore other pathways of Nrf2 activation. Nrf2 activity is regulated by not only Keap-mediated ubiquitination as described above but also phosphorylation of serine residues in the Nrf2 protein (583, 584). Several kinases reportedly phosphorylate Nrf2 at Ser40, and Nrf2 is a direct substrate of PERK, a kinase that acts as a transducer of ER stress (585). We would investigate both nuclear/cytoplasmic localization of Nrf2 and its state of phosphorylation and ubiquitination.

G6PDH activity and NADPH will be modulated in both drug-sensitive and -resistant cells using chemical G6PDH inhibitor DHEA and recombinant lentiviruses expressing G6PDH protein or shRNA. GSH levels in both drug-sensitive and resistant cells will be modulated using inhibitors of GSH synthesis (L-buthionine sulfoximine; the glutathione reductase inhibitor 2-AAPA) and GSH activator (Riluzole). Glutathione Monoethyl Ester (Santa Cruz, Inc) is a cell-permeable derivative of glutathione (GSH) that undergoes hydrolysis by intracellular esterases to release GSH. We already have a preliminary result showing that the GSH inhibitor, L-buthionine sulfoximine, sensitized chemoresistant lymphoma cells to doxorubicin. G6PDH activity and GSH levels will be determined using fluorescent- and colorimetric-based assays, respectively

(Figures 4.10 and 4.7B). The effect of UPRmt knockdown (siRNA) and upregulation (recombinant lentivirus) on G6PDH activity and GSH levels will be determined as we have done in the Preliminary Results.

We anticipate that upregulation of G6PDH will increase the levels of GSH and lower ROS, thus increasing the tolerance of drug-sensitive cells to chemotherapeutics. Upregulation of UPRmt will increase G6PDH activity and GSH, increase chemoresistance, and lower ROS. Downregulation of UPRmt will decrease G6PDH activity and GSH, reverse chemoresistance, and increase ROS.

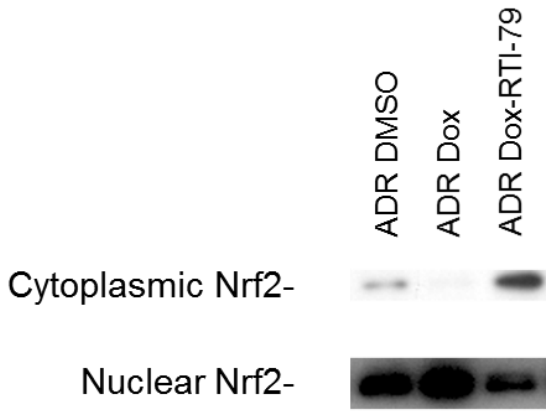

Figure 4.9 RTI-79 increases cytoplasmic Nrf2 relative to nuclear Nrf2. RTI-79 repressed doxorubicin-induced increases in Nrf2 localization with concomitant increases in the proportion of cytoplasmic-localized Nrf2 protein.

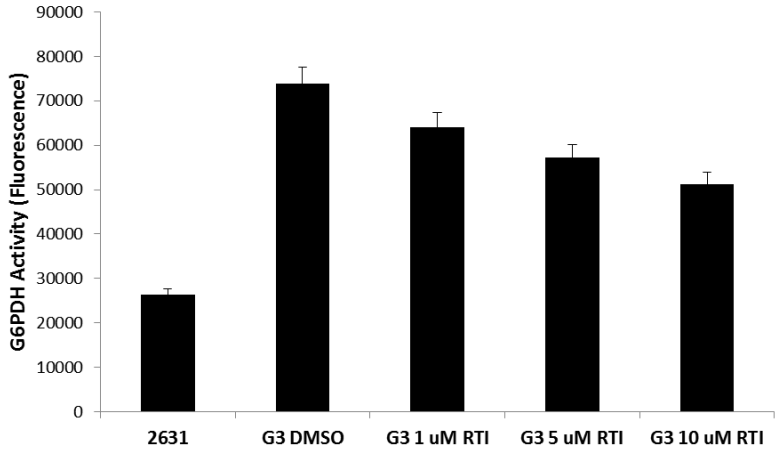

Figure 4.10 RTI-79 decreases the G6PDH activity in G3 cells. RTI-79 caused a dose-dependent decrease in G6PDH after 24 hours.

REFERENCES

1. Armitage JO, Weisenburger DD. New approach to classifying non-Hodgkin's lymphomas: clinical features of the major histologic subtypes. Non-Hodgkin's Lymphoma Classification Project. Journal of clinical oncology : official journal of the American Society of Clinical Oncology. 1998;16(8):2780-95.

2. Coiffier B. Monoclonal antibody as therapy for malignant lymphomas. C R Biol. 2006;329(4):241-54.

3. Klein U, Dalla-Favera R. Germinal centres: role in B-cell physiology and malignancy. Nat Rev Immunol. 2008;8(1):22-33.

4. Fisher RI. CHOP chemotherapy as standard therapy for treatment of patients with diffuse histiocytic lymphoma. Important Adv Oncol. 1990:217-25.

5. Czuczman MS, Leonard JP, Williams ME. Recent advances in the treatment of mantle cell lymphoma: a post-ASH 2009 discussion. Clin Adv Hematol Oncol. 2010;8(4):A1-14; quiz A5.

6. Friedberg JW, Fisher RI. Diffuse large B-cell lymphoma. Hematol Oncol Clin North Am. 2008;22(5):941-52, ix.

7. Velasquez WS. Prognostic factors in aggressive lymphoma. Journal of clinical oncology : official journal of the American Society of Clinical Oncology. 1991;9(7):1320-1.

8. Velasquez WS. Prognostic factors in intermediate high grade lymphoma. Cancer Treat Res. 1993;66:37-52.

9. Fisher RI, Gaynor ER, Dahlberg S, Oken MM, Grogan TM, Mize EM, et al. Comparison of a standard regimen (CHOP) with three intensive chemotherapy regimens for advanced non-Hodgkin's lymphoma. N Engl J Med. 1993;328(14):1002-6.

10. Multani P, White CA, Grillo-Lopez A. Non-Hodgkin's lymphoma: review of conventional treatments. Curr Pharm Biotechnol. 2001;2(4):279-91.

11. Sonneveld P, de Ridder M, van der Lelie H, Nieuwenhuis K, Schouten H, Mulder A, et al. Comparison of doxorubicin and mitoxantrone in the treatment of elderly patients with advanced diffuse non-Hodgkin's lymphoma using CHOP versus CNOP chemotherapy. Journal of clinical oncology : official journal of the American Society of Clinical Oncology. 1995;13(10):2530-9.

12. Coffey J, Hodgson DC, Gospodarowicz MK. Therapy of non-Hodgkin's lymphoma. Eur J Nucl Med Mol Imaging. 2003;30 Suppl 1:S28-36.

13. Swerdlow AJ. Epidemiology of Hodgkin's disease and non-Hodgkin's lymphoma. Eur J Nucl Med Mol Imaging. 2003;30 Suppl 1:S3-12.

14. Theodossiou C, Schwarzenberger P. Non-Hodgkin's lymphomas. Clin Obstet Gynecol. 2002;45(3):820-9.

15. Navaratnam S, Williams GJ, Rubinger M, Pettigrew NM, Mowat MR, Begleiter A, et al. Expression of p53 predicts treatment failure in aggressive non-Hodgkin's lymphomas. Leuk Lymphoma. 1998;29(1-2):139-44.

16. Wilson WH, Teruya-Feldstein J, Fest T, Harris C, Steinberg SM, Jaffe ES, et al. Relationship of p53, bcl-2, and tumor proliferation to clinical drug resistance in non-Hodgkin's lymphomas. Blood. 1997;89(2):601-9.

17. Holen KD, Saltz LB. New therapies, new directions: advances in the systemic treatment of metastatic colorectal cancer. Lancet Oncol. 2001;2(5):290-7.

18. Ansell SM, Armitage J. Non-Hodgkin lymphoma: diagnosis and treatment. Mayo Clin Proc. 2005;80(8):1087-97.

19. O'Leary HM, Savage KJ. Novel therapies in peripheral T-cell lymphomas. Current hematologic malignancy reports. 2008;3(4):213-20.

20. Cheung MC, Haynes AE, Meyer RM, Stevens A, Imrie KR. Rituximab in lymphoma: a systematic review and consensus practice guideline from Cancer Care Ontario. Cancer Treat Rev. 2007;33(2):161-76.

21. Ng AK. Diffuse large B-cell lymphoma. Semin Radiat Oncol. 2007;17(3):169-75.

22. Prichard M, Harris T, Williams ME, Densmore JJ. Treatment strategies for relapsed and refractory aggressive non-Hodgkin's lymphoma. Expert Opin Pharmacother. 2009;10(6):983-95.

23. Horning SJ. Natural history of and therapy for the indolent non-Hodgkin's lymphomas. Semin Oncol. 1993;20(5 Suppl 5):75-88.

24. Meusers P, Hense J, Brittinger G. Mantle cell lymphoma: diagnostic criteria, clinical aspects and therapeutic problems. Leukemia. 1997;11 Suppl 2:S60-4.

25. Schmidt C, Dreyling M. Therapy of mantle cell lymphoma: current standards and future strategies. Hematol Oncol Clin North Am. 2008;22(5):953-63, ix.

26. Harris NL, Jaffe ES, Stein H, Banks PM, Chan JK, Cleary ML, et al. A revised European-American classification of lymphoid neoplasms: a proposal from the International Lymphoma Study Group. Blood. 1994;84(5):1361-92.

27. Campo E, Raffeld M, Jaffe ES. Mantle-cell lymphoma. Semin Hematol. 1999;36(2):115-27.

28. Philip T, Guglielmi C, Hagenbeek A, Somers R, Van der Lelie H, Bron D, et al. Autologous bone marrow transplantation as compared with salvage chemotherapy in relapses of chemotherapy-sensitive non-Hodgkin's lymphoma. N Engl J Med. 1995;333(23):1540-5.

29. Niehans GA, Jaszcz W, Brunetto V, Perri RT, Gajl-Peczalska K, Wick MR, et al. Immunohistochemical identification of P-glycoprotein in previously untreated, diffuse large cell and immunoblastic lymphomas. Cancer Res. 1992;52(13):3768-75.

30. Bates SE, Wilson WH, Fojo AT, Alvarez M, Zhan Z, Regis J, et al. Clinical reversal of multidrug resistance. Stem Cells. 1996;14(1):56-63.

31. Webb M, Brun M, McNiven M, Le Couteur D, Craft P. MDR1 and MRP expression in chronic B-cell lymphoproliferative disorders. Br J Haematol. 1998;102(3):710-7.

32. Houldsworth J, Petlakh M, Olshen AB, Chaganti RS. Pathway activation in large B-cell non-Hodgkin lymphoma cell lines by doxorubicin reveals prognostic markers of in vivo response. Leuk Lymphoma. 2008;49(11):2170-80.

33. Alizadeh AA, Eisen MB, Davis RE, Ma C, Lossos IS, Rosenwald A, et al. Distinct types of diffuse large B-cell lymphoma identified by gene expression profiling. Nature. 2000;403(6769):503-11.

34. Rosenwald A, Wright G, Chan WC, Connors JM, Campo E, Fisher RI, et al. The use of molecular profiling to predict survival after chemotherapy for diffuse large-B-cell lymphoma. N Engl J Med. 2002;346(25):1937-47.

35. Wright G, Tan B, Rosenwald A, Hurt EH, Wiestner A, Staudt LM. A gene expression-based method to diagnose clinically distinct subgroups of diffuse large B cell lymphoma. Proc Natl Acad Sci U S A. 2003;100(17):9991-6.

36. Bea S, Zettl A, Wright G, Salaverria I, Jehn P, Moreno V, et al. Diffuse large B-cell lymphoma subgroups have distinct genetic profiles that influence tumor biology and improve gene-expression-based survival prediction. Blood. 2005;106(9):3183-90.

37. Davis RE, Brown KD, Siebenlist U, Staudt LM. Constitutive nuclear factor kappaB activity is required for survival of activated B cell-like diffuse large B cell lymphoma cells. J Exp Med. 2001;194(12):1861-74.

38. Monti S, Savage KJ, Kutok JL, Feuerhake F, Kurtin P, Mihm M, et al. Molecular profiling of diffuse large B-cell lymphoma identifies robust subtypes including one characterized by host inflammatory response. Blood. 2005;105(5):1851-61.

39. Leonard JP, Schattner EJ, Coleman M. Biology and management of mantle cell lymphoma. Curr Opin Oncol. 2001;13(5):342-7.

40. Vandenberghe E, De Wolf-Peeters C, Vaughan Hudson G, Vaughan Hudson B, Pittaluga S, Anderson L, et al. The clinical outcome of 65 cases of mantle cell lymphoma initially treated with non-intensive therapy by the British National Lymphoma Investigation Group. Br J Haematol. 1997;99(4):842-7.

41. Royo C, Salaverria I, Hartmann EM, Rosenwald A, Campo E, Bea S. The complex landscape of genetic alterations in mantle cell lymphoma. Semin Cancer Biol. 2011;21(5):322-34.

42. Jares P, Colomer D, Campo E. Genetic and molecular pathogenesis of mantle cell lymphoma: perspectives for new targeted therapeutics. Nature reviews Cancer. 2007;7(10):750-62.

43. Smith MR. Mantle cell lymphoma: advances in biology and therapy. Curr Opin Hematol. 2008;15(4):415-21.

44. Martinez N, Camacho FI, Algara P, Rodriguez A, Dopazo A, Ruiz-Ballesteros E, et al. The molecular signature of mantle cell lymphoma reveals multiple signals favoring cell survival. Cancer Res. 2003;63(23):8226-32.

45. Fu L, Lin-Lee YC, Pham LV, Tamayo A, Yoshimura L, Ford RJ. Constitutive NF-kappaB and NFAT activation leads to stimulation of the BLyS survival pathway in aggressive B-cell lymphomas. Blood. 2006;107(11):4540-8.

46. Pham LV, Tamayo AT, Yoshimura LC, Lo P, Ford RJ. Inhibition of constitutive NF-kappa B activation in mantle cell lymphoma B cells leads to induction of cell cycle arrest and apoptosis. J Immunol. 2003;171(1):88-95.

47. Shishodia S, Amin HM, Lai R, Aggarwal BB. Curcumin (diferuloylmethane) inhibits constitutive NF-kappaB activation, induces G1/S arrest, suppresses proliferation, and induces apoptosis in mantle cell lymphoma. Biochem Pharmacol. 2005;70(5):700-13.

48. Tucker CA, Kapanen AI, Chikh G, Hoffman BG, Kyle AH, Wilson IM, et al. Silencing Bcl-2 in models of mantle cell lymphoma is associated with decreases in cyclin D1, nuclear factor-kappaB, p53, bax, and p27 levels. Mol Cancer Ther. 2008;7(4):749-58.

49. Thieblemont C, Nasser V, Felman P, Leroy K, Gazzo S, Callet-Bauchu E, et al. Small lymphocytic lymphoma, marginal zone B-cell lymphoma, and mantle cell lymphoma exhibit distinct gene-expression profiles allowing molecular diagnosis. Blood. 2004;103(7):2727-37.

50. Bennaceur-Griscelli A, Bosq J, Koscielny S, Lefrere F, Turhan A, Brousse N, et al. High level of glutathione-S-transferase pi expression in mantle cell lymphomas. Clinical cancer research : an official journal of the American Association for Cancer Research. 2004;10(9):3029-34.

51. Rizzatti EG, Falcao RP, Panepucci RA, Proto-Siqueira R, Anselmo-Lima WT, Okamoto OK, et al. Gene expression profiling of mantle cell lymphoma cells reveals aberrant expression of genes from the PI3K-AKT, WNT and TGFbeta signalling pathways. Br J Haematol. 2005;130(4):516-26.

52. Rizzatti EG, Mora-Jensen H, Weniger MA, Gibellini F, Lee E, Daibata M, et al. Noxa mediates bortezomib induced apoptosis in both sensitive and intrinsically resistant mantle cell

lymphoma cells and this effect is independent of constitutive activity of the AKT and NF-kappaB pathways. Leuk Lymphoma. 2008;49(4):798-808.

53. Ghielmini M, Zucca E. How I treat mantle cell lymphoma. Blood. 2009;114(8):1469-76.

54. Alessi DR, James SR, Downes CP, Holmes AB, Gaffney PR, Reese CB, et al. Characterization of a 3-phosphoinositide-dependent protein kinase which phosphorylates and activates protein kinase Balpha. Curr Biol. 1997;7(4):261-9.

55. Kawauchi K, Ogasawara T, Yasuyama M, Otsuka K, Yamada O. The PI3K/Akt pathway as a target in the treatment of hematologic malignancies. Anticancer Agents Med Chem. 2009;9(5):550-9.

56. Manning BD, Cantley LC. AKT/PKB signaling: navigating downstream. Cell. 2007;129(7):1261-74.

57. Stokoe D, Stephens LR, Copeland T, Gaffney PR, Reese CB, Painter GF, et al. Dual role of phosphatidylinositol-3,4,5-trisphosphate in the activation of protein kinase B. Science. 1997;277(5325):567-70.

58. Jung HJ, Chen Z, McCarty N. Stem-like tumor cells confer drug resistant properties to mantle cell lymphoma. Leuk Lymphoma. 2011;52(6):1066-79.

59. Baohua Y, Xiaoyan Z, Tiecheng Z, Tao Q, Daren S. Mutations of the PIK3CA gene in diffuse large B cell lymphoma. Diagn Mol Pathol. 2008;17(3):159-65.

60. Bonavida B. Rituximab-induced inhibition of antiapoptotic cell survival pathways: implications in chemo/immunoresistance, rituximab unresponsiveness, prognostic and novel therapeutic interventions. Oncogene. 2007;26(25):3629-36.

61. Fridberg M, Servin A, Anagnostaki L, Linderoth J, Berglund M, Soderberg O, et al. Protein expression and cellular localization in two prognostic subgroups of diffuse large B-cell lymphoma: higher expression of ZAP70 and PKC-beta II in the non-germinal center group and poor survival in patients deficient in nuclear PTEN. Leuk Lymphoma. 2007;48(11):2221-32.

62. Hasselblom S, Hansson U, Olsson M, Toren L, Bergstrom A, Nilsson-Ehle H, et al. High immunohistochemical expression of p-AKT predicts inferior survival in patients with diffuse large B-cell lymphoma treated with immunochemotherapy. Br J Haematol. 2010;149(4):560-8.

63. Renne C, Willenbrock K, Martin-Subero JI, Hinsch N, Doring C, Tiacci E, et al. High expression of several tyrosine kinases and activation of the PI3K/AKT pathway in mediastinal large B cell lymphoma reveals further similarities to Hodgkin lymphoma. Leukemia. 2007;21(4):780-7.

64. Uddin S, Bu R, Ahmed M, Hussain AR, Ajarim D, Al-Dayel F, et al. Leptin receptor expression and its association with PI3K/AKT signaling pathway in diffuse large B-cell lymphoma. Leuk Lymphoma. 2010;51(7):1305-14.

65. Uddin S, Hussain AR, Ahmed M, Al-Dayel F, Bu R, Bavi P, et al. Inhibition of c-MET is a potential therapeutic strategy for treatment of diffuse large B-cell lymphoma. Lab Invest. 2010;90(9):1346-56.

66. Nakao A, Afrakhte M, Moren A, Nakayama T, Christian JL, Heuchel R, et al. Identification of Smad7, a TGFbeta-inducible antagonist of TGF-beta signalling. Nature. 1997;389(6651):631-5.

67. Imamura T, Takase M, Nishihara A, Oeda E, Hanai J, Kawabata M, et al. Smad6 inhibits signalling by the TGF-beta superfamily. Nature. 1997;389(6651):622-6.

68. Wendel HG, De Stanchina E, Fridman JS, Malina A, Ray S, Kogan S, et al. Survival signalling by Akt and eIF4E in oncogenesis and cancer therapy. Nature. 2004;428(6980):332-7.

69. Hess G, Herbrecht R, Romaguera J, Verhoef G, Crump M, Gisselbrecht C, et al. Phase III study to evaluate temsirolimus compared with investigator's choice therapy for the treatment of relapsed or refractory mantle cell lymphoma. Journal of clinical oncology : official journal of the American Society of Clinical Oncology. 2009;27(23):3822-9.

70. Shi Y, Massague J. Mechanisms of TGF-beta signaling from cell membrane to the nucleus. Cell. 2003;113(6):685-700.

71. Chen G, Ghosh P, Osawa H, Sasaki CY, Rezanka L, Yang J, et al. Resistance to TGF-beta 1 correlates with aberrant expression of TGF-beta receptor II in human B-cell lymphoma cell lines. Blood. 2007;109(12):5301-7.

72. Wang D, Long J, Dai F, Liang M, Feng XH, Lin X. BCL6 represses Smad signaling in transforming growth factor-beta resistance. Cancer Res. 2008;68(3):783-9.

73. Wendel HG, Malina A, Zhao Z, Zender L, Kogan SC, Cordon-Cardo C, et al. Determinants of sensitivity and resistance to rapamycin-chemotherapy drug combinations in vivo. Cancer Res. 2006;66(15):7639-46.

74. Allard D, Figg N, Bennett MR, Littlewood TD. Akt regulates the survival of vascular smooth muscle cells via inhibition of FoxO3a and GSK3. The Journal of biological chemistry. 2008;283(28):19739-47.

75. Datta SR, Brunet A, Greenberg ME. Cellular survival: a play in three Akts. Genes Dev. 1999;13(22):2905-27.

76. del Peso L, Gonzalez-Garcia M, Page C, Herrera R, Nunez G. Interleukin-3-induced phosphorylation of BAD through the protein kinase Akt. Science. 1997;278(5338):687-9.

77. Goldman EH, Chen L, Fu H. Activation of apoptosis signal-regulating kinase 1 by reactive oxygen species through dephosphorylation at serine 967 and 14-3-3 dissociation. The Journal of biological chemistry. 2004;279(11):10442-9.

78. Jope RS, Johnson GV. The glamour and gloom of glycogen synthase kinase-3. Trends Biochem Sci. 2004;29(2):95-102.

79. Kim I, Shu CW, Xu W, Shiau CW, Grant D, Vasile S, et al. Chemical biology investigation of cell death pathways activated by endoplasmic reticulum stress reveals cytoprotective modulators of ASK1. The Journal of biological chemistry. 2009;284(3):1593-603.

80. Yan L, Lavin VA, Moser LR, Cui Q, Kanies C, Yang E. PP2A regulates the pro-apoptotic activity of FOXO1. The Journal of biological chemistry. 2008;283(12):7411-20.

81. Suzuki E, Umezawa K, Bonavida B. Rituximab inhibits the constitutively activated PI3K-Akt pathway in B-NHL cell lines: involvement in chemosensitization to drug-induced apoptosis. Oncogene. 2007;26(42):6184-93.

82. Maxwell SA, Cherry EM, Bayless KJ. Akt, 14-3-3zeta, and vimentin mediate a drug-resistant invasive phenotype in diffuse large B-cell lymphoma. Leuk Lymphoma. 2011;52(5):849-64.

83. Maxwell SA, Li Z, Jaye D, Ballard S, Ferrell J, Fu H. 14-3-3zeta mediates resistance of diffuse large B cell lymphoma to an anthracycline-based chemotherapeutic regimen. The Journal of biological chemistry. 2009;284(33):22379-89.

84. Gupta M, Ansell SM, Novak AJ, Kumar S, Kaufmann SH, Witzig TE. Inhibition of histone deacetylase overcomes rapamycin-mediated resistance in diffuse large B-cell lymphoma by inhibiting Akt signaling through mTORC2. Blood. 2009;114(14):2926-35.

85. Smith SM, van Besien K, Karrison T, Dancey J, McLaughlin P, Younes A, et al. Temsirolimus has activity in non-mantle cell non-Hodgkin's lymphoma subtypes: The University of Chicago phase II consortium. Journal of clinical oncology : official journal of the American Society of Clinical Oncology. 2010;28(31):4740-6.

86. Witzig TE, Reeder CB, LaPlant BR, Gupta M, Johnston PB, Micallef IN, et al. A phase II trial of the oral mTOR inhibitor everolimus in relapsed aggressive lymphoma. Leukemia. 2011;25(2):341-7.

87. Schatz JH. Targeting the PI3K/AKT/mTOR pathway in non-Hodgkin’s lymphoma: results, biology, and development strategies. Current oncology reports. 2011;13(5):398-406.

88. Krammer PH. CD95's deadly mission in the immune system. Nature. 2000;407(6805):789-95.

89. Plumas J, Jacob MC, Chaperot L, Molens JP, Sotto JJ, Bensa JC. Tumor B cells from non-Hodgkin's lymphoma are resistant to CD95 (Fas/Apo-1)-mediated apoptosis. Blood. 1998;91(8):2875-85.

90. Thomas RK, Kallenborn A, Wickenhauser C, Schultze JL, Draube A, Vockerodt M, et al. Constitutive expression of c-FLIP in Hodgkin and Reed-Sternberg cells. Am J Pathol. 2002;160(4):1521-8.

91. Kelley RF, Totpal K, Lindstrom SH, Mathieu M, Billeci K, Deforge L, et al. Receptor-selective mutants of apoptosis-inducing ligand 2/tumor necrosis factor-related apoptosis-inducing ligand reveal a greater contribution of death receptor (DR) 5 than DR4 to apoptosis signaling. The Journal of biological chemistry. 2005;280(3):2205-12.

92. Scaffidi C, Kirchhoff S, Krammer PH, Peter ME. Apoptosis signaling in lymphocytes. Curr Opin Immunol. 1999;11(3):277-85.

93. Siegel RM, Chan FK, Chun HJ, Lenardo MJ. The multifaceted role of Fas signaling in immune cell homeostasis and autoimmunity. Nat Immunol. 2000;1(6):469-74.

94. Ashkenazi A, Pai RC, Fong S, Leung S, Lawrence DA, Marsters SA, et al. Safety and antitumor activity of recombinant soluble Apo2 ligand. J Clin Invest. 1999;104(2):155-62.

95. Walczak H, Miller RE, Ariail K, Gliniak B, Griffith TS, Kubin M, et al. Tumoricidal activity of tumor necrosis factor-related apoptosis-inducing ligand in vivo. Nat Med. 1999;5(2):157-63.

96. Wiley SR, Schooley K, Smolak PJ, Din WS, Huang CP, Nicholl JK, et al. Identification and characterization of a new member of the TNF family that induces apoptosis. Immunity. 1995;3(6):673-82.

97. Cillessen SA, Meijer CJ, Ossenkoppele GJ, Castricum KC, Westra AH, Niesten P, et al. Human soluble TRAIL/Apo2L induces apoptosis in a subpopulation of chemotherapy refractory nodal diffuse large B-cell lymphomas, determined by a highly sensitive in vitro apoptosis assay. Br J Haematol. 2006;134(3):283-93.

98. Bodmer JL, Holler N, Reynard S, Vinciguerra P, Schneider P, Juo P, et al. TRAIL receptor-2 signals apoptosis through FADD and caspase-8. Nature cell biology. 2000;2(4):241-3.

99. Pitti RM, Marsters SA, Ruppert S, Donahue CJ, Moore A, Ashkenazi A. Induction of apoptosis by Apo-2 ligand, a new member of the tumor necrosis factor cytokine family. The Journal of biological chemistry. 1996;271(22):12687-90.

100. Brien G, Trescol-Biemont MC, Bonnefoy-Berard N. Downregulation of Bfl-1 protein expression sensitizes malignant B cells to apoptosis. Oncogene. 2007;26(39):5828-32.

101. Grumont RJ, Rourke IJ, Gerondakis S. Rel-dependent induction of A1 transcription is required to protect B cells from antigen receptor ligation-induced apoptosis. Genes Dev. 1999;13(4):400-11.

102. Wang CY, Guttridge DC, Mayo MW, Baldwin AS, Jr. NF-kappaB induces expression of the Bcl-2 homologue A1/Bfl-1 to preferentially suppress chemotherapy-induced apoptosis. Mol Cell Biol. 1999;19(9):5923-9.

103. Zong WX, Edelstein LC, Chen C, Bash J, Gelinas C. The prosurvival Bcl-2 homolog Bfl-1/A1 is a direct transcriptional target of NF-kappaB that blocks TNFalpha-induced apoptosis. Genes Dev. 1999;13(4):382-7.

104. Werner AB, de Vries E, Tait SW, Bontjer I, Borst J. Bcl-2 family member Bfl-1/A1 sequesters truncated bid to inhibit is collaboration with pro-apoptotic Bak or Bax. The Journal of biological chemistry. 2002;277(25):22781-8.

105. Lam LT, Davis RE, Pierce J, Hepperle M, Xu Y, Hottelet M, et al. Small molecule inhibitors of IkappaB kinase are selectively toxic for subgroups of diffuse large B-cell lymphoma defined by gene expression profiling. Clinical cancer research : an official journal of the American Association for Cancer Research. 2005;11(1):28-40.

106. Danial NN, Korsmeyer SJ. Cell death: critical control points. Cell. 2004;116(2):205-19.

107. van Delft MF, Huang DC. How the Bcl-2 family of proteins interact to regulate apoptosis. Cell Res. 2006;16(2):203-13.

108. Puthalakath H, Strasser A. Keeping killers on a tight leash: transcriptional and post-translational control of the pro-apoptotic activity of BH3-only proteins. Cell Death Differ. 2002;9(5):505-12.

109. Sun Y, Orrenius S, Pervaiz S, Fadeel B. Plasma membrane sequestration of apoptotic protease-activating factor-1 in human B-lymphoma cells: a novel mechanism of chemoresistance. Blood. 2005;105(10):4070-7.

110. Johnstone RW, Ruefli AA, Lowe SW. Apoptosis: a link between cancer genetics and chemotherapy. Cell. 2002;108(2):153-64.

111. Reed JC. Bcl-2 and the regulation of programmed cell death. J Cell Biol. 1994;124(1-2):1-6.

112. Shangary S, Johnson DE. Peptides derived from BH3 domains of Bcl-2 family members: a comparative analysis of inhibition of Bcl-2, Bcl-x(L) and Bax oligomerization, induction of cytochrome c release, and activation of cell death. Biochemistry. 2002;41(30):9485-95.

113. Wang JL, Liu D, Zhang ZJ, Shan S, Han X, Srinivasula SM, et al. Structure-based discovery of an organic compound that binds Bcl-2 protein and induces apoptosis of tumor cells. Proc Natl Acad Sci U S A. 2000;97(13):7124-9.

114. Yang J, Liu X, Bhalla K, Kim CN, Ibrado AM, Cai J, et al. Prevention of apoptosis by Bcl-2: release of cytochrome c from mitochondria blocked. Science. 1997;275(5303):1129-32.

115. Kluck RM, Bossy-Wetzel E, Green DR, Newmeyer DD. The release of cytochrome c from mitochondria: a primary site for Bcl-2 regulation of apoptosis. Science. 1997;275(5303):1132-6.

116. Yang E, Korsmeyer SJ. Molecular thanatopsis: a discourse on the BCL2 family and cell death. Blood. 1996;88(2):386-401.

117. Yunis JJ, Frizzera G, Oken MM, McKenna J, Theologides A, Arnesen M. Multiple recurrent genomic defects in follicular lymphoma. A possible model for cancer. N Engl J Med. 1987;316(2):79-84.

118. Gascoyne RD, Adomat SA, Krajewski S, Krajewska M, Horsman DE, Tolcher AW, et al. Prognostic significance of Bcl-2 protein expression and Bcl-2 gene rearrangement in diffuse aggressive non-Hodgkin's lymphoma. Blood. 1997;90(1):244-51.

119. Hermine O, Haioun C, Lepage E, d'Agay MF, Briere J, Lavignac C, et al. Prognostic significance of bcl-2 protein expression in aggressive non-Hodgkin's lymphoma. Groupe d'Etude des Lymphomes de l'Adulte (GELA). Blood. 1996;87(1):265-72.

120. Hill ME, MacLennan KA, Cunningham DC, Vaughan Hudson B, Burke M, Clarke P, et al. Prognostic significance of BCL-2 expression and bcl-2 major breakpoint region rearrangement in diffuse large cell non-Hodgkin's lymphoma: a British National Lymphoma Investigation Study. Blood. 1996;88(3):1046-51.

121. Sanchez E, Chacon I, Plaza MM, Munoz E, Cruz MA, Martinez B, et al. Clinical outcome in diffuse large B-cell lymphoma is dependent on the relationship between different cell-cycle regulator proteins. Journal of clinical oncology : official journal of the American Society of Clinical Oncology. 1998;16(5):1931-9.

122. Chanan-Khan A. Bcl-2 antisense therapy in B-cell malignancies. Blood Rev. 2005;19(4):213-21.

123. Waters JS, Webb A, Cunningham D, Clarke PA, Raynaud F, di Stefano F, et al. Phase I clinical and pharmacokinetic study of bcl-2 antisense oligonucleotide therapy in patients with non-Hodgkin's lymphoma. Journal of clinical oncology : official journal of the American Society of Clinical Oncology. 2000;18(9):1812-23.

124. Kitada S, Takayama S, De Riel K, Tanaka S, Reed JC. Reversal of chemoresistance of lymphoma cells by antisense-mediated reduction of bcl-2 gene expression. Antisense Res Dev. 1994;4(2):71-9.

125. Pro B, Leber B, Smith M, Fayad L, Romaguera J, Hagemeister F, et al. Phase II multicenter study of oblimersen sodium, a Bcl-2 antisense oligonucleotide, in combination with rituximab in patients with recurrent B-cell non-Hodgkin lymphoma. Br J Haematol. 2008;143(3):355-60.

126. Rathmell JC, Thompson CB. The central effectors of cell death in the immune system. Annual review of immunology. 1999;17:781-828.

127. Duckett CS, Nava VE, Gedrich RW, Clem RJ, Van Dongen JL, Gilfillan MC, et al. A conserved family of cellular genes related to the baculovirus iap gene and encoding apoptosis inhibitors. The EMBO journal. 1996;15(11):2685-94.

128. Liston P, Roy N, Tamai K, Lefebvre C, Baird S, Cherton-Horvat G, et al. Suppression of apoptosis in mammalian cells by NAIP and a related family of IAP genes. Nature. 1996;379(6563):349-53.

129. Muris JJ, Cillessen SA, Vos W, van Houdt IS, Kummer JA, van Krieken JH, et al. Immunohistochemical profiling of caspase signaling pathways predicts clinical response to chemotherapy in primary nodal diffuse large B-cell lymphomas. Blood. 2005;105(7):2916-23.

130. Cillessen SA, Hess CJ, Hooijberg E, Castricum KC, Kortman P, Denkers F, et al. Inhibition of the intrinsic apoptosis pathway downstream of caspase-9 activation causes chemotherapy resistance in diffuse large B-cell lymphoma. Clinical cancer research : an official journal of the American Association for Cancer Research. 2007;13(23):7012-21.

131. Cillessen SA, Reed JC, Welsh K, Pinilla C, Houghten R, Hooijberg E, et al. Small-molecule XIAP antagonist restores caspase-9 mediated apoptosis in XIAP-positive diffuse large B-cell lymphoma cells. Blood. 2008;111(1):369-75.

132. Savitsky K, Bar-Shira A, Gilad S, Rotman G, Ziv Y, Vanagaite L, et al. A single ataxia telangiectasia gene with a product similar to PI-3 kinase. Science. 1995;268(5218):1749-53.

133. Korz C, Pscherer A, Benner A, Mertens D, Schaffner C, Leupolt E, et al. Evidence for distinct pathomechanisms in B-cell chronic lymphocytic leukemia and mantle cell lymphoma by quantitative expression analysis of cell cycle and apoptosis-associated genes. Blood. 2002;99(12):4554-61.

134. Pusapati RV, Rounbehler RJ, Hong S, Powers JT, Yan M, Kiguchi K, et al. ATM promotes apoptosis and suppresses tumorigenesis in response to Myc. Proc Natl Acad Sci U S A. 2006;103(5):1446-51.

135. Shreeram S, Hee WK, Demidov ON, Kek C, Yamaguchi H, Fornace AJ, Jr., et al. Regulation of ATM/p53-dependent suppression of myc-induced lymphomas by Wip1 phosphatase. J Exp Med. 2006;203(13):2793-9.

136. Reimann M, Loddenkemper C, Rudolph C, Schildhauer I, Teichmann B, Stein H, et al. The Myc-evoked DNA damage response accounts for treatment resistance in primary lymphomas in vivo. Blood. 2007;110(8):2996-3004.

137. Baldwin AS. Control of oncogenesis and cancer therapy resistance by the transcription factor NF-kappaB. J Clin Invest. 2001;107(3):241-6.

138. Jost PJ, Ruland J. Aberrant NF-kappaB signaling in lymphoma: mechanisms, consequences, and therapeutic implications. Blood. 2007;109(7):2700-7.

139. Hayden MS, Ghosh S. Signaling to NF-kappaB. Genes Dev. 2004;18(18):2195-224.

140. Karin M. Nuclear factor-kappaB in cancer development and progression. Nature. 2006;441(7092):431-6.

141. Kim HJ, Hawke N, Baldwin AS. NF-kappaB and IKK as therapeutic targets in cancer. Cell Death Differ. 2006;13(5):738-47.

142. Luo JL, Kamata H, Karin M. IKK/NF-kappaB signaling: balancing life and death--a new approach to cancer therapy. J Clin Invest. 2005;115(10):2625-32.

143. Jazirehi AR, Vega MI, Chatterjee D, Goodglick L, Bonavida B. Inhibition of the Raf-MEK1/2-ERK1/2 signaling pathway, Bcl-xL down-regulation, and chemosensitization of non-Hodgkin's lymphoma B cells by Rituximab. Cancer Res. 2004;64(19):7117-26.

144. Thomas RK, Sos ML, Zander T, Mani O, Popov A, Berenbrinker D, et al. Inhibition of nuclear translocation of nuclear factor-kappaB despite lack of functional IkappaBalpha protein overcomes multiple defects in apoptosis signaling in human B-cell malignancies. Clinical cancer research : an official journal of the American Association for Cancer Research. 2005;11(22):8186-94.

145. Bai H, Wei J, Deng C, Yang X, Wang C, Xu R. MicroRNA-21 regulates the sensitivity of diffuse large B-cell lymphoma cells to the CHOP chemotherapy regimen. International journal of hematology. 2013;97(2):223-31.

146. Hayashita Y, Osada H, Tatematsu Y, Yamada H, Yanagisawa K, Tomida S, et al. A polycistronic microRNA cluster, miR-17-92, is overexpressed in human lung cancers and enhances cell proliferation. Cancer research. 2005;65(21):9628-32.

147. He L, Thomson JM, Hemann MT, Hernando-Monge E, Mu D, Goodson S, et al. A microRNA polycistron as a potential human oncogene. Nature. 2005;435(7043):828-33.

148. Ota A, Tagawa H, Karnan S, Tsuzuki S, Karpas A, Kira S, et al. Identification and characterization of a novel gene, C13orf25, as a target for 13q31-q32 amplification in malignant lymphoma. Cancer research. 2004;64(9):3087-95.

149. Rao E, Jiang C, Ji M, Huang X, Iqbal J, Lenz G, et al. The miRNA-17~ 92 cluster mediates chemoresistance and enhances tumor growth in mantle cell lymphoma via PI3K/AKT pathway activation. Leukemia. 2012;26(5):1064-72.

150. Hayashi H, Abdollah S, Qiu Y, Cai J, Xu YY, Grinnell BW, et al. The MAD-related protein Smad7 associates with the TGFbeta receptor and functions as an antagonist of TGFbeta signaling. Cell. 1997;89(7):1165-73.

151. Tome ME, Baker AF, Powis G, Payne CM, Briehl MM. Catalase-overexpressing thymocytes are resistant to glucocorticoid-induced apoptosis and exhibit increased net tumor growth. Cancer Res. 2001;61(6):2766-73.

152. Tome ME, Briehl MM. Thymocytes selected for resistance to hydrogen peroxide show altered antioxidant enzyme profiles and resistance to dexamethasone-induced apoptosis. Cell Death Differ. 2001;8(9):953-61.

153. Wilkinson ST, Wilkinson DB, Tardif HL, Tome ME, Briehl MM. Increased cytochrome c correlates with poor survival in aggressive lymphoma. Oncology letters. 2010;1(2):227-30.

154. Tome ME, Johnson DB, Rimsza LM, Roberts RA, Grogan TM, Miller TP, et al. A redox signature score identifies diffuse large B-cell lymphoma patients with a poor prognosis. Blood. 2005;106(10):3594-601.

155. Tome ME, Lutz NW, Briehl MM. Overexpression of catalase or Bcl-2 alters glucose and energy metabolism concomitant with dexamethasone resistance. Biochimica et biophysica acta. 2004;1693(1):57-72.

156. Certo M, Del Gaizo Moore V, Nishino M, Wei G, Korsmeyer S, Armstrong SA, et al. Mitochondria primed by death signals determine cellular addiction to antiapoptotic BCL-2 family members. Cancer Cell. 2006;9(5):351-65.

157. Willis SN, Fletcher JI, Kaufmann T, van Delft MF, Chen L, Czabotar PE, et al. Apoptosis initiated when BH3 ligands engage multiple Bcl-2 homologs, not Bax or Bak. Science. 2007;315(5813):856-9.

158. Tome ME, Frye JB, Coyle DL, Jacobson EL, Samulitis BK, Dvorak K, et al. Lymphoma cells with increased anti-oxidant defenses acquire chemoresistance. Experimental and therapeutic medicine. 2012;3(5):845-52.

159. Gatenby RA, Gillies RJ. Why do cancers have high aerobic glycolysis? Nature Reviews Cancer. 2004;4(11):891-9.

160. Raghunand N, He X, van Sluis R, Mahoney B, Baggett B, Taylor CW, et al. Enhancement of chemotherapy by manipulation of tumour pH. Br J Cancer. 1999;80(7):1005-11.

161. De Milito A, Fais S. Tumor acidity, chemoresistance and proton pump inhibitors. Future Oncol. 2005;1(6):779-86.

162. Gatenby RA, Gawlinski ET. The glycolytic phenotype in carcinogenesis and tumor invasion: insights through mathematical models. Cancer Res. 2003;63(14):3847-54.

163. Sennoune SR, Luo D, Martinez-Zaguilan R. Plasmalemmal vacuolar-type H+-ATPase in cancer biology. Cell Biochem Biophys. 2004;40(2):185-206.

164. De Milito A, Iessi E, Logozzi M, Lozupone F, Spada M, Marino ML, et al. Proton pump inhibitors induce apoptosis of human B-cell tumors through a caspase-independent mechanism involving reactive oxygen species. Cancer Res. 2007;67(11):5408-17.

165. O'Brien ML, Tew KD. Glutathione and related enzymes in multidrug resistance. Eur J Cancer. 1996;32A(6):967-78.

166. Cowan KH, Batist G, Tulpule A, Sinha BK, Myers CE. Similar biochemical changes associated with multidrug resistance in human breast cancer cells and carcinogen-induced resistance to xenobiotics in rats. Proc Natl Acad Sci U S A. 1986;83(24):9328-32.

167. McGown AT, Fox BW. A proposed mechanism of resistance to cyclophosphamide and phosphoramide mustard in a Yoshida cell line in vitro. Cancer Chemother Pharmacol. 1986;17(3):223-6.

168. Robson CN, Lewis AD, Wolf CR, Hayes JD, Hall A, Proctor SJ, et al. Reduced levels of drug-induced DNA cross-linking in nitrogen mustard-resistant Chinese hamster ovary cells expressing elevated glutathione S-transferase activity. Cancer Res. 1987;47(22):6022-7.

169. Schisselbauer JC, Silber R, Papadopoulos E, Abrams K, LaCreta FP, Tew KD. Characterization of glutathione S-transferase expression in lymphocytes from chronic lymphocytic leukemia patients. Cancer Res. 1990;50(12):3562-8.

170. Teicher BA, Holden SA, Kelley MJ, Shea TC, Cucchi CA, Rosowsky A, et al. Characterization of a human squamous carcinoma cell line resistant to cis-diamminedichloroplatinum(II). Cancer Res. 1987;47(2):388-93.

171. Tew KD. Glutathione-associated enzymes in anticancer drug resistance. Cancer Res. 1994;54(16):4313-20.

172. Coiffier B, Lepage E, Briere J, Herbrecht R, Tilly H, Bouabdallah R, et al. CHOP chemotherapy plus rituximab compared with CHOP alone in elderly patients with diffuse large-B-cell lymphoma. N Engl J Med. 2002;346(4):235-42.

173. Sehn LH, Donaldson J, Chhanabhai M, Fitzgerald C, Gill K, Klasa R, et al. Introduction of combined CHOP plus rituximab therapy dramatically improved outcome of diffuse large B-cell lymphoma in British Columbia. Journal of clinical oncology : official journal of the American Society of Clinical Oncology. 2005;23(22):5027-33.

174. Coiffier B, Haioun C, Ketterer N, Engert A, Tilly H, Ma D, et al. Rituximab (anti-CD20 monoclonal antibody) for the treatment of patients with relapsing or refractory aggressive lymphoma: a multicenter phase II study. Blood. 1998;92(6):1927-32.

175. Hess G, Flohr T, Kolbe K, Bonn S, Schuler M, Derigs HG, et al. Effect of rituximab on the long-term outcome after high-dose therapy for relapsed B-cell non-Hodgkin's lymphoma. Ann Hematol. 2006;85(11):769-79.

176. Hiddemann W, Kneba M, Dreyling M, Schmitz N, Lengfelder E, Schmits R, et al. Frontline therapy with rituximab added to the combination of cyclophosphamide, doxorubicin, vincristine, and prednisone (CHOP) significantly improves the outcome for patients with advanced-stage follicular lymphoma compared with therapy with CHOP alone: results of a prospective randomized study of the German Low-Grade Lymphoma Study Group. Blood. 2005;106(12):3725-32.

177. Marcus R, Imrie K, Belch A, Cunningham D, Flores E, Catalano J, et al. CVP chemotherapy plus rituximab compared with CVP as first-line treatment for advanced follicular lymphoma. Blood. 2005;105(4):1417-23.

178. Pfreundschuh M, Trumper L, Osterborg A, Pettengell R, Trneny M, Imrie K, et al. CHOP-like chemotherapy plus rituximab versus CHOP-like chemotherapy alone in young patients with good-prognosis diffuse large-B-cell lymphoma: a randomised controlled trial by the MabThera International Trial (MInT) Group. Lancet Oncol. 2006;7(5):379-91.

179. Vellenga E, van Putten WL, van 't Veer MB, Zijlstra JM, Fibbe WE, van Oers MH, et al. Rituximab improves the treatment results of DHAP-VIM-DHAP and ASCT in relapsed/progressive aggressive CD20+ NHL: a prospective randomized HOVON trial. Blood. 2008;111(2):537-43.

180. Maloney DG, Liles TM, Czerwinski DK, Waldichuk C, Rosenberg J, Grillo-Lopez A, et al. Phase I clinical trial using escalating single-dose infusion of chimeric anti-CD20 monoclonal antibody (IDEC-C2B8) in patients with recurrent B-cell lymphoma. Blood. 1994;84(8):2457-66.

181. Press OW, Appelbaum F, Ledbetter JA, Martin PJ, Zarling J, Kidd P, et al. Monoclonal antibody 1F5 (anti-CD20) serotherapy of human B cell lymphomas. Blood. 1987;69(2):584-91.

182. Einfeld DA, Brown JP, Valentine MA, Clark EA, Ledbetter JA. Molecular cloning of the human B cell CD20 receptor predicts a hydrophobic protein with multiple transmembrane domains. The EMBO journal. 1988;7(3):711-7.

183. Kimby E. Tolerability and safety of rituximab (MabThera). Cancer Treat Rev. 2005;31(6):456-73.

184. Smith MR. Rituximab (monoclonal anti-CD20 antibody): mechanisms of action and resistance. Oncogene. 2003;22(47):7359-68.

185. Martin P, Furman RR, Coleman M, Leonard JP. Phase I to III trials of anti-B cell therapy in non-Hodgkin's lymphoma. Clinical cancer research : an official journal of the American Association for Cancer Research. 2007;13(18 Pt 2):5636s-42s.

186. Coiffier B. Rituximab therapy in malignant lymphoma. Oncogene. 2007;26(25):3603-13.

187. Colombat P, Salles G, Brousse N, Eftekhari P, Soubeyran P, Delwail V, et al. Rituximab (anti-CD20 monoclonal antibody) as single first-line therapy for patients with follicular lymphoma with a low tumor burden: clinical and molecular evaluation. Blood. 2001;97(1):101-6.

188. Ghielmini M, Schmitz SF, Cogliatti SB, Pichert G, Hummerjohann J, Waltzer U, et al. Prolonged treatment with rituximab in patients with follicular lymphoma significantly increases event-free survival and response duration compared with the standard weekly x 4 schedule. Blood. 2004;103(12):4416-23.

189. Hainsworth JD, Litchy S, Burris HA, 3rd, Scullin DC, Jr., Corso SW, Yardley DA, et al. Rituximab as first-line and maintenance therapy for patients with indolent non-hodgkin's lymphoma. Journal of clinical oncology : official journal of the American Society of Clinical Oncology. 2002;20(20):4261-7.

190. Hainsworth JD, Litchy S, Shaffer DW, Lackey VL, Grimaldi M, Greco FA. Maximizing therapeutic benefit of rituximab: maintenance therapy versus re-treatment at progression in patients with indolent non-Hodgkin's lymphoma--a randomized phase II trial of the Minnie Pearl Cancer Research Network. Journal of clinical oncology : official journal of the American Society of Clinical Oncology. 2005;23(6):1088-95.

191. Lemieux B, Bouafia F, Thieblemont C, Hequet O, Arnaud P, Tartas S, et al. Second treatment with rituximab in B-cell non-Hodgkin's lymphoma: efficacy and toxicity on 41 patients treated at CHU-Lyon Sud. Hematol J. 2004;5(6):467-71.

192. McLaughlin P, Grillo-Lopez AJ, Link BK, Levy R, Czuczman MS, Williams ME, et al. Rituximab chimeric anti-CD20 monoclonal antibody therapy for relapsed indolent lymphoma: half of patients respond to a four-dose treatment program. Journal of clinical oncology : official journal of the American Society of Clinical Oncology. 1998;16(8):2825-33.

193. Maloney DG. Immunotherapy for non-Hodgkin's lymphoma: monoclonal antibodies and vaccines. Journal of clinical oncology : official journal of the American Society of Clinical Oncology. 2005;23(26):6421-8.

194. Clynes RA, Towers TL, Presta LG, Ravetch JV. Inhibitory Fc receptors modulate in vivo cytoxicity against tumor targets. Nat Med. 2000;6(4):443-6.

195. Kennedy GA, Tey SK, Cobcroft R, Marlton P, Cull G, Grimmett K, et al. Incidence and nature of CD20-negative relapses following rituximab therapy in aggressive B-cell non-Hodgkin's lymphoma: a retrospective review. Br J Haematol. 2002;119(2):412-6.

196. Daniels I, Abulayha AM, Thomson BJ, Haynes AP. Caspase-independent killing of Burkitt lymphoma cell lines by rituximab. Apoptosis. 2006;11(6):1013-23.

197. Hofmeister JK, Cooney D, Coggeshall KM. Clustered CD20 induced apoptosis: src-family kinase, the proximal regulator of tyrosine phosphorylation, calcium influx, and caspase 3-dependent apoptosis. Blood Cells Mol Dis. 2000;26(2):133-43.

198. Popoff IJ, Savage JA, Blake J, Johnson P, Deans JP. The association between CD20 and Src-family Tyrosine kinases requires an additional factor. Mol Immunol. 1998;35(4):207-14.

199. Shan D, Ledbetter JA, Press OW. Apoptosis of malignant human B cells by ligation of CD20 with monoclonal antibodies. Blood. 1998;91(5):1644-52.

200. Shan D, Ledbetter JA, Press OW. Signaling events involved in anti-CD20-induced apoptosis of malignant human B cells. Cancer Immunol Immunother. 2000;48(12):673-83.

201. Walshe CA, Beers SA, French RR, Chan CH, Johnson PW, Packham GK, et al. Induction of cytosolic calcium flux by CD20 is dependent upon B Cell antigen receptor signaling. The Journal of biological chemistry. 2008;283(25):16971-84.

202. Olejniczak SH, Hernandez-Ilizaliturri FJ, Clements JL, Czuczman MS. Acquired resistance to rituximab is associated with chemotherapy resistance resulting from decreased Bax

and Bak expression. Clinical cancer research : an official journal of the American Association for Cancer Research. 2008;14(5):1550-60.

203. Davidson B, Konstantinovsky S, Nielsen S, Dong HP, Berner A, Vyberg M, et al. Altered expression of metastasis-associated and regulatory molecules in effusions from breast cancer patients: a novel model for tumor progression. Clinical cancer research : an official journal of the American Association for Cancer Research. 2004;10(21):7335-46.

204. Gabison EE, Hoang-Xuan T, Mauviel A, Menashi S. EMMPRIN/CD147, an MMP modulator in cancer, development and tissue repair. Biochimie. 2005;87(3-4):361-8.

205. Misra S, Ghatak S, Zoltan-Jones A, Toole BP. Regulation of multidrug resistance in cancer cells by hyaluronan. The Journal of biological chemistry. 2003;278(28):25285-8.

206. Reimers N, Zafrakas K, Assmann V, Egen C, Riethdorf L, Riethdorf S, et al. Expression of extracellular matrix metalloproteases inducer on micrometastatic and primary mammary carcinoma cells. Clinical cancer research : an official journal of the American Association for Cancer Research. 2004;10(10):3422-8.

207. Zou W, Yang H, Hou X, Zhang W, Chen B, Xin X. Inhibition of CD147 gene expression via RNA interference reduces tumor cell invasion, tumorigenicity and increases chemosensitivity to paclitaxel in HO-8910pm cells. Cancer letters. 2007;248(2):211-8.

208. Zucker S, Hymowitz M, Rollo EE, Mann R, Conner CE, Cao J, et al. Tumorigenic potential of extracellular matrix metalloproteinase inducer. Am J Pathol. 2001;158(6):1921-8.

209. Illemann M, Bird N, Majeed A, Sehested M, Laerum OD, Lund LR, et al. MMP-9 is differentially expressed in primary human colorectal adenocarcinomas and their metastases. Mol Cancer Res. 2006;4(5):293-302.

210. Jia L, Wei W, Cao J, Xu H, Miao X, Zhang J. Silencing CD147 inhibits tumor progression and increases chemosensitivity in murine lymphoid neoplasm P388D1 cells. Ann Hematol. 2009;88(8):753-60.

211. Simon SM, Schindler M. Cell biological mechanisms of multidrug resistance in tumors. Proc Natl Acad Sci U S A. 1994;91(9):3497-504.

212. Gottesman MM, Pastan I. Biochemistry of multidrug resistance mediated by the multidrug transporter. Annu Rev Biochem. 1993;62:385-427.

213. Kerb R, Hoffmeyer S, Brinkmann U. ABC drug transporters: hereditary polymorphisms and pharmacological impact in MDR1, MRP1 and MRP2. Pharmacogenomics. 2001;2(1):51-64.

214. Litman T, Druley TE, Stein WD, Bates SE. From MDR to MXR: new understanding of multidrug resistance systems, their properties and clinical significance. Cell Mol Life Sci. 2001;58(7):931-59.

215. Szakacs G, Paterson JK, Ludwig JA, Booth-Genthe C, Gottesman MM. Targeting multidrug resistance in cancer. Nature reviews Drug discovery. 2006;5(3):219-34.

216. Kang YK, Zhan Z, Regis J, Alvarez M, Robey R, Meadows B, et al. Expression of mdr-1 in refractory lymphoma: quantitation by polymerase chain reaction and validation of the assay. Blood. 1995;86(4):1515-24.

217. Pileri SA, Sabattini E, Falini B, Tazzari PL, Gherlinzoni F, Michieli MG, et al. Immunohistochemical detection of the multidrug transport protein P170 in human normal tissues and malignant lymphomas. Histopathology. 1991;19(2):131-40.

218. Ohsawa M, Ikura Y, Fukushima H, Shirai N, Sugama Y, Suekane T, et al. Immunohistochemical expression of multidrug resistance proteins as a predictor of poor response to chemotherapy and prognosis in patients with nodal diffuse large B-cell lymphoma. Oncology. 2005;68(4-6):422-31.

219. Moscow JA, Fairchild CR, Madden MJ, Ransom DT, Wieand HS, O'Brien EE, et al. Expression of anionic glutathione-S-transferase and P-glycoprotein genes in human tissues and tumors. Cancer Res. 1989;49(6):1422-8.

220. Miller TP, Grogan TM, Dalton WS, Spier CM, Scheper RJ, Salmon SE. P-glycoprotein expression in malignant lymphoma and reversal of clinical drug resistance with chemotherapy plus high-dose verapamil. Journal of clinical oncology : official journal of the American Society of Clinical Oncology. 1991;9(1):17-24.

221. Wilson WH, Bates SE, Fojo A, Bryant G, Zhan Z, Regis J, et al. Controlled trial of dexverapamil, a modulator of multidrug resistance, in lymphomas refractory to EPOCH chemotherapy. Journal of clinical oncology : official journal of the American Society of Clinical Oncology. 1995;13(8):1995-2004.

222. Yahanda AM, Alder KM, Fisher GA, Brophy NA, Halsey J, Hardy RI, et al. Phase I trial of etoposide with cyclosporine as a modulator of multidrug resistance. Journal of clinical oncology : official journal of the American Society of Clinical Oncology. 1992;10(10):1624-34.

223. Rodriguez C, Commes T, Robert J, Rossi JF. Expression of P-glycoprotein and anionic glutathione S-transferase genes in non-Hodgkin's lymphoma. Leuk Res. 1993;17(2):149-56.

224. Finnegan MC, Royds J, Goepel JR, Lorigan P, Hancock BW, Goyns MH. MDR-1 expression in non-Hodgkin's lymphomas is unrelated to treatment intensity or response to therapy. Leuk Lymphoma. 1995;18(3-4):297-302.

225. Zhan Z, Sandor VA, Gamelin E, Regis J, Dickstein B, Wilson W, et al. Expression of the multidrug resistance-associated protein gene in refractory lymphoma: quantitation by a validated polymerase chain reaction assay. Blood. 1997;89(10):3795-800.

226. Goldstein LJ, Galski H, Fojo A, Willingham M, Lai SL, Gazdar A, et al. Expression of a multidrug resistance gene in human cancers. J Natl Cancer Inst. 1989;81(2):116-24.

227. Holzmayer TA, Hilsenbeck S, Von Hoff DD, Roninson IB. Clinical correlates of MDR1 (P-glycoprotein) gene expression in ovarian and small-cell lung carcinomas. J Natl Cancer Inst. 1992;84(19):1486-91.

228. Garcia MG, Alaniz LD, Cordo Russo RI, Alvarez E, Hajos SE. PI3K/Akt inhibition modulates multidrug resistance and activates NF-kappaB in murine lymphoma cell lines. Leuk Res. 2009;33(2):288-96.

229. Kim JE, Singh RR, Cho-Vega JH, Drakos E, Davuluri Y, Khokhar FA, et al. Sonic hedgehog signaling proteins and ATP-binding cassette G2 are aberrantly expressed in diffuse large B-cell lymphoma. Modern Pathology. 2009;22(10):1312-20.

230. Singh RR, Kunkalla K, Qu C, Schlette E, Neelapu SS, Samaniego F, et al. ABCG2 is a direct transcriptional target of hedgehog signaling and involved in stroma-induced drug tolerance in diffuse large B-cell lymphoma. Oncogene. 2011;30(49):4874-86.

231. Scheper RJ, Broxterman HJ, Scheffer GL, Kaaijk P, Dalton WS, van Heijningen TH, et al. Overexpression of a M(r) 110,000 vesicular protein in non-P-glycoprotein-mediated multidrug resistance. Cancer Res. 1993;53(7):1475-9.

232. Scheffer GL, Wijngaard PL, Flens MJ, Izquierdo MA, Slovak ML, Pinedo HM, et al. The drug resistance-related protein LRP is the human major vault protein. Nat Med. 1995;1(6):578-82.

233. Kedersha NL, Rome LH. Isolation and characterization of a novel ribonucleoprotein particle: large structures contain a single species of small RNA. J Cell Biol. 1986;103(3):699-709.

234. Izquierdo MA, Shoemaker RH, Flens MJ, Scheffer GL, Wu L, Prather TR, et al. Overlapping phenotypes of multidrug resistance among panels of human cancer-cell lines. Int J Cancer. 1996;65(2):230-7.

235. Kitazono M, Sumizawa T, Takebayashi Y, Chen ZS, Furukawa T, Nagayama S, et al. Multidrug resistance and the lung resistance-related protein in human colon carcinoma SW-620 cells. J Natl Cancer Inst. 1999;91(19):1647-53.

236. Filipits M, Jaeger U, Simonitsch I, Chizzali-Bonfadin C, Heinzl H, Pirker R. Clinical relevance of the lung resistance protein in diffuse large B-cell lymphomas. Clinical cancer research : an official journal of the American Association for Cancer Research. 2000;6(9):3417-23.

237. Wolf CR, Macpherson JS, Smyth JF. Evidence for the metabolism of mitozantrone by microsomal glutathione transferases and 3-methylcholanthrene-inducible glucuronosyl transferases. Biochem Pharmacol. 1986;35(9):1577-81.

238. Batist G, Tulpule A, Sinha BK, Katki AG, Myers CE, Cowan KH. Overexpression of a novel anionic glutathione transferase in multidrug-resistant human breast cancer cells. The Journal of biological chemistry. 1986;261(33):15544-9.

239. Gupta V, Singh SV, Ahmad H, Medh RD, Awasthi YC. Glutathione and glutathione S-transferases in a human plasma cell line resistant to melphalan. Biochem Pharmacol. 1989;38(12):1993-2000.

240. Bolton MG, Colvin OM, Hilton J. Specificity of isozymes of murine hepatic glutathione S-transferase for the conjugation of glutathione with L-phenylalanine mustard. Cancer Res. 1991;51(9):2410-5.

241. Lewis AD, Hickson ID, Robson CN, Harris AL, Hayes JD, Griffiths SA, et al. Amplification and increased expression of alpha class glutathione S-transferase-encoding genes associated with resistance to nitrogen mustards. Proc Natl Acad Sci U S A. 1988;85(22):8511-5.

242. Puchalski RB, Fahl WE. Expression of recombinant glutathione S-transferase pi, Ya, or Yb1 confers resistance to alkylating agents. Proc Natl Acad Sci U S A. 1990;87(7):2443-7.

243. Ribrag V, Koscielny S, Carpiuc I, Cebotaru C, Vande Walle H, Talbot M, et al. Prognostic value of GST-pi expression in diffuse large B-cell lymphomas. Leukemia. 2003;17(5):972-7.

244. Katahira T, Takayama T, Miyanishi K, Hayashi T, Ikeda T, Takahashi Y, et al. Plasma glutathione S-Transferase P1-1 as a prognostic factor in patients with advanced non-Hodgkin's lymphoma (stages III and IV). Clinical cancer research : an official journal of the American Association for Cancer Research. 2004;10(23):7934-40.

245. O'Brien KA, Muscarella DE, Bloom SE. Differential induction of apoptosis and MAP kinase signaling by mitochondrial toxicants in drug-sensitive compared to drug-resistant B-lineage lymphoid cell lines. Toxicol Appl Pharmacol. 2001;174(3):245-56.

246. Greenland C, Touriol C, Chevillard G, Morris SW, Bai R, Duyster J, et al. Expression of the oncogenic NPM-ALK chimeric protein in human lymphoid T-cells inhibits drug-induced, but not Fas-induced apoptosis. Oncogene. 2001;20(50):7386-97.

247. Liu Q, Schwaller J, Kutok J, Cain D, Aster JC, Williams IR, et al. Signal transduction and transforming properties of the TEL-TRKC fusions associated with t(12;15)(p13;q25) in congenital fibrosarcoma and acute myelogenous leukemia. The EMBO journal. 2000;19(8):1827-38.

248. Masumoto N, Nakano S, Fujishima H, Kohno K, Niho Y. v-src induces cisplatin resistance by increasing the repair of cisplatin-DNA interstrand cross-links in human gallbladder adenocarcinoma cells. Int J Cancer. 1999;80(5):731-7.

249. Pietras RJ, Fendly BM, Chazin VR, Pegram MD, Howell SB, Slamon DJ. Antibody to HER-2/neu receptor blocks DNA repair after cisplatin in human breast and ovarian cancer cells. Oncogene. 1994;9(7):1829-38.

250. Raitano AB, Whang YE, Sawyers CL. Signal transduction by wild-type and leukemogenic Abl proteins. Biochimica et biophysica acta. 1997;1333(3):F201-16.

251. Sattler M, Salgia R. Activation of hematopoietic growth factor signal transduction pathways by the human oncogene BCR/ABL. Cytokine Growth Factor Rev. 1997;8(1):63-79.

252. Zou X, Calame K. Signaling pathways activated by oncogenic forms of Abl tyrosine kinase. The Journal of biological chemistry. 1999;274(26):18141-4.

253. Thomas SM, Brugge JS. Cellular functions regulated by Src family kinases. Annu Rev Cell Dev Biol. 1997;13:513-609.

254. Dal Porto JM, Gauld SB, Merrell KT, Mills D, Pugh-Bernard AE, Cambier J. B cell antigen receptor signaling 101. Mol Immunol. 2004;41(6-7):599-613.

255. Monroe JG. ITAM-mediated tonic signalling through pre-BCR and BCR complexes. Nat Rev Immunol. 2006;6(4):283-94.

256. Hollmann CA, Tzankov A, Martinez-Marignac VL, Baker K, Grygorczyk C, Grygorczyk R, et al. Therapeutic implications of Src independent calcium mobilization in diffuse large B-cell lymphoma. Leuk Res. 2010;34(5):585-93.

257. Brave M, Goodman V, Kaminskas E, Farrell A, Timmer W, Pope S, et al. Sprycel for chronic myeloid leukemia and Philadelphia chromosome-positive acute lymphoblastic leukemia resistant to or intolerant of imatinib mesylate. Clinical cancer research : an official journal of the American Association for Cancer Research. 2008;14(2):352-9.

258. Morris SW, Naeve C, Mathew P, James PL, Kirstein MN, Cui X, et al. ALK, the chromosome 2 gene locus altered by the t(2;5) in non-Hodgkin's lymphoma, encodes a novel neural receptor tyrosine kinase that is highly related to leukocyte tyrosine kinase (LTK). Oncogene. 1997;14(18):2175-88.

259. Greenstein S, Ghias K, Krett NL, Rosen ST. Mechanisms of glucocorticoid-mediated apoptosis in hematological malignancies. Clinical cancer research : an official journal of the American Association for Cancer Research. 2002;8(6):1681-94.

260. Pui CH, Relling MV, Downing JR. Acute lymphoblastic leukemia. N Engl J Med. 2004;350(15):1535-48.

261. Gaynon PS, Carrel AL. Glucocorticosteroid therapy in childhood acute lymphoblastic leukemia. Adv Exp Med Biol. 1999;457:593-605.

262. Kaspers GJ, Pieters R, Klumper E, De Waal FC, Veerman AJ. Glucocorticoid resistance in childhood leukemia. Leuk Lymphoma. 1994;13(3-4):187-201.

263. Schrappe M, Reiter A, Zimmermann M, Harbott J, Ludwig WD, Henze G, et al. Long-term results of four consecutive trials in childhood ALL performed by the ALL-BFM study group from 1981 to 1995. Berlin-Frankfurt-Munster. Leukemia. 2000;14(12):2205-22.

264. Tissing WJ, Meijerink JP, den Boer ML, Brinkhof B, van Rossum EF, van Wering ER, et al. Genetic variations in the glucocorticoid receptor gene are not related to glucocorticoid

resistance in childhood acute lymphoblastic leukemia. Clinical cancer research : an official journal of the American Association for Cancer Research. 2005;11(16):6050-6.

265. Morris SW, Kirstein MN, Valentine MB, Dittmer K, Shapiro DN, Look AT, et al. Fusion of a kinase gene, ALK, to a nucleolar protein gene, NPM, in non-Hodgkin's lymphoma. Science. 1995;267(5196):316-7.

266. Cessna MH, Zhou H, Sanger WG, Perkins SL, Tripp S, Pickering D, et al. Expression of ALK1 and p80 in inflammatory myofibroblastic tumor and its mesenchymal mimics: a study of 135 cases. Mod Pathol. 2002;15(9):931-8.

267. Gascoyne RD, Lamant L, Martin-Subero JI, Lestou VS, Harris NL, Muller-Hermelink HK, et al. ALK-positive diffuse large B-cell lymphoma is associated with Clathrin-ALK rearrangements: report of 6 cases. Blood. 2003;102(7):2568-73.

268. Jazii FR, Najafi Z, Malekzadeh R, Conrads TP, Ziaee AA, Abnet C, et al. Identification of squamous cell carcinoma associated proteins by proteomics and loss of beta tropomyosin expression in esophageal cancer. World J Gastroenterol. 2006;12(44):7104-12.

269. Soda M, Choi YL, Enomoto M, Takada S, Yamashita Y, Ishikawa S, et al. Identification of the transforming EML4-ALK fusion gene in non-small-cell lung cancer. Nature. 2007;448(7153):561-6.

270. Li R, Morris SW. Development of anaplastic lymphoma kinase (ALK) small-molecule inhibitors for cancer therapy. Med Res Rev. 2008;28(3):372-412.

271. Gu L, Gao J, Li Q, Zhu YP, Jia CS, Fu RY, et al. Rapamycin reverses NPM-ALK-induced glucocorticoid resistance in lymphoid tumor cells by inhibiting mTOR signaling pathway, enhancing G1 cell cycle arrest and apoptosis. Leukemia. 2008;22(11):2091-6.

272. Marzec M, Kasprzycka M, Liu X, Raghunath PN, Wlodarski P, Wasik MA. Oncogenic tyrosine kinase NPM/ALK induces activation of the MEK/ERK signaling pathway independently of c-Raf. Oncogene. 2007;26(6):813-21.

273. Vega F, Medeiros LJ, Leventaki V, Atwell C, Cho-Vega JH, Tian L, et al. Activation of mammalian target of rapamycin signaling pathway contributes to tumor cell survival in anaplastic lymphoma kinase-positive anaplastic large cell lymphoma. Cancer Res. 2006;66(13):6589-97.

274. Fan S, el-Deiry WS, Bae I, Freeman J, Jondle D, Bhatia K, et al. p53 gene mutations are associated with decreased sensitivity of human lymphoma cells to DNA damaging agents. Cancer Res. 1994;54(22):5824-30.

275. Foroutan B, Ali Ruf A, Jerwood D, Anderson D. In vitro studies of DNA damage and its repair in cells from NHL patients with different p53 mutant protein status, resistant (p53(+)) and sensitive (p53(-)) to cancer chemotherapy. J Pharmacol Toxicol Methods. 2007;55(1):58-64.

276. Kerbauy FR, Colleoni GW, Saad ST, Regis Silva MR, Correa Alves A, Aguiar KC, et al. Detection and possible prognostic relevance of p53 gene mutations in diffuse large B-cell lymphoma. An analysis of 51 cases and review of the literature. Leuk Lymphoma. 2004;45(10):2071-8.

277. Drexler HG, Fombonne S, Matsuo Y, Hu ZB, Hamaguchi H, Uphoff CC. p53 alterations in human leukemia-lymphoma cell lines: in vitroartifact or prerequisite for cell immortalization? Leukemia. 2000;14(1):198-206.

278. Ichikawa A, Kinoshita T, Watanabe T, Kato H, Nagai H, Tsushita K, et al. Mutations of the p53 gene as a prognostic factor in aggressive B-cell lymphoma. N Engl J Med. 1997;337(8):529-34.

279. Moller MB, Gerdes AM, Skjodt K, Mortensen LS, Pedersen NT. Disrupted p53 function as predictor of treatment failure and poor prognosis in B- and T-cell non-Hodgkin's lymphoma. Clinical cancer research : an official journal of the American Association for Cancer Research. 1999;5(5):1085-91.

280. Koduru PR, Raju K, Vadmal V, Menezes G, Shah S, Susin M, et al. Correlation between mutation in P53, p53 expression, cytogenetics, histologic type, and survival in patients with B-cell non-Hodgkin's lymphoma. Blood. 1997;90(10):4078-91.

281. Happo L, Cragg MS, Phipson B, Haga JM, Jansen ES, Herold MJ, et al. Maximal killing of lymphoma cells by DNA damage-inducing therapy requires not only the p53 targets Puma and Noxa, but also Bim. Blood. 2010;116(24):5256-67.

282. Adams J. The development of proteasome inhibitors as anticancer drugs. Cancer Cell. 2004;5(5):417-21.

283. Richardson PG, Mitsiades C, Hideshima T, Anderson KC. Proteasome inhibition in the treatment of cancer. Cell Cycle. 2005;4(2):290-6.

284. Orlowski RZ, Kuhn DJ. Proteasome inhibitors in cancer therapy: lessons from the first decade. Clinical cancer research : an official journal of the American Association for Cancer Research. 2008;14(6):1649-57.

285. Stapnes C, Doskeland AP, Hatfield K, Ersvaer E, Ryningen A, Lorens JB, et al. The proteasome inhibitors bortezomib and PR-171 have antiproliferative and proapoptotic effects on primary human acute myeloid leukaemia cells. Br J Haematol. 2007;136(6):814-28.

286. Strauss SJ, Higginbottom K, Juliger S, Maharaj L, Allen P, Schenkein D, et al. The proteasome inhibitor bortezomib acts independently of p53 and induces cell death via apoptosis and mitotic catastrophe in B-cell lymphoma cell lines. Cancer Res. 2007;67(6):2783-90.

287. Meister S, Schubert U, Neubert K, Herrmann K, Burger R, Gramatzki M, et al. Extensive immunoglobulin production sensitizes myeloma cells for proteasome inhibition. Cancer Res. 2007;67(4):1783-92.

288. Obeng EA, Carlson LM, Gutman DM, Harrington WJ, Jr., Lee KP, Boise LH. Proteasome inhibitors induce a terminal unfolded protein response in multiple myeloma cells. Blood. 2006;107(12):4907-16.

289. McConkey DJ, Zhu K. Mechanisms of proteasome inhibitor action and resistance in cancer. Drug Resist Updat. 2008;11(4-5):164-79.

290. Fisher RI, Bernstein SH, Kahl BS, Djulbegovic B, Robertson MJ, de Vos S, et al. Multicenter phase II study of bortezomib in patients with relapsed or refractory mantle cell lymphoma. Journal of clinical oncology : official journal of the American Society of Clinical Oncology. 2006;24(30):4867-74.

291. Goy A, Younes A, McLaughlin P, Pro B, Romaguera JE, Hagemeister F, et al. Phase II study of proteasome inhibitor bortezomib in relapsed or refractory B-cell non-Hodgkin's lymphoma. Journal of clinical oncology : official journal of the American Society of Clinical Oncology. 2005;23(4):667-75.

292. O'Connor OA, Wright J, Moskowitz C, Muzzy J, MacGregor-Cortelli B, Stubblefield M, et al. Phase II clinical experience with the novel proteasome inhibitor bortezomib in patients with indolent non-Hodgkin's lymphoma and mantle cell lymphoma. Journal of clinical oncology : official journal of the American Society of Clinical Oncology. 2005;23(4):676-84.

293. Ruckrich T, Kraus M, Gogel J, Beck A, Ovaa H, Verdoes M, et al. Characterization of the ubiquitin-proteasome system in bortezomib-adapted cells. Leukemia. 2009;23(6):1098-105.

294. Glas R, Bogyo M, McMaster JS, Gaczynska M, Ploegh HL. A proteolytic system that compensates for loss of proteasome function. Nature. 1998;392(6676):618-22.

295. Princiotta MF, Schubert U, Chen W, Bennink JR, Myung J, Crews CM, et al. Cells adapted to the proteasome inhibitor 4-hydroxy- 5-iodo-3-nitrophenylacetyl-Leu-Leu-leucinal-vinyl sulfone require enzymatically active proteasomes for continued survival. Proc Natl Acad Sci U S A. 2001;98(2):513-8.

296. Turk V, Turk B, Turk D. Lysosomal cysteine proteases: facts and opportunities. The EMBO journal. 2001;20(17):4629-33.

297. Li J, Lee AS. Stress induction of GRP78/BiP and its role in cancer. Current molecular medicine. 2006;6(1):45-54.

298. Mozos A, Roué G, López-Guillermo A, Jares P, Campo E, Colomer D, et al. The expression of the endoplasmic reticulum stress sensor BiP/GRP78 predicts response to chemotherapy and determines the efficacy of proteasome inhibitors in diffuse large b-cell lymphoma. The American journal of pathology. 2011;179(5):2601-10.

299. Esteller M. Epigenetics in cancer. N Engl J Med. 2008;358(11):1148-59.

300. Ropero S, Esteller M. The role of histone deacetylases (HDACs) in human cancer. Mol Oncol. 2007;1(1):19-25.

301. Yang XJ, Seto E. The Rpd3/Hda1 family of lysine deacetylases: from bacteria and yeast to mice and men. Nat Rev Mol Cell Biol. 2008;9(3):206-18.

302. Kikuchi J, Wada T, Shimizu R, Izumi T, Akutsu M, Mitsunaga K, et al. Histone deacetylases are critical targets of bortezomib-induced cytotoxicity in multiple myeloma. Blood. 2010;116(3):406-17.

303. Maiso P, Carvajal-Vergara X, Ocio EM, Lopez-Perez R, Mateo G, Gutierrez N, et al. The histone deacetylase inhibitor LBH589 is a potent antimyeloma agent that overcomes drug resistance. Cancer Res. 2006;66(11):5781-9.

304. Marks PA, Richon VM, Rifkind RA. Histone deacetylase inhibitors: inducers of differentiation or apoptosis of transformed cells. J Natl Cancer Inst. 2000;92(15):1210-6.

305. Sakai E, Bottaro A, Alt FW. The Ig heavy chain intronic enhancer core region is necessary and sufficient to promote efficient class switch recombination. Int Immunol. 1999;11(10):1709-13.

306. Marks P, Rifkind RA, Richon VM, Breslow R, Miller T, Kelly WK. Histone deacetylases and cancer: causes and therapies. Nature reviews Cancer. 2001;1(3):194-202.

307. Schreiber SL, Bernstein BE. Signaling network model of chromatin. Cell. 2002;111(6):771-8.

308. Kim MS, Kwon HJ, Lee YM, Baek JH, Jang JE, Lee SW, et al. Histone deacetylases induce angiogenesis by negative regulation of tumor suppressor genes. Nat Med. 2001;7(4):437-43.

309. Mitsiades CS, Mitsiades NS, McMullan CJ, Poulaki V, Shringarpure R, Hideshima T, et al. Transcriptional signature of histone deacetylase inhibition in multiple myeloma: biological and clinical implications. Proc Natl Acad Sci U S A. 2004;101(2):540-5.

310. Duan H, Heckman CA, Boxer LM. Histone deacetylase inhibitors down-regulate bcl-2 expression and induce apoptosis in t(14;18) lymphomas. Mol Cell Biol. 2005;25(5):1608-19.

311. Bhalla S, Balasubramanian S, David K, Sirisawad M, Buggy J, Mauro L, et al. PCI-24781 induces caspase and reactive oxygen species-dependent apoptosis through NF-kappaB mechanisms and is synergistic with bortezomib in lymphoma cells. Clinical cancer research : an official journal of the American Association for Cancer Research. 2009;15(10):3354-65.

312. Dasmahapatra G, Lembersky D, Kramer L, Fisher RI, Friedberg J, Dent P, et al. The pan-HDAC inhibitor vorinostat potentiates the activity of the proteasome inhibitor carfilzomib in human DLBCL cells in vitro and in vivo. Blood. 2010;115(22):4478-87.

313. Shimizu R, Kikuchi J, Wada T, Ozawa K, Kano Y, Furukawa Y. HDAC inhibitors augment cytotoxic activity of rituximab by upregulating CD20 expression on lymphoma cells. Leukemia. 2010;24(10):1760-8.

314. Aaltonen LA, Peltomaki P, Leach FS, Sistonen P, Pylkkanen L, Mecklin JP, et al. Clues to the pathogenesis of familial colorectal cancer. Science. 1993;260(5109):812-6.

315. Fishel R, Lescoe MK, Rao MR, Copeland NG, Jenkins NA, Garber J, et al. The human mutator gene homolog MSH2 and its association with hereditary nonpolyposis colon cancer. Cell. 1993;75(5):1027-38.

316. Ionov Y, Peinado MA, Malkhosyan S, Shibata D, Perucho M. Ubiquitous somatic mutations in simple repeated sequences reveal a new mechanism for colonic carcinogenesis. Nature. 1993;363(6429):558-61.

317. Peltomaki P, Lothe RA, Aaltonen LA, Pylkkanen L, Nystrom-Lahti M, Seruca R, et al. Microsatellite instability is associated with tumors that characterize the hereditary non-polyposis colorectal carcinoma syndrome. Cancer Res. 1993;53(24):5853-5.

318. Thibodeau SN, Bren G, Schaid D. Microsatellite instability in cancer of the proximal colon. Science. 1993;260(5109):816-9.

319. Miyashita K, Fujii K, Yamada Y, Hattori H, Taguchi K, Yamanaka T, et al. Frequent microsatellite instability in non-Hodgkin lymphomas irresponsive to chemotherapy. Leuk Res. 2008;32(8):1183-95.

320. Eckstein N, Servan K, Hildebrandt B, Politz A, von Jonquieres G, Wolf-Kummeth S, et al. Hyperactivation of the insulin-like growth factor receptor I signaling pathway is an essential event for cisplatin resistance of ovarian cancer cells. Cancer Res. 2009;69(7):2996-3003.

321. Williams RT, den Besten W, Sherr CJ. Cytokine-dependent imatinib resistance in mouse BCR-ABL+, Arf-null lymphoblastic leukemia. Genes Dev. 2007;21(18):2283-7.

322. Bajenoff M, Egen JG, Koo LY, Laugier JP, Brau F, Glaichenhaus N, et al. Stromal cell networks regulate lymphocyte entry, migration, and territoriality in lymph nodes. Immunity. 2006;25(6):989-1001.

323. Okada T, Ngo VN, Ekland EH, Forster R, Lipp M, Littman DR, et al. Chemokine requirements for B cell entry to lymph nodes and Peyer's patches. J Exp Med. 2002;196(1):65-75.

324. Meads MB, Hazlehurst LA, Dalton WS. The bone marrow microenvironment as a tumor sanctuary and contributor to drug resistance. Clinical cancer research : an official journal of the American Association for Cancer Research. 2008;14(9):2519-26.

325. Linderoth J, Eden P, Ehinger M, Valcich J, Jerkeman M, Bendahl PO, et al. Genes associated with the tumour microenvironment are differentially expressed in cured versus primary chemotherapy-refractory diffuse large B-cell lymphoma. Br J Haematol. 2008;141(4):423-32.

326. Walker A, Taylor ST, Hickman JA, Dive C. Germinal center-derived signals act with Bcl-2 to decrease apoptosis and increase clonogenicity of drug-treated human B lymphoma cells. Cancer Res. 1997;57(10):1939-45.

327. Taylor ST, Hickman JA, Dive C. Survival signals within the tumour microenvironment suppress drug-induced apoptosis: lessons learned from B lymphomas. Endocr Relat Cancer. 1999;6(1):21-3.

328. Shu HB, Hu WH, Johnson H. TALL-1 is a novel member of the TNF family that is down-regulated by mitogens. J Leukoc Biol. 1999;65(5):680-3.

329. Mercurio F, DiDonato JA, Rosette C, Karin M. p105 and p98 precursor proteins play an active role in NF-kappa B-mediated signal transduction. Genes Dev. 1993;7(4):705-18.

330. Naumann M, Wulczyn FG, Scheidereit C. The NF-kappa B precursor p105 and the proto-oncogene product Bcl-3 are I kappa B molecules and control nuclear translocation of NF-kappa B. The EMBO journal. 1993;12(1):213-22.

331. Lwin T, Crespo LA, Wu A, Dessureault S, Shu HB, Moscinski LC, et al. Lymphoma cell adhesion-induced expression of B cell-activating factor of the TNF family in bone marrow stromal cells protects non-Hodgkin's B lymphoma cells from apoptosis. Leukemia. 2009;23(1):170-7.

332. Briones J, Timmerman JM, Hilbert DM, Levy R. BLyS and BLyS receptor expression in non-Hodgkin's lymphoma. Exp Hematol. 2002;30(2):135-41.

333. A predictive model for aggressive non-Hodgkin's lymphoma. The International Non-Hodgkin's Lymphoma Prognostic Factors Project. N Engl J Med. 1993;329(14):987-94.

334. Dive C, Hickman JA. Drug-target interactions: only the first step in the commitment to a programmed cell death? Br J Cancer. 1991;64(1):192-6.

335. Raff MC. Social controls on cell survival and cell death. Nature. 1992;356(6368):397-400.

336. Reed JC. Double identity for proteins of the Bcl-2 family. Nature. 1997;387(6635):773-6.

337. Taylor ST, Hickman JA, Dive C. Epigenetic determinants of resistance to etoposide regulation of Bcl-X(L) and Bax by tumor microenvironmental factors. J Natl Cancer Inst. 2000;92(1):18-23.

338. Trikha M, Corringham R, Klein B, Rossi JF. Targeted anti-interleukin-6 monoclonal antibody therapy for cancer: a review of the rationale and clinical evidence. Clinical cancer research : an official journal of the American Association for Cancer Research. 2003;9(13):4653-65.

339. Gilbert LA, Hemann MT. DNA damage-mediated induction of a chemoresistant niche. Cell. 2010;143(3):355-66.

340. Trentin L, Cabrelle A, Facco M, Carollo D, Miorin M, Tosoni A, et al. Homeostatic chemokines drive migration of malignant B cells in patients with non-Hodgkin lymphomas. Blood. 2004;104(2):502-8.

341. Burger JA, Burger M, Kipps TJ. Chronic lymphocytic leukemia B cells express functional CXCR4 chemokine receptors that mediate spontaneous migration beneath bone marrow stromal cells. Blood. 1999;94(11):3658-67.

342. Burkle A, Niedermeier M, Schmitt-Graff A, Wierda WG, Keating MJ, Burger JA. Overexpression of the CXCR5 chemokine receptor, and its ligand, CXCL13 in B-cell chronic lymphocytic leukemia. Blood. 2007;110(9):3316-25.

343. Sipkins DA, Wei X, Wu JW, Runnels JM, Cote D, Means TK, et al. In vivo imaging of specialized bone marrow endothelial microdomains for tumour engraftment. Nature. 2005;435(7044):969-73.

344. Burger JA, Kipps TJ. Chemokine receptors and stromal cells in the homing and homeostasis of chronic lymphocytic leukemia B cells. Leuk Lymphoma. 2002;43(3):461-6.

345. Lenz G, Wright G, Dave SS, Xiao W, Powell J, Zhao H, et al. Stromal gene signatures in large-B-cell lymphomas. N Engl J Med. 2008;359(22):2313-23.

346. Allen CD, Ansel KM, Low C, Lesley R, Tamamura H, Fujii N, et al. Germinal center dark and light zone organization is mediated by CXCR4 and CXCR5. Nat Immunol. 2004;5(9):943-52.

347. Reif K, Ekland EH, Ohl L, Nakano H, Lipp M, Forster R, et al. Balanced responsiveness to chemoattractants from adjacent zones determines B-cell position. Nature. 2002;416(6876):94-9.

348. Springer TA. Traffic signals for lymphocyte recirculation and leukocyte emigration: the multistep paradigm. Cell. 1994;76(2):301-14.

349. Byers RJ, Sakhinia E, Joseph P, Glennie C, Hoyland JA, Menasce LP, et al. Clinical quantitation of immune signature in follicular lymphoma by RT-PCR-based gene expression profiling. Blood. 2008;111(9):4764-70.

350. Dave SS, Wright G, Tan B, Rosenwald A, Gascoyne RD, Chan WC, et al. Prediction of survival in follicular lymphoma based on molecular features of tumor-infiltrating immune cells. N Engl J Med. 2004;351(21):2159-69.

351. Farinha P, Masoudi H, Skinnider BF, Shumansky K, Spinelli JJ, Gill K, et al. Analysis of multiple biomarkers shows that lymphoma-associated macrophage (LAM) content is an independent predictor of survival in follicular lymphoma (FL). Blood. 2005;106(6):2169-74.

352. Wang Y, Liu Y, Wu C, Zhang H, Zheng X, Zheng Z, et al. Epm2a suppresses tumor growth in an immunocompromised host by inhibiting Wnt signaling. Cancer Cell. 2006;10(3):179-90.

353. Cuvillier O, Pirianov G, Kleuser B, Vanek PG, Coso OA, Gutkind S, et al. Suppression of ceramide-mediated programmed cell death by sphingosine-1-phosphate. Nature. 1996;381(6585):800-3.

354. Maceyka M, Payne SG, Milstien S, Spiegel S. Sphingosine kinase, sphingosine-1-phosphate, and apoptosis. Biochimica et biophysica acta. 2002;1585(2-3):193-201.

355. Macchia M, Barontini S, Bertini S, Di Bussolo V, Fogli S, Giovannetti E, et al. Design, synthesis, and characterization of the antitumor activity of novel ceramide analogues. J Med Chem. 2001;44(23):3994-4000.

356. Bayerl MG, Bruggeman RD, Conroy EJ, Hengst JA, King TS, Jimenez M, et al. Sphingosine kinase 1 protein and mRNA are overexpressed in non-Hodgkin lymphomas and are attractive targets for novel pharmacological interventions. Leuk Lymphoma. 2008;49(5):948-54.

357. Ageberg M, Rydstrom K, Linden O, Linderoth J, Jerkeman M, Drott K. Inhibition of geranylgeranylation mediates sensitivity to CHOP-induced cell death of DLBCL cell lines. Exp Cell Res. 2011;317(8):1179-91.

358. Novick P, Zerial M. The diversity of Rab proteins in vesicle transport. Curr Opin Cell Biol. 1997;9(4):496-504.

359. Wright LP, Philips MR. Thematic review series: lipid posttranslational modifications. CAAX modification and membrane targeting of Ras. J Lipid Res. 2006;47(5):883-91.

360. Zerial M, McBride H. Rab proteins as membrane organizers. Nat Rev Mol Cell Biol. 2001;2(2):107-17.

361. Chitambar CR, Zahir SA, Ritch PS, Anderson T. Evaluation of continuous-infusion gallium nitrate and hydroxyurea in combination for the treatment of refractory non-Hodgkin's lymphoma. Am J Clin Oncol. 1997;20(2):173-8.

362. Keller J, Bartolucci A, Carpenter JT, Jr., Feagler J. Phase II evaluation of bolus gallium nitrate in lymphoproliferative disorders: a Southeastern Cancer Study Group trial. Cancer Treat Rep. 1986;70(10):1221-3.

363. Straus DJ. Gallium nitrate in the treatment of lymphoma. Semin Oncol. 2003;30(2 Suppl 5):25-33.

364. Warrell RP, Jr., Coonley CJ, Straus DJ, Young CW. Treatment of patients with advanced malignant lymphoma using gallium nitrate administered as a seven-day continuous infusion. Cancer. 1983;51(11):1982-7.

365. Weick JK, Stephens RL, Baker LH, Jones SE. Gallium nitrate in malignant lymphoma: a Southwest Oncology Group study. Cancer Treat Rep. 1983;67(9):823-5.

366. Chitambar CR, Zivkovic Z. Uptake of gallium-67 by human leukemic cells: demonstration of transferrin receptor-dependent and transferrin-independent mechanisms. Cancer Res. 1987;47(15):3929-34.

367. Esserman L, Takahashi S, Rojas V, Warnke R, Levy R. An epitope of the transferrin receptor is exposed on the cell surface of high-grade but not low-grade human lymphomas. Blood. 1989;74(8):2718-29.

368. Habeshaw JA, Lister TA, Stansfeld AG, Greaves MF. Correlation of transferrin receptor expression with histological class and outcome in non-Hodgkin lymphoma. Lancet. 1983;1(8323):498-501.

369. Harris WR, Pecoraro VL. Thermodynamic binding constants for gallium transferrin. Biochemistry. 1983;22(2):292-9.

370. Kiratli PO, Canpinar H, Ruacan S, Kansu E. Correlation of flow cytometric parameters and transferrin receptors with gallium-67 scintigraphic images in lymphoma patients. Nucl Med Commun. 2000;21(10):925-31.

371. Larson SM, Rasey JS, Allen DR, Nelson NJ, Grunbaum Z, Harp GD, et al. Common pathway for tumor cell uptake of gallium-67 and iron-59 via a transferrin receptor. J Natl Cancer Inst. 1980;64(1):41-53.

372. Yang M, Kroft SH, Chitambar CR. Gene expression analysis of gallium-resistant and gallium-sensitive lymphoma cells reveals a role for metal-responsive transcription factor-1, metallothionein-2A, and zinc transporter-1 in modulating the antineoplastic activity of gallium nitrate. Mol Cancer Ther. 2007;6(2):633-43.

373. Shapiro-Shelef M, Calame K. Regulation of plasma-cell development. Nat Rev Immunol. 2005;5(3):230-42.

374. Shapiro-Shelef M, Lin KI, Savitsky D, Liao J, Calame K. Blimp-1 is required for maintenance of long-lived plasma cells in the bone marrow. J Exp Med. 2005;202(11):1471-6.

375. Gyory I, Fejer G, Ghosh N, Seto E, Wright KL. Identification of a functionally impaired positive regulatory domain I binding factor 1 transcription repressor in myeloma cell lines. J Immunol. 2003;170(6):3125-33.

376. Johnson K, Shapiro-Shelef M, Tunyaplin C, Calame K. Regulatory events in early and late B-cell differentiation. Mol Immunol. 2005;42(7):749-61.

377. Garcia JF, Roncador G, Sanz AI, Maestre L, Lucas E, Montes-Moreno S, et al. PRDM1/BLIMP-1 expression in multiple B and T-cell lymphoma. Haematologica. 2006;91(4):467-74.

378. Friedman HS, Colvin OM, Kaufmann SH, Ludeman SM, Bullock N, Bigner DD, et al. Cyclophosphamide resistance in medulloblastoma. Cancer Res. 1992;52(19):5373-8.

379. Jones RJ, Barber JP, Vala MS, Collector MI, Kaufmann SH, Ludeman SM, et al. Assessment of aldehyde dehydrogenase in viable cells. Blood. 1995;85(10):2742-6.

380. Brennan SK, Meade B, Wang Q, Merchant AA, Kowalski J, Matsui W. Mantle cell lymphoma activation enhances bortezomib sensitivity. Blood. 2010;116(20):4185-91.

381. Corti S, Locatelli F, Papadimitriou D, Donadoni C, Salani S, Del Bo R, et al. Identification of a primitive brain-derived neural stem cell population based on aldehyde dehydrogenase activity. Stem Cells. 2006;24(4):975-85.

382. Hess DA, Meyerrose TE, Wirthlin L, Craft TP, Herrbrich PE, Creer MH, et al. Functional characterization of highly purified human hematopoietic repopulating cells isolated according to aldehyde dehydrogenase activity. Blood. 2004;104(6):1648-55.

383. Jones RJ, Gocke CD, Kasamon YL, Miller CB, Perkins B, Barber JP, et al. Circulating clonotypic B cells in classic Hodgkin lymphoma. Blood. 2009;113(23):5920-6.

384. Matsui W, Huff CA, Wang Q, Malehorn MT, Barber J, Tanhehco Y, et al. Characterization of clonogenic multiple myeloma cells. Blood. 2004;103(6):2332-6.

385. Hilton J. Role of aldehyde dehydrogenase in cyclophosphamide-resistant L1210 leukemia. Cancer Res. 1984;44(11):5156-60.

386. Kastan MB, Schlaffer E, Russo JE, Colvin OM, Civin CI, Hilton J. Direct demonstration of elevated aldehyde dehydrogenase in human hematopoietic progenitor cells. Blood. 1990;75(10):1947-50.

387. Kohn FR, Sladek NE. Aldehyde dehydrogenase activity as the basis for the relative insensitivity of murine pluripotent hematopoietic stem cells to oxazaphosphorines. Biochem Pharmacol. 1985;34(19):3465-71.

388. Magni M, Shammah S, Schiro R, Mellado W, Dalla-Favera R, Gianni AM. Induction of cyclophosphamide-resistance by aldehyde-dehydrogenase gene transfer. Blood. 1996;87(3):1097-103.

389. Russo JE, Hilton J. Characterization of cytosolic aldehyde dehydrogenase from cyclophosphamide resistant L1210 cells. Cancer Res. 1988;48(11):2963-8.

390. Compagno M, Lim WK, Grunn A, Nandula SV, Brahmachary M, Shen Q, et al. Mutations of multiple genes cause deregulation of NF-kappaB in diffuse large B-cell lymphoma. Nature. 2009;459(7247):717-21.

391. Dunleavy K, Pittaluga S, Czuczman MS, Dave SS, Wright G, Grant N, et al. Differential efficacy of bortezomib plus chemotherapy within molecular subtypes of diffuse large B-cell lymphoma. Blood. 2009;113(24):6069-76.

392. Catley L, Weisberg E, Kiziltepe T, Tai YT, Hideshima T, Neri P, et al. Aggresome induction by proteasome inhibitor bortezomib and alpha-tubulin hyperacetylation by tubulin deacetylase (TDAC) inhibitor LBH589 are synergistic in myeloma cells. Blood. 2006;108(10):3441-9.

393. Dai Y, Chen S, Kramer LB, Funk VL, Dent P, Grant S. Interactions between bortezomib and romidepsin and belinostat in chronic lymphocytic leukemia cells. Clinical cancer research : an official journal of the American Association for Cancer Research. 2008;14(2):549-58.

394. Lewis TS, McCormick RS, Emmerton K, Lau JT, Yu SF, McEarchern JA, et al. Distinct apoptotic signaling characteristics of the anti-CD40 monoclonal antibody dacetuzumab and rituximab produce enhanced antitumor activity in non-Hodgkin lymphoma. Clinical cancer research : an official journal of the American Association for Cancer Research. 2011;17(14):4672-81.

395. Hutter G, Rieken M, Pastore A, Weigert O, Zimmermann Y, Weinkauf M, et al. The proteasome inhibitor bortezomib targets cell cycle and apoptosis and acts synergistically in a sequence-dependent way with chemotherapeutic agents in mantle cell lymphoma. Annals of hematology. 2012;91(6):847-56.

396. Lancet JE, Duong VH, Winton EF, Stuart RK, Burton M, Zhang S, et al. A phase I clinical-pharmacodynamic study of the farnesyltransferase inhibitor tipifarnib in combination with the proteasome inhibitor bortezomib in advanced acute leukemias. Clinical Cancer Research. 2011;17(5):1140-6.

397. Zhao XF, Gartenhaus RB. Phospho-p70S6K and cdc2/cdk1 as therapeutic targets for diffuse large B-cell lymphoma. Expert opinion on therapeutic targets. 2009;13(9):1085-93.

398. Deng J, Carlson N, Takeyama K, Dal Cin P, Shipp M, Letai A. BH3 profiling identifies three distinct classes of apoptotic blocks to predict response to ABT-737 and conventional chemotherapeutic agents. Cancer cell. 2007;12(2):171-85.

399. Pall ML, Levine S. Nrf2, a master regulator of detoxification and also antioxidant, anti-inflammatory and other cytoprotective mechanisms, is raised by health promoting factors. Sheng li xue bao : [Acta physiologica Sinica]. 2015;67(1):1-18.

400. Harder B, Jiang T, Wu T, Tao S, Rojo de la Vega M, Tian W, et al. Molecular mechanisms of Nrf2 regulation and how these influence chemical modulation for disease intervention. Biochemical Society transactions. 2015;43(4):680-6.

401. Gorrini C, Harris IS, Mak TW. Modulation of oxidative stress as an anticancer strategy. Nature reviews Drug discovery. 2013;12(12):931-47.

402. Wang X-J, Sun Z, Villeneuve NF, Zhang S, Zhao F, Li Y, et al. Nrf2 enhances resistance of cancer cells to chemotherapeutic drugs, the dark side of Nrf2. Carcinogenesis. 2008;29(6):1235-43.

403. Lau A, Villeneuve NF, Sun Z, Wong PK, Zhang DD. Dual roles of Nrf2 in cancer. Pharmacological research. 2008;58(5):262-70.

404. de la Vega MR, Dodson M, Chapman E, Zhang DD. NRF2-targeted therapeutics: New targets and modes of NRF2 regulation. Current Opinion in Toxicology. 2016;1:62-70.

405. Ren D, Villeneuve NF, Jiang T, Wu T, Lau A, Toppin HA, et al. Brusatol enhances the efficacy of chemotherapy by inhibiting the Nrf2-mediated defense mechanism. Proceedings of the National Academy of Sciences of the United States of America. 2011;108(4):1433-8.

406. Bryan HK, Olayanju A, Goldring CE, Park BK. The Nrf2 cell defence pathway: Keap1-dependent and -independent mechanisms of regulation. Biochem Pharmacol. 2013;85(6):705-17.

407. Jang HJ, Hong EM, Kim M, Kim JH, Jang J, Park SW, et al. Simvastatin induces heme oxygenase-1 via NF-E2-related factor 2 (Nrf2) activation through ERK and PI3K/Akt pathway in colon cancer. Oncotarget. 2016;7(29):46219-29.

408. Wang L, Chen Y, Sternberg P, Cai J. Essential roles of the PI3 kinase/Akt pathway in regulating Nrf2-dependent antioxidant functions in the RPE. Investigative ophthalmology & visual science. 2008;49(4):1671-8.

409. Niture SK, Jaiswal AK. Nrf2 protein up-regulates antiapoptotic protein Bcl-2 and prevents cellular apoptosis. Journal of Biological Chemistry. 2012;287(13):9873-86.

410. Niture SK, Jaiswal AK. INrf2 (Keap1) targets Bcl-2 degradation and controls cellular apoptosis. Cell Death & Differentiation. 2011;18(3):439-51.

411. Ryu H, Son A-r, Seo B, Kim J, Jung S-Y, Song J-Y, et al. TGF-β and hypoxia/reoxygenation promote radioresistance of A549 lung cancer cells through activation of Nrf2 and EGFR. Oxidative medicine and cellular longevity. 2016;2016.

412. No JH, Kim Y-B, Song YS. Targeting nrf2 signaling to combat chemoresistance. Journal of cancer prevention. 2014;19(2):111-7.

413. Rotblat B, Melino G, Knight RA. NRF2 and p53: Januses in cancer? Oncotarget. 2012;3(11):1272-83.

414. Chen W, Sun Z, Wang XJ, Jiang T, Huang Z, Fang D, et al. Direct interaction between Nrf2 and p21(Cip1/WAF1) upregulates the Nrf2-mediated antioxidant response. Mol Cell. 2009;34(6):663-73.

415. Kruger A, Gruning NM, Wamelink MM, Kerick M, Kirpy A, Parkhomchuk D, et al. The pentose phosphate pathway is a metabolic redox sensor and regulates transcription during the antioxidant response. Antioxid Redox Signal. 2011;15(2):311-24.

416. Heiss EH, Schachner D, Zimmermann K, Dirsch VM. Glucose availability is a decisive factor for Nrf2-mediated gene expression. Redox biology. 2013;1:359-65.

417. Lushchak VI. Glutathione homeostasis and functions: potential targets for medical interventions. Journal of amino acids. 2012;2012:736837.

418. De Paepe P, De Wolf-Peeters C. Diffuse large B-cell lymphoma: a heterogeneous group of non-Hodgkin lymphomas comprising several distinct clinicopathological entities. Leukemia. 2007;21(1):37-43.

419. Zelenetz AD, Abramson JS, Advani RH, Andreadis CB, Byrd JC, Czuczman MS, et al. NCCN Clinical Practice Guidelines in Oncology: non-Hodgkin's lymphomas. Journal of the National Comprehensive Cancer Network : JNCCN. 2010;8(3):288-334.

420. Martelli M, Ferreri AJ, Agostinelli C, Di Rocco A, Pfreundschuh M, Pileri SA. Diffuse large B-cell lymphoma. Critical reviews in oncology/hematology. 2013;87(2):146-71.

421. Schneider C, Pasqualucci L, Dalla-Favera R. Molecular pathogenesis of diffuse large B-cell lymphoma. Seminars in diagnostic pathology. 2011;28(2):167-77.

422. Koff JL, Chihara D, Phan A, Nastoupil LJ, Williams JN, Flowers CR. To Each Its Own: Linking the Biology and Epidemiology of NHL Subtypes. Current hematologic malignancy reports. 2015;10(3):244-55.

423. Blombery PA, Wall M, Seymour JF. The molecular pathogenesis of B-cell non-Hodgkin lymphoma. European journal of haematology. 2015;95(4):280-93.

424. Habermann TM, Weller EA, Morrison VA, Gascoyne RD, Cassileth PA, Cohn JB, et al. Rituximab-CHOP versus CHOP alone or with maintenance rituximab in older patients with diffuse large B-cell lymphoma. Journal of clinical oncology : official journal of the American Society of Clinical Oncology. 2006;24(19):3121-7.

425. Friedberg JW. Relapsed/refractory diffuse large B-cell lymphoma. Hematology / the Education Program of the American Society of Hematology American Society of Hematology Education Program. 2011;2011:498-505.

426. Shaffer AL, 3rd, Young RM, Staudt LM. Pathogenesis of human B cell lymphomas. Annual review of immunology. 2012;30:565-610.

427. Roman E, Smith AG. Epidemiology of lymphomas. Histopathology. 2011;58(1):4-14.

428. George A, Tam CS, Seymour JF. High-risk diffuse large B-cell lymphoma: can we do better than rituximab, cyclophosphamide, doxorubicin, vincristine and prednisone? Leuk Lymphoma. 2013;54(12):2575-6.

429. Maxwell SA, Mousavi-Fard S. Non-Hodgkin's B-cell lymphoma: advances in molecular strategies targeting drug resistance. Experimental biology and medicine (Maywood, NJ). 2013;238(9):971-90.

430. Camicia R, Winkler HC, Hassa PO. Novel drug targets for personalized precision medicine in relapsed/refractory diffuse large B-cell lymphoma: a comprehensive review. Molecular cancer. 2015;14:207.

431. Sullivan LB, Chandel NS. Mitochondrial reactive oxygen species and cancer. Cancer & metabolism. 2014;2:17.

432. Thanan R, Oikawa S, Hiraku Y, Ohnishi S, Ma N, Pinlaor S, et al. Oxidative stress and its significant roles in neurodegenerative diseases and cancer. International journal of molecular sciences. 2015;16(1):193-217.

433. Trachootham D, Alexandre J, Huang P. Targeting cancer cells by ROS-mediated mechanisms: a radical therapeutic approach? Nature reviews Drug discovery. 2009;8(7):579-91.

434. DeNicola GM, Karreth FA, Humpton TJ, Gopinathan A, Wei C, Frese K, et al. Oncogene-induced Nrf2 transcription promotes ROS detoxification and tumorigenesis. Nature. 2011;475(7354):106-9.

435. Shi X, Zhang Y, Zheng J, Pan J. Reactive oxygen species in cancer stem cells. Antioxid Redox Signal. 2012;16(11):1215-28.

436. Landriscina M, Maddalena F, Laudiero G, Esposito F. Adaptation to oxidative stress, chemoresistance, and cell survival. Antioxid Redox Signal. 2009;11(11):2701-16.

437. Sporn MB, Liby KT. NRF2 and cancer: the good, the bad and the importance of context. Nature reviews Cancer. 2012;12(8):564-71.

438. Taguchi K, Motohashi H, Yamamoto M. Molecular mechanisms of the Keap1-Nrf2 pathway in stress response and cancer evolution. Genes to cells : devoted to molecular & cellular mechanisms. 2011;16(2):123-40.

439. Hayes JD, Dinkova-Kostova AT. The Nrf2 regulatory network provides an interface between redox and intermediary metabolism. Trends Biochem Sci. 2014;39(4):199-218.

440. Giudice A, Arra C, Turco MC. Review of molecular mechanisms involved in the activation of the Nrf2-ARE signaling pathway by chemopreventive agents. Methods in molecular biology (Clifton, NJ). 2010;647:37-74.

441. Jaramillo MC, Zhang DD. The emerging role of the Nrf2-Keap1 signaling pathway in cancer. Genes Dev. 2013;27(20):2179-91.

442. Biswas C, Shah N, Muthu M, La P, Fernando AP, Sengupta S, et al. Nuclear heme oxygenase-1 (HO-1) modulates subcellular distribution and activation of Nrf2, impacting metabolic and anti-oxidant defenses. The Journal of biological chemistry. 2014;289(39):26882-94.

443. Gallorini M, Petzel C, Bolay C, Hiller KA, Cataldi A, Buchalla W, et al. Activation of the Nrf2-regulated antioxidant cell response inhibits HEMA-induced oxidative stress and supports cell viability. Biomaterials. 2015;56:114-28.

444. Thimmulappa RK, Mai KH, Srisuma S, Kensler TW, Yamamoto M, Biswal S. Identification of Nrf2-regulated genes induced by the chemopreventive agent sulforaphane by oligonucleotide microarray. Cancer Res. 2002;62(18):5196-203.

445. Berndt N, Yang H, Trinczek B, Betzi S, Zhang Z, Wu B, et al. The Akt activation inhibitor TCN-P inhibits Akt phosphorylation by binding to the PH domain of Akt and blocking its recruitment to the plasma membrane. Cell Death Differ. 2010;17(11):1795-804.

446. Abazari-Kia AH, Mohammadi-Sangcheshmeh A, Dehghani-Mohammadabadi M, Jamshidi-Adegani F, Veshkini A, Zhandi M, et al. Intracellular glutathione content, developmental competence and expression of apoptosis-related genes associated with G6PDH-activity in goat oocyte. Journal of assisted reproduction and genetics. 2014;31(3):313-21.

447. Riganti C, Gazzano E, Polimeni M, Aldieri E, Ghigo D. The pentose phosphate pathway: an antioxidant defense and a crossroad in tumor cell fate. Free radical biology & medicine. 2012;53(3):421-36.

448. Stanton RC. Glucose-6-phosphate dehydrogenase, NADPH, and cell survival. IUBMB life. 2012;64(5):362-9.

449. Barcia-Vieitez R, Ramos-Martinez JI. The regulation of the oxidative phase of the pentose phosphate pathway: new answers to old problems. IUBMB life. 2014;66(11):775-9.

450. Dodson M, Darley-Usmar V, Zhang J. Cellular metabolic and autophagic pathways: traffic control by redox signaling. Free radical biology & medicine. 2013;63:207-21.

451. Jiang P, Du W, Wu M. Regulation of the pentose phosphate pathway in cancer. Protein & cell. 2014;5(8):592-602.

452. Mitsuishi Y, Taguchi K, Kawatani Y, Shibata T, Nukiwa T, Aburatani H, et al. Nrf2 redirects glucose and glutamine into anabolic pathways in metabolic reprogramming. Cancer Cell. 2012;22(1):66-79.

453. Piccirillo S, Filomeni G, Brune B, Rotilio G, Ciriolo MR. Redox mechanisms involved in the selective activation of Nrf2-mediated resistance versus p53-dependent apoptosis in adenocarcinoma cells. The Journal of biological chemistry. 2009;284(40):27721-33.

454. Liu B, Fang M, He Z, Cui D, Jia S, Lin X, et al. Hepatitis B virus stimulates G6PD expression through HBx-mediated Nrf2 activation. Cell death & disease. 2015;6:e1980.

455. Mine N, Yamamoto S, Kufe DW, Von Hoff DD, Kawabe T. Activation of Nrf2 pathways correlates with resistance of NSCLC cell lines to CBP501 in vitro. Mol Cancer Ther. 2014;13(9):2215-25.

456. Vegliante R, Desideri E, Di Leo L, Ciriolo MR. Dehydroepiandrosterone triggers autophagic cell death in human hepatoma cell line HepG2 via JNK-mediated p62/SQSTM1 expression. Carcinogenesis. 2016;37(3):233-44.

457. Gupte SA, Li KX, Okada T, Sato K, Oka M. Inhibitors of pentose phosphate pathway cause vasodilation: involvement of voltage-gated potassium channels. The Journal of pharmacology and experimental therapeutics. 2002;301(1):299-305.

458. Tsutsui EA, Marks PA, Reich P. Effect of dehydroepiandrosterone on glucose 6-phosphate dehydrogenase activity and reduced triphosphopyridine nucleotide formation in adrenal tissue. The Journal of biological chemistry. 1962;237:3009-13.

459. Costa Rosa LF, Curi R, Murphy C, Newsholme P. Effect of adrenaline and phorbol myristate acetate or bacterial lipopolysaccharide on stimulation of pathways of macrophage glucose, glutamine and O2 metabolism. Evidence for cyclic AMP-dependent protein kinase mediated inhibition of glucose-6-phosphate dehydrogenase and activation of NADP+-dependent 'malic' enzyme. The Biochemical journal. 1995;310 (Pt 2):709-14.

460. Xu Y, Osborne BW, Stanton RC. Diabetes causes inhibition of glucose-6-phosphate dehydrogenase via activation of PKA, which contributes to oxidative stress in rat kidney cortex. American journal of physiology Renal physiology. 2005;289(5):F1040-7.

461. Napier MA, Lipari MT, Courter RG, Cheng CH. Epidermal growth factor receptor tyrosine kinase phosphorylation of glucose-6-phosphate dehydrogenase in vitro. Arch Biochem Biophys. 1987;259(2):296-304.

462. Matta A, Masui O, Siu KW, Ralhan R. Identification of 14-3-3zeta associated protein networks in oral cancer. Proteomics. 2016.

463. Cordeiro AT, Godoi PH, Silva CH, Garratt RC, Oliva G, Thiemann OH. Crystal structure of human phosphoglucose isomerase and analysis of the initial catalytic steps. Biochimica et biophysica acta. 2003;1645(2):117-22.

464. Somarowthu S, Brodkin HR, D'Aquino JA, Ringe D, Ondrechen MJ, Beuning PJ. A tale of two isomerases: compact versus extended active sites in ketosteroid isomerase and phosphoglucose isomerase. Biochemistry. 2011;50(43):9283-95.

465. Wagle A, Jivraj S, Garlock GL, Stapleton SR. Insulin regulation of glucose-6-phosphate dehydrogenase gene expression is rapamycin-sensitive and requires phosphatidylinositol 3-kinase. The Journal of biological chemistry. 1998;273(24):14968-74.

466. Abdullah LN, Chow EK-H. Mechanisms of chemoresistance in cancer stem cells. Clinical and translational medicine. 2013;2(1):1.

467. Hayes JD, McLELLAN LI. Glutathione and glutathione-dependent enzymes represent a co-ordinately regulated defence against oxidative stress. Free radical research. 1999;31(4):273-300.

468. Ledermann J, Kristeleit R. Optimal treatment for relapsing ovarian cancer. Annals of oncology. 2010;21(suppl 7):vii218-vii22.

469. Maiti AK. Genetic determinants of oxidative stress-mediated sensitization of drug-resistant cancer cells. International journal of cancer. 2012;130(1):1-9.

470. Perera RM, Bardeesy N. Cancer: when antioxidants are bad. Nature. 2011;475(7354):43-4.

471. Watson J. Oxidants, antioxidants and the current incurability of metastatic cancers. Open biology. 2013;3(1):120144.

472. Pelicano H, Carney D, Huang P. ROS stress in cancer cells and therapeutic implications. Drug Resistance Updates. 2004;7(2):97-110.

473. Wondrak GT. Redox-directed cancer therapeutics: molecular mechanisms and opportunities. Antioxidants & redox signaling. 2009;11(12):3013-69.

474. Copple IM. The Keap1-Nrf2 cell defense pathway--a promising therapeutic target? Advances in pharmacology (San Diego, Calif). 2011;63:43-79.

475. Geismann C, Arlt A, Sebens S, Schäfer H. Cytoprotection "gone astray": Nrf2 and its role in cancer. Onco Targets Ther. 2014;7:1497-518.

476. Mitsuishi Y, Motohashi H, Yamamoto M. The Keap1-Nrf2 system in cancers: stress response and anabolic metabolism. Frontiers in oncology. 2011;2:200-.

477. Suzuki T, Motohashi H, Yamamoto M. Toward clinical application of the Keap1–Nrf2 pathway. Trends in pharmacological sciences. 2013;34(6):340-6.

478. Ames JR, Ryan MD, Kovacic P. Mechanism of antibacterial action: electron transfer and oxy radicals. Journal of free radicals in biology & medicine. 1986;2(5-6):377-91.

479. Quinlan GJ, Gutteridge JM. Oxidative damage to DNA and deoxyribose by β-lactam antibiotics in the presence of iron and copper salts. Free radical research communications. 1988;5(3):149-58.

480. Dwyer DJ, Belenky PA, Yang JH, MacDonald IC, Martell JD, Takahashi N, et al. Antibiotics induce redox-related physiological alterations as part of their lethality. Proceedings of the National Academy of Sciences. 2014;111(20):E2100-E9.

481. Kohanski MA, Dwyer DJ, Hayete B, Lawrence CA, Collins JJ. A common mechanism of cellular death induced by bactericidal antibiotics. Cell. 2007;130(5):797-810.

482. Kohanski MA, Dwyer DJ, Wierzbowski J, Cottarel G, Collins JJ. Mistranslation of membrane proteins and two-component system activation trigger antibiotic-mediated cell death. Cell. 2008;135(4):679-90.

483. Kohanski MA, DePristo MA, Collins JJ. Sublethal antibiotic treatment leads to multidrug resistance via radical-induced mutagenesis. Molecular cell. 2010;37(3):311-20.

484. Kalghatgi S, Spina CS, Costello JC, Liesa M, Morones-Ramirez JR, Slomovic S, et al. Bactericidal antibiotics induce mitochondrial dysfunction and oxidative damage in mammalian cells. Science translational medicine. 2013;5(192):192ra85-ra85.

485. Liu Y, Imlay JA. Cell death from antibiotics without the involvement of reactive oxygen species. Science. 2013;339(6124):1210-3.

486. Keren I, Wu Y, Inocencio J, Mulcahy LR, Lewis K. Killing by bactericidal antibiotics does not depend on reactive oxygen species. Science. 2013;339(6124):1213-6.

487. Yasuhisa K. Oxygen enhancement of bactericidal activity of rifamycin SV on Escherichia coli and aerobic oxidation of rifamycin SV to rifamycin S catalyzed by manganous ions: the role of superoxide. Journal of biochemistry. 1982;91(1):381-95.

488. Yasuhisa K, Sugiura Y. Electron spin resonance studies on the oxidation of rifamycin SV catalyzed by metal ions. Journal of biochemistry. 1982;91(1):397-401.

489. Scrutton MC. Divalent metal ion catalysis of the oxidation of rifamycin SV to refamycin S. FEBS letters. 1977;78(2):216-20.

490. Quinlan GJ, Gutteridge JM. Oxygen radical damage to DNA by rifamycin SV and copper ions. Biochemical Pharmacology. 1987;36(21):3629-33.

491. Quinlan GJ, Gutteridge JM. DNA base damage by β-lactam, tetracycline, bacitracin and rifamycin antibacterial antibiotics. Biochemical pharmacology. 1991;42(8):1595-9.

492. Cederbaum AI. Stimulation of microsomal production of reactive oxygen intermediates by rifamycin SV: effect of ferric complexes and comparisons between NADPH and NADH. Archives of biochemistry and biophysics. 1992;298(2):602-11.

493. Rao DR, Cederbaum AI. A comparative study of the redox-cycling of a quinone (Rifamycin S) and a quinonimine (Rifabutin) antibiotic by rat liver microsomes. Free Radical Biology and Medicine. 1997;22(3):439-46.

494. Hanson GT, Aggeler R, Oglesbee D, Cannon M, Capaldi RA, Tsien RY, et al. Investigating mitochondrial redox potential with redox-sensitive green fluorescent protein indicators. Journal of Biological Chemistry. 2004;279(13):13044-53.

495. Cannon MB, James Remington S. Redox-sensitive green fluorescent protein: probes for dynamic intracellular redox responses. A review. Redox-Mediated Signal Transduction: Methods and Protocols. 2009:50-64.

496. Lohman JR, Remington SJ. Development of a Family of Redox-Sensitive Green Fluorescent Protein Indicators for Use in Relatively Oxidizing Subcellular Environments†‡. Biochemistry. 2008;47(33):8678-88.

497. Jiang P, Yamauchi K, Yang M, Tsuji K, Xu M, Maitra A, et al. Tumor cells genetically labeled with GFP in the nucleus and RFP in the cytoplasm for imaging cellular dynamics. Cell Cycle. 2006;5(11):1198-201.

498. Langmead B, Salzberg SL. Fast gapped-read alignment with Bowtie 2. Nature methods. 2012;9(4):357-9.

499. Trapnell C, Hendrickson DG, Sauvageau M, Goff L, Rinn JL, Pachter L. Differential analysis of gene regulation at transcript resolution with RNA-seq. Nature biotechnology. 2013;31(1):46-53.

500. Mohammad RM, Mohamed AN, Smith MR, Jawadi NS, Al-Katib A. A unique EBV-negative low-grade lymphoma line (WSU-FSCCL) exhibiting both t (14; 18) and t (8; 11). Cancer genetics and cytogenetics. 1993;70(1):62-7.

501. Amini R-M, Berglund M, Rosenquist R, von Heideman A, Lagercrantz S, Thunberg U, et al. A novel B-cell line (U-2932) established from a patient with diffuse large B-cell lymphoma following Hodgkin lymphoma. Leukemia & lymphoma. 2002;43(11):2179-89.

502. Drexler HG, Eberth S, Nagel S, MacLeod RA. Malignant hematopoietic cell lines: in vitro models for double-hit B-cell lymphomas. Leukemia & lymphoma. 2016;57(5):1015-20.

503. Foley OW, Del Carmen MG. Recurrent epithelial ovarian cancer: an update on treatment. Oncology. 2013;27(4):288.

504. Cain JW, Hauptschein RS, Stewart JK, Bagci T, Sahagian GG, Jay DG. Identification of CD44 as a surface biomarker for drug resistance by surface proteome signature technology. Molecular Cancer Research. 2011;9(5):637-47.

505. Wu L, Smythe AM, Stinson SF, Mullendore LA, Monks A, Scudiero DA, et al. Multidrug-resistant phenotype of disease-oriented panels of human tumor cell lines used for anticancer drug screening. Cancer research. 1992;52(11):3029-34.

506. Ke W, Yu P, Wang J, Wang R, Guo C, Zhou L, et al. MCF-7/ADR cells (re-designated NCI/ADR-RES) are not derived from MCF-7 breast cancer cells: a loss for breast cancer multidrug-resistant research. Medical oncology. 2011;28(1):135-41.

507. Kalyanaraman B, Perez-Reyes E, Mason RP. Spin-trapping and direct electron spin resonance investigations of the redox metabolism of quinone anticancer drugs. Biochimica et Biophysica Acta (BBA)-General Subjects. 1980;630(1):119-30.

508. Gutierrez PL. The metabolism of quinone-containing alkylating agents: free radical production and measurement. Front Biosci. 2000;5:629-38.

509. Lin Y, Shi R, Wang X, Shen H-M. Luteolin, a flavonoid with potential for cancer prevention and therapy. Current cancer drug targets. 2008;8(7):634-46.

510. Kensler TW, Wakabayashi N, Biswal S. Cell survival responses to environmental stresses via the Keap1-Nrf2-ARE pathway. Annu Rev Pharmacol Toxicol. 2007;47:89-116.

511. Kobayashi A, Kang M-I, Okawa H, Ohtsuji M, Zenke Y, Chiba T, et al. Oxidative stress sensor Keap1 functions as an adaptor for Cul3-based E3 ligase to regulate proteasomal degradation of Nrf2. Molecular and cellular biology. 2004;24(16):7130-9.

512. Cullinan SB, Gordan JD, Jin J, Harper JW, Diehl JA. The Keap1-BTB protein is an adaptor that bridges Nrf2 to a Cul3-based E3 ligase: oxidative stress sensing by a Cul3-Keap1 ligase. Molecular and cellular biology. 2004;24(19):8477-86.

513. Wu T, Zhao F, Gao B, Tan C, Yagishita N, Nakajima T, et al. Hrd1 suppresses Nrf2-mediated cellular protection during liver cirrhosis. Genes & development. 2014;28(7):708-22.

514. Malhotra JD, Kaufman RJ. Endoplasmic reticulum stress and oxidative stress: a vicious cycle or a double-edged sword? Antioxidants & redox signaling. 2007;9(12):2277-94.

515. Woehlbier U, Hetz C. Modulating stress responses by the UPRosome: a matter of life and death. Trends in biochemical sciences. 2011;36(6):329-37.

516. Teicher BA. Tumor models for efficacy determination. Molecular cancer therapeutics. 2006;5(10):2435-43.

517. Day C-P, Merlino G, Van Dyke T. Preclinical mouse cancer models: a maze of opportunities and challenges. Cell. 2015;163(1):39-53.

518. Johnson J, Decker S, Zaharevitz D, Rubinstein L, Venditti J, Schepartz S, et al. Relationships between drug activity in NCI preclinical in vitro and in vivo models and early clinical trials. British journal of cancer. 2001;84(10):1424.

519. Swerdlow SH. Diagnosis of 'double hit'diffuse large B-cell lymphoma and B-cell lymphoma, unclassifiable, with features intermediate between DLBCL and Burkitt lymphoma: when and how, FISH versus IHC. ASH Education Program Book. 2014;2014(1):90-9.

520. Aukema SM, Siebert R, Schuuring E, van Imhoff GW, Kluin-Nelemans HC, Boerma E-J, et al. Double-hit B-cell lymphomas. Blood. 2011;117(8):2319-31.

521. Kurosu T, Fukuda T, Miki T, Miura O. BCL6 overexpression prevents increase in reactive oxygen species and inhibits apoptosis induced by chemotherapeutic reagents in B-cell lymphoma cells. Oncogene. 2003;22(29):4459-68.

522. Wang Y-Q, Xu M-D, Weng W-W, Wei P, Yang Y-S, Du X. BCL6 is a negative prognostic factor and exhibits pro-oncogenic activity in ovarian cancer. American journal of cancer research. 2015;5(1):255.

523. Kaneko YS, Takayanagi T, Nagasaki H, Kodani Y, Nakashima A, Mori K, et al. Aripiprazole increases NAD(P)H-quinone oxidoreductase-1 and heme oxygenase-1 in PC12 cells. Journal of neural transmission (Vienna, Austria : 1996). 2015;122(6):757-72.

524. Du W, Jiang P, Mancuso A, Stonestrom A, Brewer MD, Minn AJ, et al. TAp73 enhances the pentose phosphate pathway and supports cell proliferation. Nature cell biology. 2013;15(8):991-1000.

525. Marí M, Morales A, Colell A, García-Ruiz C, Fernández-Checa JC. Mitochondrial glutathione, a key survival antioxidant. Antioxidants & redox signaling. 2009;11(11):2685-700.

526. Leopold JA, Loscalzo J. Cyclic strain modulates resistance to oxidant stress by increasing G6PDH expression in smooth muscle cells. American Journal of Physiology-Heart and Circulatory Physiology. 2000;279(5):H2477-H85.

527. Quiroz N, Rivas N, del Pozo T, Burkhead J, Suazo M, Gonzalez M, et al. Transcriptional activation of glutathione pathways and role of glucose homeostasis during copper imbalance. Biometals : an international journal on the role of metal ions in biology, biochemistry, and medicine. 2015;28(2):321-8.

528. Sandoval JM, Arenas FA, Vasquez CC. Glucose-6-phosphate dehydrogenase protects Escherichia coli from tellurite-mediated oxidative stress. PLoS One. 2011;6(9):e25573.

529. Wolf MB, Baynes JW. The anti-cancer drug, doxorubicin, causes oxidant stress-induced endothelial dysfunction. Biochimica et Biophysica Acta (BBA)-General Subjects. 2006;1760(2):267-71.

530. Zhang HS, Wang SQ. Nrf2 is involved in the effect of tanshinone IIA on intracellular redox status in human aortic smooth muscle cells. Biochem Pharmacol. 2007;73(9):1358-66.

531. Zhang M, Liu H, Guo R, Ling Y, Wu X, Li B, et al. Molecular mechanism of gossypol-induced cell growth inhibition and cell death of HT-29 human colon carcinoma cells. Biochem Pharmacol. 2003;66(1):93-103.

532. Cramer CT, Cooke S, Ginsberg LC, Kletzien RF, Stapleton SR, Ulrich RG. Upregulation of glucose-6-phosphate dehydrogenase in response to hepatocellular oxidative stress: studies with diquat. Journal of biochemical toxicology. 1995;10(6):293-8.

533. Nguyen TT, Kitajima S, Izawa S. Importance of glucose-6-phosphate dehydrogenase (G6PDH) for vanillin tolerance in Saccharomyces cerevisiae. Journal of bioscience and bioengineering. 2014;118(3):263-9.

534. Rodrigues JR, Ferrer R, Gamboa N, Charris J, Antunes F. Potential antitumour and pro-oxidative effects of (E)-methyl 2-(7-chloroquinolin-4-ylthio)-3-(4-hydroxyphenyl) acrylate (QNACR). Journal of enzyme inhibition and medicinal chemistry. 2013;28(6):1300-6.

535. Gupta S, Igoillo-Esteve M, Michels PA, Cordeiro AT. Glucose-6-phosphate dehydrogenase of trypanosomatids: characterization, target validation, and drug discovery. Molecular biology international. 2011;2011.

536. Valderrama R, Corpas FJ, Carreras A, Gomez-Rodriguez MV, Chaki M, Pedrajas JR, et al. The dehydrogenase-mediated recycling of NADPH is a key antioxidant system against salt-induced oxidative stress in olive plants. Plant Cell Environ. 2006;29(7):1449-59.

537. Haynes CM, Ron D. The mitochondrial UPR–protecting organelle protein homeostasis. J Cell Sci. 2010;123(22):3849-55.

538. Zhao Q, Wang J, Levichkin IV, Stasinopoulos S, Ryan MT, Hoogenraad NJ. A mitochondrial specific stress response in mammalian cells. The EMBO journal. 2002;21(17):4411-9.

539. Al-Furoukh N, Ianni A, Nolte H, Hölper S, Krüger M, Wanrooij S, et al. ClpX stimulates the mitochondrial unfolded protein response (UPR mt) in mammalian cells. Biochimica et Biophysica Acta (BBA)-Molecular Cell Research. 2015;1853(10):2580-91.

540. Guaragnella N, Giannattasio S, Moro L. Mitochondrial dysfunction in cancer chemoresistance. Biochemical pharmacology. 2014;92(1):62-72.

541. Pellegrino MW, Nargund AM, Haynes CM. Signaling the mitochondrial unfolded protein response. Biochimica et Biophysica Acta (BBA)-Molecular Cell Research. 2013;1833(2):410-6.

542. Yaguchi T, Aida S, Kaul SC, Wadhwa R. Involvement of mortalin in cellular senescence from the perspective of its mitochondrial import, chaperone, and oxidative stress management functions. Annals of the New York Academy of Sciences. 2007;1100(1):306-11.

543. Liu Y, Liu W, Song X-D, Zuo J. Effect of GRP75/mthsp70/PBP74/mortalin overexpression on intracellular ATP level, mitochondrial membrane potential and ROS accumulation following glucose deprivation in PC12 cells. Molecular and cellular biochemistry. 2005;268(1-2):45-51.

544. Jin J, Hulette C, Wang Y, Zhang T, Pan C, Wadhwa R, et al. Proteomic identification of a stress protein, mortalin/mthsp70/GRP75 relevance to Parkinson disease. Molecular & Cellular Proteomics. 2006;5(7):1193-204.

545. Burbulla LF, Schelling C, Kato H, Rapaport D, Woitalla D, Schiesling C, et al. Dissecting the role of the mitochondrial chaperone mortalin in Parkinson's disease: functional impact of disease-related variants on mitochondrial homeostasis. Human molecular genetics. 2010:ddq370.

546. Kaul SC, Deocaris CC, Wadhwa R. Three faces of mortalin: a housekeeper, guardian and killer. Experimental gerontology. 2007;42(4):263-74.

547. Kaul SC, Yaguchi T, Taira K, Reddel RR, Wadhwa R. Overexpressed mortalin (mot-2)/mthsp70/GRP75 and hTERT cooperate to extend the in vitro lifespan of human fibroblasts. Experimental cell research. 2003;286(1):96-101.

548. Kotiadis VN, Duchen MR, Osellame LD. Mitochondrial quality control and communications with the nucleus are important in maintaining mitochondrial function and cell health. Biochimica et Biophysica Acta (BBA)-General Subjects. 2014;1840(4):1254-65.

549. Arnould T, Michel S, Renard P. Mitochondria retrograde signaling and the UPRmt: where are we in mammals? International journal of molecular sciences. 2015;16(8):18224-51.

550. Jovaisaite V, Mouchiroud L, Auwerx J. The mitochondrial unfolded protein response, a conserved stress response pathway with implications in health and disease. Journal of Experimental Biology. 2014;217(1):137-43.

551. Horibe T, Hoogenraad NJ. The chop gene contains an element for the positive regulation of the mitochondrial unfolded protein response. PloS one. 2007;2(9):e835.

552. Jones AW, Yao Z, Vicencio JM, Karkucinska-Wieckowska A, Szabadkai G. PGC-1 family coactivators and cell fate: Roles in cancer, neurodegeneration, cardiovascular disease and retrograde mitochondria–nucleus signalling. Mitochondrion. 2012;12(1):86-99.

553. Torelli NQ, Ferreira-Júnior JR, Kowaltowski AJ, da Cunha FM. RTG1-and RTG2-dependent retrograde signaling controls mitochondrial activity and stress resistance in Saccharomyces cerevisiae. Free Radical Biology and Medicine. 2015;81:30-7.

554. Murata S, Minami Y, Minami M, Chiba T, Tanaka K. CHIP is a chaperone-dependent E3 ligase that ubiquitylates unfolded protein. EMBO reports. 2001;2(12):1133-8.

555. Connell P, Ballinger CA, Jiang J, Wu Y, Thompson LJ, Höhfeld J, et al. The co-chaperone CHIP regulates protein triage decisions mediated by heat-shock proteins. Nature cell biology. 2001;3(1):93-6.

556. Tang X, Wen S, Zheng D, Tucker L, Cao L, Pantazatos D, et al. Acetylation of drosha on the N-terminus inhibits its degradation by ubiquitination. PloS one. 2013;8(8):e72503.

557. Soss SE, Rose KL, Hill S, Jouan S, Chazin WJ. Biochemical and proteomic analysis of ubiquitination of HSC70 and HSP70 by the E3 ligase chip. PloS one. 2015;10(5):e0128240.

558. Kästle M, Reeg S, Rogowska-Wrzesinska A, Grune T. Chaperones, but not oxidized proteins, are ubiquitinated after oxidative stress. Free Radical Biology and Medicine. 2012;53(7):1468-77.

559. Benedetti C, Haynes CM, Yang Y, Harding HP, Ron D. Ubiquitin-like protein 5 positively regulates chaperone gene expression in the mitochondrial unfolded protein response. Genetics. 2006;174(1):229-39.

560. Ross JM, Olson L, Coppotelli G. Mitochondrial and ubiquitin proteasome system dysfunction in ageing and disease: two sides of the same coin? International journal of molecular sciences. 2015;16(8):19458-76.

561. Livnat-Levanon N, Glickman MH. Ubiquitin–proteasome system and mitochondria—reciprocity. Biochimica et Biophysica Acta (BBA)-Gene Regulatory Mechanisms. 2011;1809(2):80-7.

562. Karbowski M, Youle RJ. Regulating mitochondrial outer membrane proteins by ubiquitination and proteasomal degradation. Current opinion in cell biology. 2011;23(4):476-82.

563. Heo J-M, Rutter J. Ubiquitin-dependent mitochondrial protein degradation. The international journal of biochemistry & cell biology. 2011;43(10):1422-6.

564. Kanazawa H, Nagatsuka T, Miyazaki M, Matsushima Y. Determination of peptides by high-performance liquid chromatography with laser-induced fluorescence detection. Journal of Chromatography A. 1997;763(1):23-9.

565. Jacobs AT, Marnett LJ. Heat shock factor 1 attenuates 4-hydroxynonenal-mediated apoptosis critical role for heat shock protein 70 induction and stabilization of Bcl-xl. Journal of Biological Chemistry. 2007;282(46):33412-20.

566. Suliman HB, Sweeney TE, Withers CM, Piantadosi CA. Co-regulation of nuclear respiratory factor-1 by NFκB and CREB links LPS-induced inflammation to mitochondrial biogenesis. J Cell Sci. 2010;123(15):2565-75.

567. Grossmann C, Wuttke M, Ruhs S, Seiferth A, Mildenberger S, Rabe S, et al. Mineralocorticoid receptor inhibits CREB signaling by calcineurin activation. The FASEB Journal. 2010;24(6).

568. Chowanadisai W, Bauerly KA, Tchaparian E, Wong A, Cortopassi GA, Rucker RB. Pyrroloquinoline quinone stimulates mitochondrial biogenesis through cAMP response element-binding protein phosphorylation and increased PGC-1α expression. Journal of Biological Chemistry. 2010;285(1):142-52.

569. Hou X-D, Li N, Zong M-H. Significantly enhancing enzymatic hydrolysis of rice straw after pretreatment using renewable ionic liquid–water mixtures. Bioresource technology. 2013;136:469-74.

570. Clague MJ, Urbé S. Endocytosis: the DUB version. Trends in cell biology. 2006;16(11):551-9.

571. Park JK, Park SH, So K, Bae IH, Yoo YD, Um HD. ICAM-3 enhances the migratory and invasive potential of human non-small cell lung cancer cells by inducing MMP-2 and MMP-9 via Akt and CREB. Int J Oncol. 2010;36(1):181-92.

572. Yonashiro R, Sugiura A, Miyachi M, Fukuda T, Matsushita N, Inatome R, et al. Mitochondrial ubiquitin ligase MITOL ubiquitinates mutant SOD1 and attenuates mutant SOD1-induced reactive oxygen species generation. Molecular biology of the cell. 2009;20(21):4524-30.

573. Zhang B, Huang J, Li HL, Liu T, Wang YY, Waterman P, et al. GIDE is a mitochondrial E3 ubiquitin ligase that induces apoptosis and slows growth. Cell Res. 2008;18(9):900-10.

574. Yang H, Zhou X, Liu X, Yang L, Chen Q, Zhao D, et al. Mitochondrial dysfunction induced by knockdown of mortalin is rescued by Parkin. Biochemical and biophysical research communications. 2011;410(1):114-20.

575. Wang Y, Serricchio M, Jauregui M, Shanbhag R, Stoltz T, Di Paolo CT, et al. Deubiquitinating enzymes regulate PARK2-mediated mitophagy. Autophagy. 2015;11(4):595-606.

576. Yoneda T, Benedetti C, Urano F, Clark SG, Harding HP, Ron D. Compartment-specific perturbation of protein handling activates genes encoding mitochondrial chaperones. Journal of cell science. 2004;117(18):4055-66.

577. Runkel ED, Liu S, Baumeister R, Schulze E. Surveillance-Activated Defenses Block the ROS–Induced Mitochondrial Unfolded Protein Response. PLoS Genet. 2013;9(3):e1003346.

578. Nargund AM, Pellegrino MW, Fiorese CJ, Baker BM, Haynes CM. Mitochondrial import efficiency of ATFS-1 regulates mitochondrial UPR activation. Science. 2012;337(6094):587-90.

579. Mottis A, Jovaisaite V, Auwerx J. The mitochondrial unfolded protein response in mammalian physiology. Mammalian Genome. 2014;25(9-10):424-33.

580. Itoh K, Ye P, Matsumiya T, Tanji K, Ozaki T. Emerging functional cross-talk between the Keap1-Nrf2 system and mitochondria. Journal of clinical biochemistry and nutrition. 2015;56(2):91-7.

581. Ricart KC, Bolisetty S, Johnson MS, Perez J, Agarwal A, Murphy MP, et al. The permissive role of mitochondria in the induction of haem oxygenase-1 in endothelial cells. Biochemical Journal. 2009;419(2):427-36.

582. Itoh K, Wakabayashi N, Katoh Y, Ishii T, Igarashi K, Engel JD, et al. Keap1 represses nuclear activation of antioxidant responsive elements by Nrf2 through binding to the amino-terminal Neh2 domain. Genes & development. 1999;13(1):76-86.

583. Surh Y-J, Kundu JK, Na H-K. Nrf2 as a master redox switch in turning on the cellular signaling involved in the induction of cytoprotective genes by some chemopreventive phytochemicals. Planta medica. 2008;74(13):1526-39.

584. Vargas MR, Johnson JA. The Nrf2–ARE cytoprotective pathway in astrocytes. Expert reviews in molecular medicine. 2009;11:e17.

585. Cullinan SB, Zhang D, Hannink M, Arvisais E, Kaufman RJ, Diehl JA. Nrf2 is a direct PERK substrate and effector of PERK-dependent cell survival. Molecular and cellular biology. 2003;23(20):7198-209.